Processing Fibrous Plants to High Quantity and Quality Fibres

by

Vahid Sadrmanesh

A Thesis Submitted to The Faculty of Graduate Studies of

The University of Manitoba

In partial fulfilment of the requirements of the degree of

DOCTOR OF PHILOSOPHY

Department of Biosystems Engineering

University of Manitoba

Winnipeg

Abstract

Insufficient resources of plant fibre for developing bio-based products and processing fibrous plant stalks to high quality and quantity fibres are two challenges of the natural fibre industry. Considering the first challenge, two alternative plant fibres including canola and sweet clover fibres were characterized and compared to hemp and flax fibres which are two traditional fibres. Their characteristics, including microstructural, surface, thermal, and mechanical properties, were measured. Mechanical behaviour of fibres was also simulated using the Discrete Element Method (DEM). Considering the second challenge, fibre extraction experiments were conducted on both traditional and alternative fibrous plants. In the experiments, hemp fibre was mechanically extracted using a decorticator. Mechanical extraction of canola fibres was not successful; therefore, canola fibre was extracted through retting. Results demonstrated that the microstructural, surface, and thermal properties of the alternative fibres (canola and sweet clover) were in the same ranges with the traditional fibres (hemp and flax). However, the alternative fibres had lower Young's modulus, while the traditional fibres had higher stiffness and tensile strength. Simulation results indicated that the DEM model generated comparable results to the tensile test experiments in terms of Young's modulus and tensile strength. For mechanical extraction of hemp fibre using the decorticator, the most effective parameters, in terms of quantity and quality of the fibres, were the retting condition of the feed stalks, the number of pass of stalks through the decorticator rollers, and the feed amount. For retting extraction of canola fibre using chemical solution, when the time, temperature, and $NaHCO_3$ concentration were set to 37.8 h, 57.7 ºC, and 5.62%, respectively, the highest quantity and quality canola fibres were achieved. The results from this study have important implications to applications of plant fibres.

Acknowledgments

There are no proper words to convey my deepest appreciation and respect for my advisor, Dr. Ying Chen. Without her encouragement, support and continuous optimism, the completion of my dissertation would not have been possible. She was and remains my role model for a scientist, mentor, and teacher. Besides, I am deeply indebted to my thesis advisory committee members, Dr. Simon Potter and Dr. Malcom Xing, for their constructive inputs which allowed me to take advantage from their vast experience.

I wish to express my sincere thanks to Dr. Mashiur Rahman for his advice and guidance. A special thanks goes to the past and present members of my lab-mates for their assistance. I would like to give special thanks to the teaching, administrative and technical staff of the Department of Biosystems Engineering, the University of Manitoba.

This journey would not have been possible without my family members for the unconditional love and support during my life. I wish to express my deep indebtedness to my wife, Mahdieh Farahani, for her support and encouragement. Immense thanks to my youngest brother, Milad, who has indirectly pushed me to work very hard by saying that “Vahid, you are my role model”.

I would like to express my deep sense of gratuities and appreciation to the following organizations because of their financial support provided as research grants or scholarships throughout the program: NSERC, MITACS, University of Manitoba, and Composite Innovation Center.

My cordial thanks are because of everyone not mentioned but most importantly not forgotten.

“This thesis is dedicated to my beloved wife and parents”

Table of Contents

Lists of Tables

List of Figures

Chapter 1: Introductory Materials, Scope and Objectives of the Thesis

1.1. INTRODUCTION

Over the past decades, researchers have been trying to replace synthetic fibres, especially glass fibres, with plant bast fibres because of favorable properties of plant fibres, such as high biodegradation, low energy consumption for production, low density, and low price. Although plant fibres have some disadvantages, such as low tensile strength, low decomposition temperature, tendency to absorb moisture, and poor adhesion with polymer matrix, these undesirable properties are being addressed during processing fibrous plants and making bioproducts.

The traditionally used bast fibres are hemp and flax fibres. However, increasing demand for using bio-based products will create a shortage of such fibres in the future. Therefore, we are facing a challenge of identifying new bast fibres with acceptable technical properties. Another challenge with bast fibres is the fibre extraction. Biological retting and mechanical decortication are the two main fibre extraction methods. When performed correctly, retting generates the highest purity fibre; but it is time-consuming and produces large amounts of wastewater. In contrast, mechanical extraction is faster and more environmentally friendly; however, the resultant fibre has low purity. Thus, obtaining the optimize condition for both mechanical and retting extraction of bast fibres is important to improve the effectiveness of extraction and fibre quality.

In this study, four types of bast fibres were investigated. They were canola and sweet clover as two alternative bast fibres and hemp and flax fibres as traditionally used bast fibres. Canola fibre

was explored because Canada is one of the leading countries in the world to grow canola. The current situation is that almost all canola stalks remain in the field as wastes after the seeds are harvested. Wild sweet clover fibre was explored because it can be found Canada wide.

1.2. OBJECTIVES

The overall intention of this study was to predict the optimal condition for extraction of bast fibres. Results from this investigation will contribute to obtain high quantity and quality fibres in terms of fibre yield and properties (chemical compositions, crystallinity index, thermal stability, and maximum degradation temperature). The specific objectives of this study were to:

(1) review bast fibres and their properties;

(2) characterise canola and sweet clover fibres as two alternative bast fibres;

(3) simulate tensile behavior of hemp fibres using the Discrete Element Method;

(4) prioritise the most influential parameters affecting mechanical extraction of hemp fibres;

(5) optimize canola fibres extraction conditions using a hybrid algorithm.

1.3. THESIS STRUCTURE

This thesis is structured in paper format where each paper focuses on some specific objectives. General introduction and literature review are presented in Chapter 1 and Chapter 2. Chapter 3 reviewed all aspects of bast fibres which has already been published (*Sadrmanesh V, Chen Y. Bast fibres: structure, processing, properties, and applications. International Material Reviews 2018; 64:381–406. https://doi.org/10.1080/09506608.2018.1501171*). In Chapter 4, two alternative bast fibres were introduced and they were compared with traditional fibres. The manuscript of Chapter 4 titled “Canola and sweet clover fibres: alternative plant fibres for industrial applications” has been submitted to a scientific journal. In Chapter 5, the tensile behavior of plant fibre was

simulated using the Discrete Element Method. This chapter has been published (*Sadrmanesh V, Chen Y. Simulation of tensile behavior of plant fibres using the Discrete Element Method (DEM). Composite Part A Applied Science Manufacturing 2018; 114:196–203. https://doi.org/10.1016/J.COMPOSITESA.2018.08.023*.). Chapter 6 prioritized the most important parameters which influence mechanical extraction of bast fibres. This chapter has also been published (*Sadrmanesh V, Chen Y, Rahman M, AL-Oqla FM. Developing a decision making model to identify the most influential parameters affecting mechanical extraction of bast fibres. Journal of Cleaner Production 2019; 238:117891. https://doi.org/10.1016/j.jclepro.2019.117891*.). The manuscript based on Chapter 7 titled "Multi-objective optimization of canola fibre extraction using a hybrid algorithm" has been submitted to a scientific journal. General conclusion and recommendations are presented in Chapter 8.

In all the manuscripts brought in this thesis, the candidate is the first author and Dr. Ying Chen, the candidate's advisor, is the corresponding author. Chapter 4 is co-authored by Alain Lagasse, a summer student, who performed tensile test on the studied fibres and data processing. Chapter 6 is co-authored by Dr. Mashiur Rahman (Senior Instructor, Department of Biosystems Engineering, University of Manitoba) who provided Instrument for doing tensile test, and Dr. Faris M. AL-Oqla (Assistant Professor, Department of Mechanical Engineering, Hashemite University, Zarqa, Jordan) who contributed to develop the decision-making model. Chapter 7 is co-authored by Dr. Mashiur Rahman who contributed to the testing protocol and discussion, and Hamid Reza Fazeli (Graduate Student, Department of Mechanical Engineering, University of Manitoba) who contributed to the development of the hybrid algorithm.

Chapter 2: General Literature Review

2.1. PLANT FIBRES

Plant fibres are referred to as the fibres which are extracted from plant bark, leaf, fruit, wood, straw, and grasses [1]. Plant fibres include seed fibres, hard fibres, and bast fibres. Among these fibres, bast fibres are the most popular fibres because of their specific mechanical properties. This study focused on bast fibres from various plants, including hemp, flax, canola, and wild sweet clover. Bast fibres are referred to plant fibres which are extracted from the phloem surrounding the stem of certain dicotyledonous plants. Figure 2.1 shows all aspects of bast fibres from processing to future trends. Bast fibres are in the form of fibre bundles when they are extracted from the phloem. Fibre bundles consist of several individual single fibres. The main chemical compositions of bast fibres are cellulose, hemicellulose, lignin, pectin, and small amounts of wax and fats. The percentage of these elements varies with age, fibre source, and fibre extraction methods. Bast fibres are extracted from plant stalks using mechanical, biological, or chemical (e.g. retting) extraction. Mechanical extraction is faster and more environmentally friendly; however, it produces low-purity fibre. In contrast, retting extraction, when performed properly, provides high purity fibres, but it is time-consuming and generates large amounts of wastewater [3].

Bast fibres have been used in many applications, for examples in, insulation, automotive, construction, biomedical, military, marine, sports, electrical, and geotextile industries. The ideal application of bast fibres is determined by the properties of the fibre. Properties of fibre can be classified as physical, mechanical, dielectric, degradation, hygroscopic, and surface properties. Properties of bast fibre-based products are affected by the properties of the bast fibres. For

example, the dielectric properties of bast fibres determine the conductivity of the bio-products, and surface properties of bast fibres affect the strength of the bio-composites.

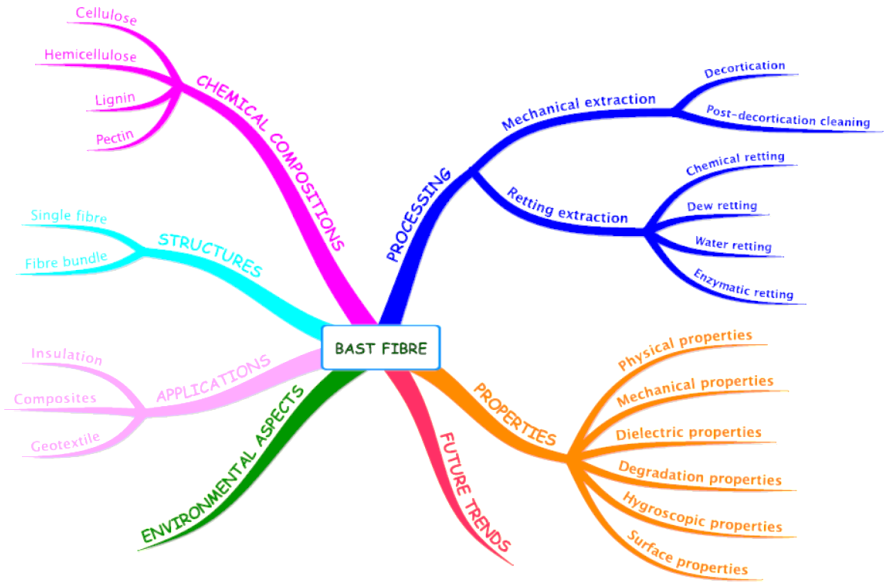

Figure 2.1. All aspects of bast fibres

Compared to glass fibres, plant fibres are less expensive and more environmentally friendly. A comprehensive study was done to compare Life Cycle Inventory of producing glass and plant fibres (flax fibres) [2]. The product system for flax fibres involves several agricultural operations (e.g. tillage, fertilization, seeding, weed control, and harvest), followed by fibre extraction (e.g. retting or decortication) and fibre preparation (e.g. hackling and carding). The inputs to the system include seeds, fertilizer, pesticides, water, diesel, and electricity. The output product is bast fibre that can have different qualities, such as flax yarn or flax fibre mat. Producing yarn is more energy intensive than producing a flax mat. The outputs also include coproducts (e.g. fibre, shive/core, dust, and plant residues), waste and emissions (derived from diesel combustion, electricity generation, chemical fertiliser and pesticide production) into water and air (Figure 2.2). The energy analysis of the life cycle of flax fibre showed that producing glass fibre reinforcement was more

efficient than producing flax yarn, but flax fibre mat and glass fibre silver consumed equal energy per tonne. Glass fibre silver is glass fibre which is coated using electroless silver plating. Regarding environmental issues, flax silver was highly recommended to replace glass fibre as reinforcement in polymer matrix composites [2].

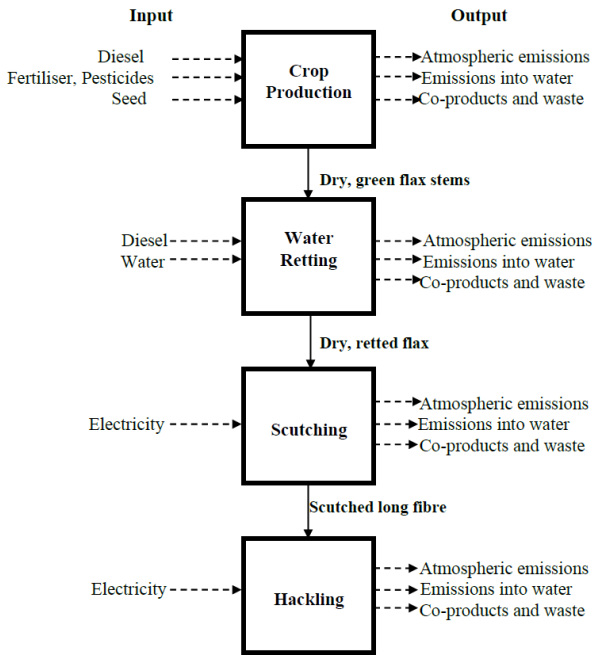

©Figure 2.2. Inputs and outputs of flax production for LCI [2]

Using bast fibre-based products assists to alleviate environmental issues that arise from using fossil fuel-based products. However, there are some restrictions to develop bast fibre-based products in the large industrial scale due to lack of understanding of bast fibre properties, and lack of high-performance fibre extraction methods, which must be addressed before bast fibre can be widely used for bioproduct industries. Readers are referred to Chapter 3 for more discussion about bast fibres. The following sections focus on aspects of fibre related modeling.

2.2. MODELLING OF FIBRE AND FIBRE PROCESSING

Applying some modelling methods to the natural fibre area of research is one of the innovations of this work. These methods include application of a numerical simulation to predict tensile behavior of bast fibres, application of a decision-making model to identify the most influential parameters in the decortication process, and application of a multi-objective optimization algorithm to predict the optimal parameters for retting extraction of bast fibres. These methods are discussed in detail as follows.

2.2.1. Numerical simulations

Traditional experimental methods to study mechanical behaviors of plant fibres are time-consuming and require special equipment. Thus, simulating behaviors of plant fibres using numerical modelling approaches is an advantage. The Discrete Element Method (DEM) and the Finite Element Method (FEM) are two popular numerical modelling approaches. In the DEM, the domain of interest is simulated using an assembly of rigid particles which are in interaction with each other based on the Newton's interaction laws and maybe connected using bonds, if the material to be simulated is cohesive. It helps to examine micro-level dynamics of individual particles using the DEM [4]. The DEM is also suitable for simulations of discontinuous medias, for example, material fracturing under tensile load. In contrast, the FEM is used mainly to examine macro-level dynamics at the element level. Also, in the FEM, the associated governing equations arise from continuum mechanics, based on a predefined mesh or grid. Consequently, it faces some problems to predict discontinuous systems. While, because the DEM works based on the discrete mechanics, it can be applied to both discrete and continuum materials. Further explanation about DEM method is brought below.

Materials in a DEM model are corresponded with discrete rigid elements, which are particles of disks in 2D and spheres in 3D, and are connected with their neighboring particles by contacts [5]. The DEM is a time-step algorithm; an algorithm is repeated in every time-step, and the result of the previous time-step is applied for the current time-step. There are two interactions in each time-step: 1) the overlaps between particles generate contacting forces, and 2) the previous movement information and previous contact forces are applied to update the current movements of particles. In the first interaction, the controlling parameter of the resultant force alteration is the contact force between neighbor particles. Therefore, the Force-Displacement law is applied. In the second interaction, an estimation is done based on the Newton's Second Law to check how the contacting force controls the movement of particles. The computations conducted in the DEM alternate between the Force-Displacement law and Newton's Second Law.

DEM model requires model parameters. The basic model parameters for particles are normal stiffness, shear stiffness, and particle friction coefficient. The parameters for contacts are normal stiffness, shear stiffness, bond radius multiplier, tensile strength, and shear strength. The main challenge of applying DEM is calibrating these parameters. Two major methods to calibrate input parameters are direct measurement and bulk calibration [6]. In the direct measuring method, the properties of particles and contacts are quantified straightly and defined as the inputs. The main struggle of this method is to determine particles and contacts properties. In the bulk calibration strategy, some experimental tests are carried out or literature data are used to estimate preliminary inputs, and the data are then continuously changed to reach passable outcomes.

There are many softwares to develop a DEM model. Some of the popular Open Source software for DEM simulation are Kratos Multiphysics, Woo, LAMMPS, LIGGGHTS, and GranOO. Commercially available softwares are EDEM, Rocky DEM, and PFC. In this research, the PFC^{3D}

(Particle Flow Code in Three Dimensions) was used. It is developed by Itasca Consulting Group, Inc., Minneapolis, MN [5].

The DEM has been applied to simulate mechanical behaviour of different materials, including granular and solid materials. Lately, the DEM has been adopted to simulate the mechanics of fibres and composites, for examples, synthetic fibre reinforcement composites [7], muscle tendon complex [8], and high carbon steel [9]. The DEM has also been used to simulate the tensile behaviour of hemp fibres [10]. However, the total number of particles used to develop a fibre model was limited, which is insufficient to demonstrate the structural failure of a hemp fibre under loads. Therefore, developing a better DEM model for predicting tensile behaviour of plant fibres is essential.

2.2.2. Decision making models

Extracting bast fibre using either mechanical or retting process is controlled by multiple factors. Identifying the factors which have the highest influence on the extraction process is useful to improve the process. Some of the factors may increase the quantity of the fibres but at the same time decrease the quality and vice versa. This is a multi-criterion decision-making problem (MCDM) where an appropriate decision must be made based on a set of optimal values of affecting factors.

There are many methods to solve a MCDM problem. The most popular methods include Technique of Ranking Preferences by Similarity to the Ideal Solution (TOPSIS), Elimination and Choice Expressing Reality (ELECTRE), and Analytic Hierarchy Process (AHP) [11]. The TOPSIS is a useful method for qualitative and quantitative data. This method is comparatively easy and fast and allocates a numerical value to the candidate factors which helps to identify the differences

and similarities among the decision options. However, TOPSIS is unable to rank many decision options especially when there are many evaluation criteria. The ELECTRE has been used to sort the influence factors from the best to the worst. The main limitations of ELECTRE are large amounts of calculation when the number of decision options increases and inability to allocate the numerical value to the candidate factors. The AHP is the most powerful flexible decision-making model which can identify one set of priorities; however, the maximum number of decision options should not be more that 15. The AHP is simple and easy to use. Furthermore, during developing an AHP model, the experts' knowledge is validated using an inconsistency test which assists to remove the inconsistencies of the expert judgment. The AHP has been used in many research to prioritize the available choices which meeting conflicting objectives [12–14]. The AHP model in this study was used to rank the most influential parameters affecting mechanical extraction of bast fibres. Further discussions for devolving an AHP model are brought as follows.

There are three main steps to develop an AHP model including 1) making the hierarchy structure of the problem, 2) performing pairwise comparison (compare the criteria and decision options), and 3) ranking the decision options. All theses steps are discussed in detail as follows.

Making the hierarchy structure of the problem: The hierarchy structure of a problem has three main levels including main objective, criteria, and alternatives.

Pairwise comparison: In this step, pairwise matrices are developed to compare each sub-criterion in the lower level with its main criteria in the higher level. Equation 2.1 shows a $n \times n$ pairwise comparison matrix where n in the size of the matrix.

$$A = \begin{bmatrix} a_{11} & \cdots & a_{1n} \\ \vdots & \ddots & \vdots \\ a_{n1} & \cdots & a_{nn} \end{bmatrix} \qquad \text{Eq. (2.1)}$$

For completing the matrix, the transitivity and reciprocity rules (Eq. 2.2 and Eq. 2.3, respectively) should be followed [15].

$$a_{ij} = a_{ik} \,.\, a_{kj} \qquad \text{Eq. (2.2)}$$

$$a_{ij} = {}^{1}/_{a_{ji}} \qquad \text{Eq. (2.3)}$$

To complete the comparisons judgment matrices, the comparisons are done by either the experts' knowledge, literature review, or the experimental tests. Saaty's 1 to 9 scale is used to do the comparisons [16]. The main diagonal of the matrix where a factor is compared with itself is set to 1. Then, the matrices is completed according to transitivity and reciprocity rules [15]. To validate the experts' knowledge, the logical inconsistencies of the expert judgment is measured using the inconsistency test. An expert's idea is accepted for further processing if the consistency ratio is smaller than or equal to 10% [15]. The following steps are done to estimate the consistency ratio: (1) dividing each element of matrix A by the sum of its column to normalize the whole column of the matrix, (2) taking average of the resultant rows of the matrix to estimate the corresponding weight of each criteria (priority vector), (3) multiplying matrix A by the priority vector, and then dividing the resultant vector by the priority vector to constitute the consistency vector, (4) taking average of the elements of the consistency vector to obtain the largest eigenvalue (λ_{max}), (5) calculating consistency index (I_C) and consistency ratio (R) based on the Eq. (2.4) and Eq. (2.5).

$$I_c = \frac{\lambda_{max} - n}{n-1} \qquad \text{Eq. (2.4)}$$

$$R = \frac{I_c}{I_R} \qquad \text{Eq. (2.5)}$$

where *n* is the matrix size and I_R is random index which is equal to 0, 0, 0.58, 0.90, 1.12, 1.24, 1.32, 1.41, 1.45, 1.49, 1.51, and 1.58 when the size of the pairwise comparison *n* is 1, 2, 3, 4, 5, 6,

7, 8, 9, 10, 11, and 12, respectively.

Ranking the decision options: After checking the inconsistency ratio, the decision can be ranked according to the measured criteria in the AHP model.

2.2.3. Multi-objective optimization

Mechanical extraction of bast fibres is not always applicable for processing fibrous plants into fibres. Preliminary tests showed that mechanical extraction of canola fibres is impossible. Retting extraction is an alternative for this purpose. Chemical retting is one of the popular extractions which can be controlled by chemical concentration, reaction time, and temperature. If executed properly, retting generates the high purity fibre. However, uncontrolled retting produces low quality and quantity fibres. Thus, predicting the optimal retting condition for optimal fibre quality and quantity is necessary. This is a multi-objective problem where the maximum values for fibre quality and quantity are desirable. Optimal retting parameters can be predicted using certain algorithms such as evolutionary or/and gradient-based algorithms.

The commonly used evolutionary algorithms and gradient based algorithm are Genetic Algorithm (GA) and Sequential Quadratic Programming (SQP), respectively. The GA is strong to identify global optima but poor to find the local optima. In contrast, the SQP is strong to identify the local optima for constrained nonlinear optimization problems but it is not guaranteed that the solution is the global optimum. When SQP starts to run with a point from a possible initial solution, it can be guaranteed that the solution is the global optimum. Therefore, a hybrid GA-SQP algorithm can identify an appropriate starting point, assure a faster convergence speed, and a higher convergence accuracy to predict the optimal solution [17]. In the following sections, both GA and SQP algorithms are discussed in detail.

GA algorithm: The GA algorithm works based on natural genetic and natural selection mechanism. The algorithm operates over an initial set of chromosomes named population which may or may not include the optimum values. This step is called “initialize population”. The second step is “selection”. In this step, the value of objective function (e.g. fitting value) for each chromosome is calculated. According to the fitness values, the suitable chromosomes from the population which have the probability of generating desirable values of fitness function are selected and used for subsequent operations. The third step is “crossover”. In this step, two parent chromosomes are combined to develop a new chromosome named offspring. It is anticipated that the generated offspring inherit good gens since parent selection is based on the fitting value. “Mutation” is the fourth step where very small random changes are applied into the existing chromosomes. The characteristics of the new chromosome are not significantly different with the original ones. The mutation is only applied to maintain genetic diversity. If one of the chromosomes generates the target fitness value, the algorithm stops; otherwise, the second to forth step is repeated with a new population until the condition is met [18].

SQP algorithm: The SQP algorithm is a robust algorithm for nonlinear continuous optimization which works based on the gradient information [17]. Choosing a reasonable start point to run the algorithm increases the possibility of finding an acceptable solution and avoids the local optima. The starting point is taken from the output of GA algorithm. Sequential Quadratic Programming is an iterative method. In each iteration, a Quadratic Programming (QP) sub-problem is generated by estimating a Hessian matrix of the Lagrangian function. The solution of the sub-problem is used to develop a search direction for a line search procedure. For each iteration, the Hessian matrix is updated according to quasi-Newton updating method.

2.3. REFERENCES

[1] Sadek M. Modelling biofibre (hemp) processing using the Discrete Element Method (DEM) [dissertation]. Winnipeg (MB): University of Manitoba; 2013. 2013.

[2] Roos S, Szpieg M. Life Cycle Assessment of flax fibres. 2011. https://doi.org/10.1002/ieam.1756.

[3] Sadrmanesh V, Chen Y. Bast fibres: structure, processing, properties, and applications. Int Mater Rev 2018;0:1–26. https://doi.org/10.1080/09506608.2018.1501171.

[4] Jebahi M, Andre D, Terreros I, Iordanoff I. Discrete element model and simulation of continuous materials behavior set. London, England: Wiley; 2015.

[5] Itasca Consulting Group. PFC- Particle Flow Code, Version 5.0, Minneapolis, MN 2014.

[6] Coetzee CJ. Review: Calibration of the discrete element method. Powder Technol 2017;310:104–42. https://doi.org/10.1016/j.powtec.2017.01.015.

[7] Khattak MJ, Khattab A. Modelling Tensile Response of Fibre-Reinforced Polymer Composites Using Discrete Element Method. Polym Compos 2013;34:877–86. https://doi.org/10.1002/pc.

[8] Roux A. JLGL-LLSII. Tensile response of muscle-tendon complex using discrete element modelling. 3rd SIMBIO-M Conf Marseille , Fr June 19-20 2014:1–8.

[9] Chen G, Schott DL, Lodewijks G. Tensile test simulation of high-carbon steel by discrete element method. Eng Comput 2016;33:1224–45. https://doi.org/10.1108/EC-03-2015-0064.

[10] Sadek MA, Guzman L, Chen Y, Laguë C, Landry H. Simulation of tensile tests of hemp

fibre using discrete element method. Agric Eng Int CIGR J 2014;16:126–35.

[11] AL-Oqla FM, Salit MS. Materials selection for natural fibre composites. 2017.

[12] Al-Oqla FM, Sapuan SM, Ishak MR, Nuraini AA. A Model for evaluating and determining the most appropriate polymer matrix type for natural fibre composites. Int J Polym Anal Charact 2015;20:191–205. https://doi.org/10.1080/1023666X.2015.990184.

[13] AL-Oqla FM, Sapuan S, Ishak M. Predicting the potential of agro waste fibres for sustainable automotive industry using a decision making model. Comput Electron Agric 2015;113:116–27. https://doi.org/10.1016/j.compag.2015.01.011.

[14] Kaur B, Bhatia R. Prioritizing parameters for software project selection using Analytical Hierarchical Process. vol. 118. 2015.

[15] Saaty TL. The Analytic Hierarchy Process. New York: 1980.

[16] Saaty TL. Decision making with the analytic hierarchy process. Int J Serv Sci 2008;1:83–98.

[17] Yengui F, Labrak L, Frantz F, Daviot R, Abouchi N, O'Connor I. A Hybrid GA-SQP Algorithm for Analog Circuits Sizing. Circuits Syst 2012;03:146–52. https://doi.org/10.4236/cs.2012.32019.

[18] Deb K. Multi-objective optimization using evolutionary algorithms. vol. 16. John Wiley & Sons; 2001. https://doi.org/10.1001/jama.1943.02840160014004.

Chapter 3: Review - Bast Fibres: Structure, Processing, Properties, and Applications

3.1. ABSTRACT

There is an increasing demand for natural fibres worldwide due to their renewable and biodegradable nature. This paper reviews many aspects of natural fibres, focussing on the bast fibres of plants including hemp, flax, kenaf, jute, and ramie. Important characteristics of these plant fibres include physical, mechanical, dielectric, degradation, hygroscopic, and surface properties. These properties are highly variable, depending on both the chemical composition of the fibre and the environmental conditions. Retting and mechanical are the two main fibre extraction methods. When executed properly, retting produces the highest purity fibre; however, it is time-consuming and generates large amounts of wastewater. In contrast, mechanical extraction is faster and more environmentally friendly but results in low-purity fibre. Despite the drawbacks of bast fibres (e.g. low thermal stability, low hygroscopicity, low surface energy), they have been successfully used in insulation, composite, and geotextiles and many further applications are currently being explored.

3.2. INTRODUCTION

Fibres can be classified into two broad groups: human-made and natural. The demand for natural fibres has increased considerably in recent decades, as they are perceived to be environmentally friendly, low cost when sourced locally, and low density with adequate tensile strength (300-1200 MPa) and stiffness (30-70 GPa) [1,2]. Natural fibres have low toxic fume emission during the recycling process. High density, high cost in production and environmental burdens, and

difficulties to recycle human-made fibres (e.g. synthetic fibres) are other rational motives to switch focus to natural fibres [3].

Natural fibres are derived from three sources: animals, minerals, and plants (Figure 3.1). Animal fibres include animal hair and silk fibres. Mineral fibres are mainly asbestos and basalt but with major health issues. Plant fibres can be divided into wood and non-wood fibres. Cellulose is the main component in all plant fibres, whereas the primary elements in animal and mineral fibres are protein and natural rock materials, respectively. In terms of biodegradability, plant fibres are easier to recycle than mineral fibres [4]. In general, plant fibres have greater strength and stiffness than most animal fibres, except silk fibres. Furthermore, animal fibres are relatively pricey and less easily accessible [5]. Therefore, the most suitable and economic fibres for the production of bioproducts are plant-based fibres [6]. In the last 25 years, the number of publications in the area of plant fibres and plant fibre composites has increased by eighteen-fold (Figure 3.2). This reflects the increasing demand for plant fibres.

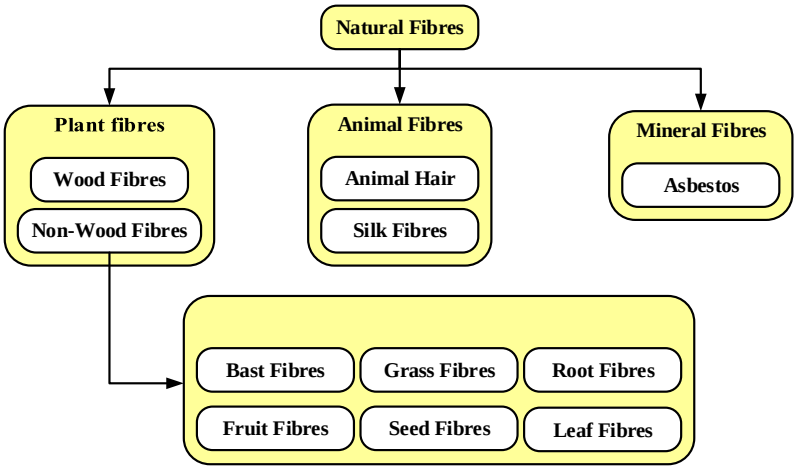

Figure 3.1. General classification of natural fibres

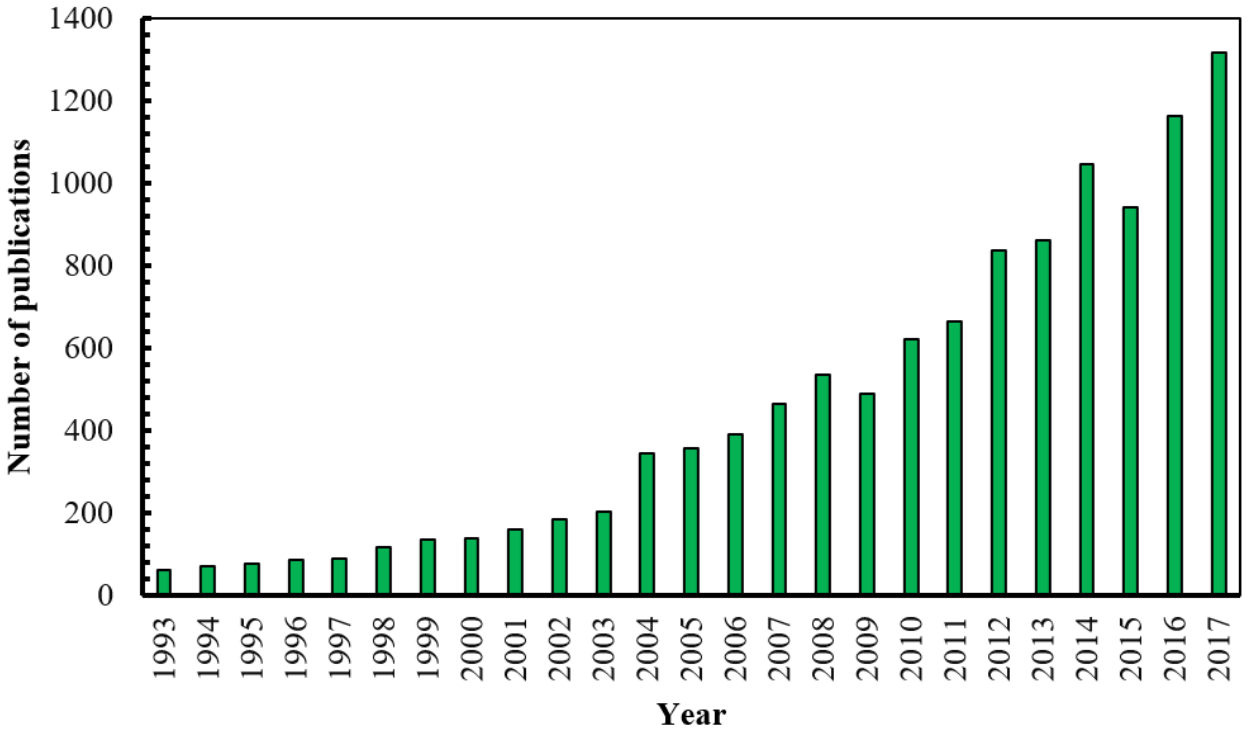

©Figure 3.2. The number of scientific publications in the area of plant fibres and plant fibre-reinforced composites. Adapted from Fortea-Verdejo et al. [7] and further updated using a title-abstract-keyword search of 'natural fib* AND composite*' on Scopus.

There are approximately 2000 species of plants used as a source of natural fibres, but only a few of these are commercially prominent, constituting around 90% of the natural fibres in the world [7]. Non-wood fibres, a branch of plant fibres called lignocellulosic fibres, are subdivided into bast, seed, straw, leaf, and grass fibres. The focus of this review is bast fibres and their extraction, characteristics, properties, and applications. Numerous reports have been written on bast fibres, but none thoroughly study the techniques used for extraction, particularly mechanical extraction. Furthermore, the applications of bast fibres are not documented comprehensively in the literature. This paper discusses many aspects of bast fibres, including their physical, mechanical, dielectric, degradation, hygroscopic, and surface characteristics, as well as their current and future applications.

3.2.1. Bast fibres

Bast fibres have been applied in many industries including geotextiles, insulation, and composite. For example, they have been used in temporary roads over soft land, agricultural and automotive exterior panels, acoustic and thermal insulation, furniture, recreational sports products, and marine products [8,9]. Biocomposites made from bast fibres are reliable, inexpensive, lightweight, non-toxic, and structurally sound [10].

The most important bast fibre plants include hemp, flax, kenaf, jute, and ramie. Hemp and flax are cultivated in almost all countries and harvested for both grain/seed and fibre. Hemp (Cannabis sativa) is a good source of fibre and biomass. Hemp plants range from 1.5 to 2.5 m in height and with an average stem diameter between 7 and 16 mm [11]. Hemp originated from Central Asia and has since been cultivated in all continents, regions, and countries. Canada reintroduced hemp as an industrial crop in 1998, after being banned for some 60 years. Hemp fibres have long been used for making clothes, ropes, and insulating materials. Recently, the use of hemp fibre as a reinforcement in composite materials has been increasing [12].

Flax (Linum usitatissimum L.) is one of the species in the family Linaceae, which is comprised of 13 genera and 300 species [13]. The height and diameter of the flax stem are approximately 1 to 1.3 m and 4 to 5 mm respectively [14]. The plant originates from the Mediterranean and Southwest Asian regions [15] and is now one of the more important crops grown in Canada. Flax fibre has previously been used as a textile material but lately, it has found use in other applications too, such as making cigarette papers in North America.

Kenaf (Hibiscus cannabinus L.), which can be grown under diverse climate conditions, is a member of the Malvaceae family. Kenaf plants can grow to a height of 2.5 to 4.0 m under optimal

temperature (22 - 30°C) and soil pH (6.0 - 6.8) conditions. The diameters of the kenaf stem range from 10 to 20 mm [16–19].

Jute is a species of the Tiliaceae family that has two commercial varieties: C. capsularis L. and C. olitorius L. It grows to a height of approximately 2.5 to 3.5 m with a diameter of approximately 20 mm. Bangladesh, India, China, and Thailand are the leading producers of raw jute and its associated fibre. Among the natural fibres, jute is considered to be the cheapest and strongest [20–22].

Ramie (Boehmeria nivea) is a species of the Urticaceae family, known as a China grass [23]. In 2014, over 94% of the world's ramie was harvested in China. The plant is between 1.0 and 2.5 m tall, and its leaves are 7 - 15 cm long and 6 - 12 cm broad [23]. The diameter of ramie stalks is between 4.5 and 10 mm [24]. Ramie is primarily cultivated for its fibres. It has been reported that the optimum conditions for ramie production are in warm and humid regions with an average rainfall of 1 m per year [23].

3.2.2. Bast fibre structure

Bast fibres are taken from the phloem, a substance within the stem of fibrous plants. For example, a flax plant stem is composed of three main parts: bark or skin, fibre bundles, and a combination of xylem, shives, and the woody core (Figure 3.3.a). The primary role of the bark/skin is to protect the plant from moisture evaporation and unanticipated temperature changes. Bark/skin also helps the stem resist moderate mechanical damage. The fibres are located in the phloem where they appear as bundles (a bundle consists of several individual single fibres) under the skin. Fibres are responsible for supporting the conductive cells of the phloem and also provide stiffness and strength to the stem [25]. The role of xylem, shives, and woody core is to transfer water and

nutritive substances from the centre of the stem to the fibres [26].

Single fibres in a bundle are connected by a substance called middle lamella (Figure 3.3.b), which is primarily composed of pectin and acts as glue [3]. Single fibres have two major components, a primary wall and a secondary wall; these walls surround a small channel, called the lumen, which is filled with proteins and pectin (Figure 3.3.c) [3]. The primary wall is made of an inflexible framework of cellulose microfibrils within a network of hemicellulose, pectin compounds, and glycoproteins [27]. The thickness of the primary wall in a single fibre is smaller than the secondary wall. The secondary wall is a three-layer structure (S1-S3) in which the middle layer (S2) forms the bulk of the fibre. All three layers consist of cellulose, hemicellulose, and lignin. Approximately 70 - 80% of the mass of a single fibre comes from the S2 layer [28,29]. Therefore, the attributes of a single fibre are predominantly controlled by the characteristics of this layer. Baley [31] stated that the S2 layer determines the mechanical strength of the fibres.

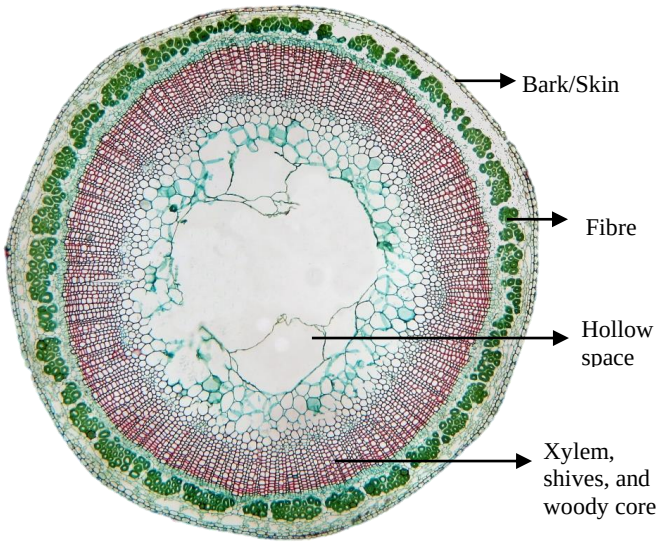

a

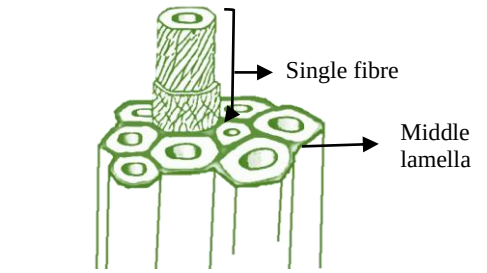

b

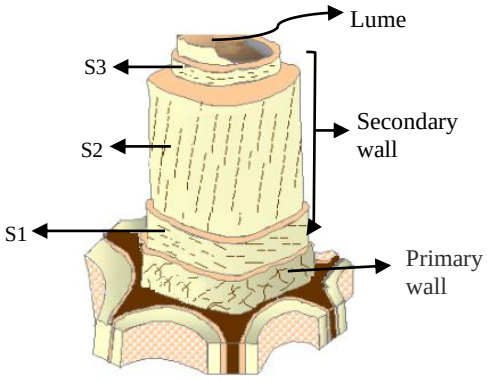

c

© Figure 3.3.a. The cross-section of common flax (Linum usitatissimum) stem (Source: [32] with permission from Shutterstock); b. A fibre bundle (Source: [33] with permission from National Programme on Technology Enhanced Learning (NPTEL)); c. Elements of a single fibre (Source: [34] with permission from Martin Hubbe).

Single fibres have a polygonal cross-section that varies along the fibre length. Many researchers use the average width of a single fibre as the diameter for calculating the apparent cross section area (CSA) assuming a circular CSA for the fibre [31]. However, this gives inaccurate results when computing the fibre's mechanical properties or developing a model to predict mechanical properties of the composites fabricated from single fibres. To address this issue, the fibre area correction factor (FACF) was introduced, which is calculated by dividing the apparent CSA by the true CSA. The predictions of tensile modulus and the strength of jute-epoxy composite was improved upon inclusion of the FACF [31].

3.2.3. Bast fibre chemical compositions

The chemical composition of the bast fibres differs between each plant and within a plant (Figure 3.4). It also varies with age, fibre source, and conditions during fibre extraction [32]. However, the major component of all fibres is cellulose, followed by hemicellulose, and then lignin, pectin, and small amounts of wax and fat mainly in the S2 layer (Figure 3.3.c) [33]. Hemp has the highest cellulose content (70 - 92%), kenaf has the lowest (44 - 65%), and flax, ramie, and jute are in between. The hemicellulose content of these fibres also varies, with upper values around 24% in all fibres except for the ramie fibre (up to 15% hemicellulose). The percentage of lignin in hemp and flax is low (2 - 6%) and kenaf has the highest proportion of lignin (15 - 21.5%). Wax and pectin, present together at approximately 1 to 4%, are the smallest components of natural fibres chemically [27,34–36].

Cellulose is a long polymer of glucose molecules, which, in turn, is connected into microfibrils (Figure 3.4). The number of chains within microfibrils varies from 30 to 100. Cellulose is the principal element that provides the strength, stiffness, and stability to the fibres. Higher fibre cellulose content increases the economic benefit of fibre extraction. Moreover, high-cellulose fibres have extensive applications [37].

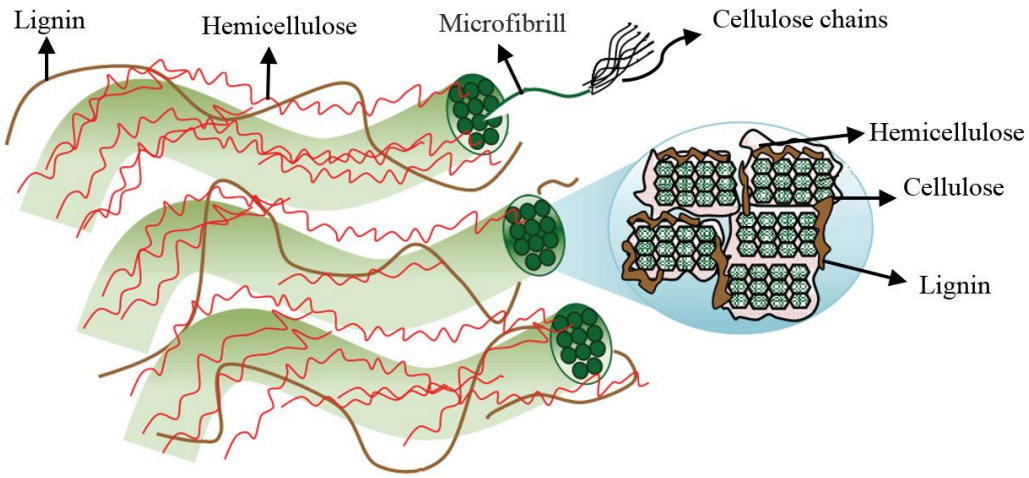

©Figure 3.4. Main chemical compositions of natural fibres and microfibril cross section. Source: [45] with unrestricted permission.

Hemicellulose is a class of complex polysaccharides composed of xyloglucans, xylans, mannans, glucomannans, and beta-glucans. Hemicellulose is highly hydrophilic; however, there is no universal chemical structure that defines them. Hemicellulose, along with lignin, constitutes the matrix for the cellulose microfibrils. Compared to cellulose, hemicellulose has low molecular weights [27,38]. It is susceptible to biodegradation, micro-absorption, and thermal degradation [39]. From a mechanical standpoint, hemicellulose does not provide stiffness or strength to fibres [40].

Lignin is a high molecular weight, three-dimensional polymer of amorphous structure. It provides increasing rigidity to plants during ageing due to its high percentage of carbon and a moderate amount of hydrogen [38]. Lignin can also be used as raw materials in the production of adhesives [38]. The flexibility of fibrous plants is conferred by pectin: plants with high pectin content are more flexible. Since pectin is degradable, it reduces the overall fibre strength, which is not desirable. Hence, fibres with lower pectin content are of better quality. Waxes are esters of

long-chain fatty alcohols with long-chain fatty acids. Waxes create a barrier that protects plants from drying and prevents microbial invasion [38].

3.3. BAST FIBRE PROCESSING

The first step in fibre preparation is to extract the fibres from the straws. In this process, the outer layer of fibre bundles is separated from the other plant parts, such as xylem and hurd/shives (referred to as cores going forward, for simplicity). Therefore, extraction can be defined as the breaking of the bonds between fibre bundles and cores. During extraction processes, fibre bundles are separated into pieces that can be as long as the plant stem height [41]. Each fibre bundle contains one to ten single fibres (Figure 3.2.b). A schematic diagram of this plant fibre processing is shown in Figure 3.5. There are three main techniques used to extract bast fibres from plants: retting, mechanical extraction, or a combination of the two. Retting is a biological process, which detaches fibre bundles from the surrounding tissue with minimal destruction of the fibre. A strong relationship exists between the quality of extracted fibres and the retting conditions (e.g. duration and temperature). Over-retting causes the bonds between the cells of a single fibre to break, thereby making the fibres weaker [42]. Under-retting produces fibre bundles that are still attached to the core, which adversely affects fibre purity. Mechanical extraction involves using mechanical forces to break the bonds between the fibre and its core. This technique is much more efficient than retting in terms of processing tonnes per hour. However, it is difficult to control the mechanical forces applied to the plant stalk and the bond breakage does not respond well to mechanical forces. Also, this technique produces highly variable fibre lengths, which is another drawback of mechanical extraction [42]. Therefore, mechanical extraction alone is not highly effective. Pre-retting plant stalks can improve fibre separation from mechanical extraction. Thus, combinations of retting and

mechanical extraction have been used to improve the efficacy and efficiency of fibre extraction. This section provides comprehensive information on the aforementioned extraction techniques.

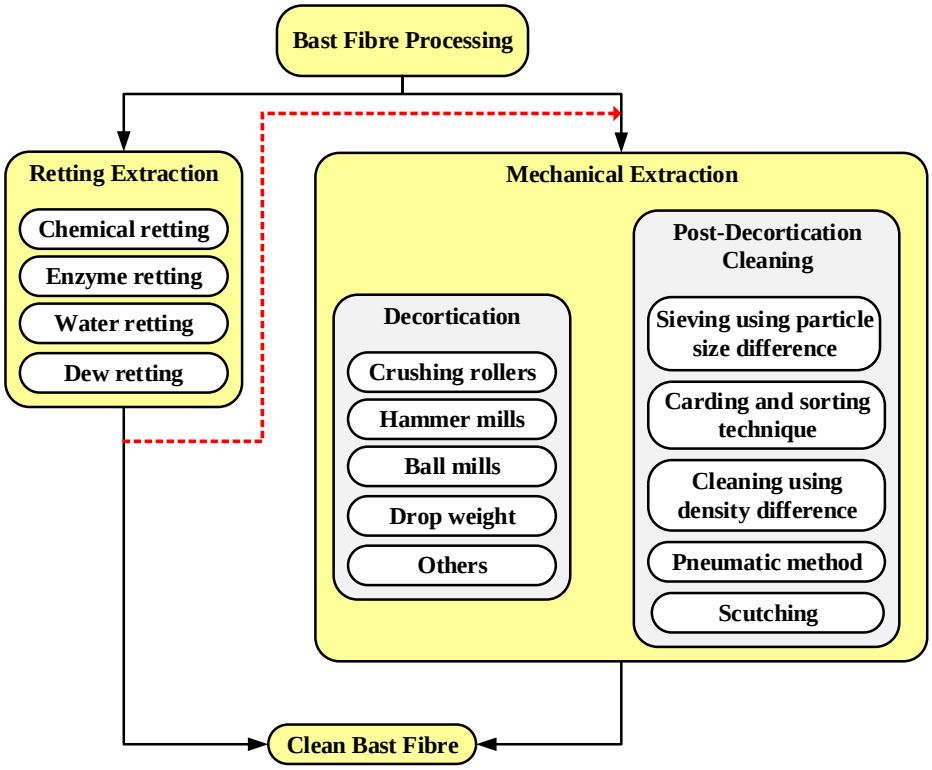

Figure 3.5. A schematic diagram of bast fibre processing

3.3.1. Retting extraction

The most common retting methods for bast fibre extraction include chemical, dew, water, and enzymatic retting.

3.3.1.1. Chemical retting

Chemical retting degrades the lignin, pectin, and hemicellulose within the plant stalk. If over-retting occurs, the cellulose will also degrade. Three important factors affect the efficacy and quality of fibre extraction in chemical retting: chemical concentration, temperature, and reaction

time [43]. Many substances have been used for chemical retting, the most common being alkalis (e.g. sodium hydroxide), mild acids, enzymes, salts (e.g. sodium benzoate), as well as a combination of acids (e.g. sulfuric acid and oxalic) with a detergent [43,44]. Applying high temperature to alkali treatments efficiently degrades the bonding material in the plant stalk, with little effect on the cellulose [45]. The major drawback to chemical retting is the disposal of used chemicals and wastewater.

3.3.1.2. Dew retting

In dew retting, plants are left in the field after harvest to absorb dew. These conditions allow for bacterial and microorganism growth to occur, thereby producing degradatory enzymes within the plants. As a result, cortex fibres are incrementally separated into fibre bundles. This natural technique is inexpensive and does not require excessive amounts of water. The drawback of dew retting is the lack of consistency due to variations in weather conditions. Plants may be insufficiently retted or over-retted, which reduces the strength and colour of the fibres. Hence, to ensure high fibre quality, regular monitoring must be an indispensable part of dew retting [46].

3.3.1.3. Water retting

Unlike dew retting, which occurs naturally, water retting takes place in a controlled environment. Water temperature and retting duration can be regulated to prevent adverse effects on fibre quality. Compared with fibres from dew retting, fibres obtained by this approach are uniform and high quality [47]. However, water retting is costly and generates a considerable amount of wastewater that must be dealt appropriately with for environmental reasons [48]. Also, water retting presents a risk of rot, fungus and mould production [49].

3.3.1.4. Enzymatic retting

Enzymatic retting addresses the issues of weather effects in dew retting and wastewater generation in water retting. One study evaluated the impact of various preparations of alkaline pectate lyase with a reported activity of 3000 alkaline pectinase standard units (APSU)/g and ethylenediaminetetraacetic acid (EDTA) on the retting of flax fibres [50]. This study concluded that the highest-quality fibres were obtained under the following conditions: Pectate lyase at levels of about 2% of the commercial product for 1 hour at 55°C and subsequently 18 mM EDTA for 23–24 hours at 55°C. Song and Obendorf [56] reported that enzymatic retting was the most effective technique for reducing the proportion of lignin in kenaf bast fibres. Yu and Yu [57] applied fungi treatment to kenaf stalks and found that approximately 91% of the pectin was eradicated from the kenaf fibres. Enzymatic retting using fungi on flax stems was explored by Evans et al. [58]. Their findings revealed that the most suitable enzyme was *Aspergillus Niger PGase*, which produced a fibre yield of 62% of dry stalk weight. The investigators also reported that no noticeable differences in fibre strength were observed between the mentioned treatment and treatments with other fungal sources.

In summary, different retting methods carry different advantages and disadvantages. Chemical retting requires energy and generates harmful waste [54]. Meanwhile, enzyme retting produces higher quality fibres with lower pollution potential. Chemical and enzyme retting are more controllable and sustainable than dew and water retting [55]. When compared to the chemical and water retting of kenaf stalks, fibres obtained from water retting had more tensile strength and brighter colour [56].

3.3.2. Mechanical extraction

Mechanical extraction of plant fibres is typically completed in two stages. The first stage is decortication. Decortication detaches the outer fibre bundle from the inner core of the plant stalk. The output from decortication is a mixture of fibre bundles and cores, and the cores must be separated from the fibres. This is achieved in the second stage referred to as post-decortication cleaning.

3.3.2.1. Decortication

Plant stalks are fed into a decorticator where they are subjected to compressive, shear, and impact forces. The stalks are broken into pieces, resulting in bast fibres that are detached or partially detached from the core [57]. The fibre bundles are the primary product of decortication, and the core is the by-product. Different types of decorticators have been used for fibre processing, including hammer mills, crushing rollers, ball mills, and more.

Hammer mills: A hammer mill consists of a high-speed rotor affixed with pivoted hammers inside of a chamber. Plant stalks are fed into the chamber where they are subjected to impact forces from the rotating hammers that detach the fibre from the core. In most cases, hammer mills fail to completely detach the fibre from the core, especially for unretted stalks. Thus, the output from hammer mills is usually of low fibre purity, which has limited applications [58,59]. Another drawback of hammer mill decortication is that the output fibres are short with variable lengths, for example, decorticated flax fibre varies in length from 17 to 101 mm [60]. The high energy requirement is another downside of the hammer mill, and energy demand increases with increased feeding mass [61].

The major advantage of this method over others is its high extraction productivity [63]. Baker [66] evaluated a hammer mill for decortication of retted, green, and unretted hemp to determine the effects of feeding mass, screen, and pre-cutting scenarios on power and energy requirements, fibre yield, and productivity of the decorticator. The results revealed that the combination of 19.3 mm screen pore size, 75 g feeding mass, and pre-cut feedstock for retted hemp produced the highest fibre yield.

Crushing rollers: A crushing roller consists of two or more pairs of rollers, which can vary in diameter from 0.2 to 0.3 m and the length to diameter ratio also varies [62]. Roller pairs are positioned parallel to one another and rotate in opposing directions. Plant stalks are fed between the rollers, ideally in a uniform and constant fashion, where they are subjected to the force from the rollers. Roller decorticators are typically designed to be adjustable [63]. The roller's surface can be flat, fluted, or pinned to permit the input materials to be compressed, crimped, or combed. A tearing or grinding force is applied when the rolls are grooved [62]. The roll gap indicates the distance between a pair of rollers. Roll gap and speed play a crucial role in determining the primary forces applied to the stalk. If rollers of equal diameter rotate at the same rate, compression is the major force applied to the stalk. If they rotate at different speeds, the stalk is subject to a combination of shearing and compression forces, which may be more effective for fibre decortication. Roll speed differential and roll gap are the two prominent factors affecting decorticator performance and Fang et al. [69] evaluated the impact of these parameters on the performance of a crushing roller decorticator. They observed that at lower differential roller speeds, less energy was required to crush the feedstock into coarse particle sizes. In contrast, at higher differential roll speeds, finer particle sizes were obtained, and more energy was required due to the greater shearing forces applied to the feedstock. They found that the roll gap also

influenced the particle size, particle size distribution, roller mill capacity, and energy required. Compared to hammer mills, crushing rollers require less energy because of their lower rotational speeds. Crushing rollers also produce longer fibres that have a higher market value. However, crushing rollers only work well for retted stalk. For unretted stalk, the decorticated fibres have low purity. Leduc et al. [68] manufactured a crushing roller decorticator, with a capacity of around 4,500 kg per hour and a fibre purity ranging from 55 to 60%.

Fibres wrapping around rotating machine parts (e.g. bearings, rollers, shafts, etc.) is a common problem when using hammer mills and crushing rollers for fibre decortication. Fibre wrapping can lead to overheating of rotating machine parts, which can cause damage to the decorticators and potentially start a fire. To solve this problem, Baker et al. [70] proposed using a ball milling method and Khan et al. [71] proposed using the drop weight method as alternatives for fibre decortication. When decorticating using these methods, fibre stalks do not contact rotating machine parts, thereby eliminating the possibility of fibre wrapping.

Ball mills: Ball mills utilize grinding balls to grind material in a grinding container. The grinding container rotates, causing the grinding balls to tumble. The tumbling balls create shear forces on the material. Grinding speed, grinding duration, and the number of grinding balls are variables that affect ball mill output. For decortication, plant stalks are fed into the container to be impacted and sheared by the tumbling balls. The intention is to grind the cores while the fibres are kept intact. A lab-scale planetary ball mill was employed for decorticating retted hemp stalks [65]. The effects of three grinding durations (2, 4, and 6 minutes) and seven grinding speeds (ranging from 100 to 400 rpm with 50 rpm intervals) on fibre yield and fibre-core detaching efficiency were studied. The results confirmed that grinding duration and rotational speed significantly impact the output. At the slowest and fastest grinding speeds, the detaching efficiencies were 52.6% and 99.7%

respectively. The best ball mill performance, in terms of both fibre yield and detaching efficiency, was observed at 200 and 250 rpm grinding speeds regardless of grinding duration. Although ball mills do not have fibre-wrapping problems, fibre losses are still high, as a considerable portion of the stalk becomes fine particles after grinding. Furthermore, ball mill efficacy, in terms of tonnes per hour, is much lower than hammer mills and crushing rollers.

Drop weight method: Drop weight is an alternative method for mechanical extraction proposed by Khan et al. [71] to solve the problems of fibre wrapping around rotating machine parts and excessive fraction of fines in the final product from ball milling. The working principle of the drop weight method is to apply impact forces to plant stalks through dropping weights on the stalk, and the fibre is thus detached from the core. The intensity of impact can be quantified by the input energy to the stalk, which is determined by the mass of the weight and the drop height. The results from Khan et al. [71] showed that higher energy inputs detached more fibre from the core and produced a higher fibre yield. The fibre-detaching was not effective for unretted hemp. It has been suggested to use the drop weight method only for retted stalk. The best fibre yield produced using this method was 24%. It must be noted that these previous results were obtained from lab-scale trials. More research is therefore required before using this method for industrial applications. It is expected that this method will have low capacity in terms of tonnes of stalk per hour.

Other extraction methods: Gratton and Chen [63] modified a forage harvester for in-field hemp decortication. The original cutter-head of the harvester had 12 knives; this was changed to three knives and nine scutching bars. The purpose of reducing the number of knives was to increase the cut length of hemp stalks, and therefore, fibre length. The addition of scutching bars provides impact forces on the hemp stalks. Greater fibre purity was obtained, and more cores were removed using the modified cutter-head configuration compared to the original cutter-head. Moreover, a

lower feeding rate and longer retting time resulted in higher fibre purity. The advantage of in-field decortication is its low investment cost compared with centralized processing facilities. In-field decortication also avoids the costs associated with baling swaths and transportation of fibre stalks to central facilities.

In summary, choosing an appropriate decorticator depends on the fibre quality and processing capacity requirements. If high processing capacity is essential, hammer mills are preferred [67]. Cutter-heads are more appropriate for obtaining short, uniform-length fibres due to the built-in cutting function of the cutter heads [68]. Crushing rollers produce long fibres and are more suitable for retted plant stalk; however, they have lower capacities than hammer mills. Hammer mills, crushing rollers, and cutter heads all have fibre wrapping issues due to the direct contact between the plant material and the rotating machine parts [42]. Ball mills avoid this fibre wrapping issue but have a low capacity. All the mechanical extraction methods detailed above are more effective using retted stalks, in terms of fibre purity. Using hammer mills, Thakur et al. [65] reported that flax fibres had a purity of 15 to 51%, and Parvin et al. [74] found the purity of hemp fibre to be 55%. It is difficult, if not impossible, to obtain high purity fibres through mechanical extraction. Post-decortication cleaning is often necessary to improve the fibre purity.

3.3.2.2. Post-decortication cleaning

Decorticator products consist of several fractions: fibres, loose-cores, fibre-bound-to-core, and fines [69]. Fibres are completely free of cores. Loose-cores are completely free of fibres. Fibre-bound-to-core is the fibre still attached to the core pieces after decortication. Fines are small particles in the mixture. These fractions are illustrated in Figure 3.6. The purpose of post-decortication cleaning is to separate the pure fibre fraction from the mixture, further detach the

fibre from the fibre-bound-to-core fraction and remove the fines. Post-decortication cleaning considerably improves the fibre purity and, therefore, increases the market value [60].

Figure 3.6. (a) pure fibre, (b) loose-core, (c) fibre-bound-to-core, and (d) fines.

Scutching: Scutching is a common method for cleaning decorticated materials that involves separating fibres as seen on industrial processing lines. A scutcher is fabricated from a large rotating wheel that transports material over grid bars enclosed within a metal housing. The fed material is rubbed over the grid bars to separate fibre bundles and remove cores. This method works well for cleaning fibre-bound-to-cores, however, it does not work well for unretted feedstock [70].

Sieving by particle size difference: Sieving or screening techniques have been commonly used to clean decorticated material based on size. Münder et al. [76] utilized a multiple ultra-cleaner to segregate fibres from the decorticated hemp. They describe how the cleaner intensely vibrates the

material, which successfully separates long fibres from short fibres and cores. Separation efficiency using a vibratory screen varied by working parameter, such as vibration frequency and amplitude. Using various parameter settings, Sadek [77] observed separation efficiencies ranging from 23 to 86% with a vibratory shaker for cleaning hemp fibres. Pecenka and Furll [78] developed a unique screening tool comprised of a fixed screen with an oscillating comb attached on top of the screen to serve as a transporting device. They explained that this mechanism loosened the decorticated mixture and assisted in untangling fibres. Their findings showed that the fibre purity was significantly enhanced. Nonetheless, most screening machines are ineffective when used for fibre cleaning since fibres and cores are tangled together [61]. The best use of the screening method is to sieve the fine (i.e. particles smaller than 20 mm) out of the fibre mixture.

Carding and sorting technique: Drum carding machines used for cleaning decorticated stalks include a licker-in cylinder, a larger cylinder known as the main cylinder, and a feeding tray. The material is fed by the feeding tray and moved through the cylinders where the carding action happens. During this process, non-fibre particles are eliminated, and fibre clusters are opened and cleaned. Cylinder rotation speed, feeding mass, and carding duration all significantly impact fibre cleanness. The efficacy of carding on cotton fibre openness and cleanness was enhanced by increasing the licker-in cylinder speed [74]. Göktepe et al. [80] reported that at increased licker-in cylinder speeds, the amount of extracted short fibre increased, fibre strength dropped, and more waste was produced. Parvin [81] investigated the effects of carding duration and feeding mass on fibre purity using a small manual carder. Their results showed no significant differences in fibre purity across all carding durations and feeding mass levels. However, carding itself improved fibre purity by 15%.

Preliminary trials by Thakur et al. [65] determined that carding was more effective for long fibres. For example, flax fibre decorticated by a hammer mill would be too short to be cleaned by carding. The large rotating cylinder does not easily catch short fibres and these fibres are then lost along with the cores. To address this issue, sorters have been used prior to fibre cleaning. Sorting works on a similar principle as carding i.e. the material is processed through a series of rollers. However, a sorter machine has smaller rollers and functions mainly to separate long and short fibres. Cores are also removed during the sorting process and, thus, the output fibre is cleaner. Using a sorter originally designed for animal fibres, the purity of decorticated flax fibre was improved from 51% to 80% and from 15% to 60% [60]. As with decortication, fibre wrapping is also an issue in carding and sorting since they utilize rotating rollers.

Cleaning by density difference: The decorticated material can also be cleaned based on density differences. The flotation method uses water to separate material based on density. Parvin et al. [74] assessed the flotation approach for post-decortication cleaning of a hemp mixture. They observed that the fibres sank in the water, while the cores floated, and found that better fibre-core separation could be obtained by agitating the water. This study demonstrated that flotation of decorticated hemp materials in agitated water produced a fibre purity of up to 90% from an initial fibre purity of 55%. Density-based cleaning has two main drawbacks: wastewater generation and the additional energy consumption required to dry the separated material.

Pneumatic method: The pneumatic method has previously been used for post-decortication fibre cleaning. This approach uses airflow to separate different particles based on their density and surface area. Since there are no rotating machine parts, fibre wrapping is not an issue in the pneumatic method. Its feasibility depends on differences in the terminal velocities of the fibre and its core. Using a wind tunnel, Parvin et al. [74] found that the terminal velocities of hemp fibres

(0.56 - 1.36 m/s) were lower than for those of hemp core particles (1.28 - 3.52 m/s). Using the same wind tunnel, Thakur et al. [65] reported that the terminal velocities of flax fibres (0.41 - 1.14 m/s) were lower than those of flax core particles (1.22 - 4.1 m/s). The large differences in the terminal velocities of the fibres and cores suggested that they could potentially be separated by the pneumatic method. Nevertheless, the researchers pointed out that in practice, the pneumatic method did not work well as the fibres and cores became entangled as they travelled together in the airstream. They stated that the simultaneous use of an airstream and a fibre opener (to separate the tangled clusters) improves the efficacy of the pneumatic cleaning.

In summary, post-decortication cleaning is necessary to improve fibre purity for certain applications such as textiles and biocomposites. Traditionally, the sieving method has been used for biomaterial separation based on particle size. However, this method does not clean the fibres, as the cores are held within tangled fibre clusters, which prevents them from falling through the screens. Scutching can further detach the fibre from the core but it may fail to remove all of the impurities required to obtain high-purity fibres. Technically, fibre and core particles can be separated using the pneumatic method based on differences in their terminal velocities. However, it is technically difficult to use airflow to separate fibre and core particles as they are often tangled together. The addition of openers (machines to separate the tangled clusters) together with sieving and aerodynamic techniques may prove ideal for fibre cleaning. However, the opening and sieving actions would need to be synchronized, which might be challenging. The water flotation method is also technically sound based on the literature. However, management of the generated wastewater prevents this method from being economical and environmentally friendly. Carding is more suitable for long or fine fibres, such as cotton and animal fibres but not useful for short fibres. Overall, there have been several alternatives proposed in the literature for post-decortication

cleaning. Challenges remain in the use of these options, due to the high level of impurities within the decorticated material and the tangling tendencies of bast fibres. Further research is required to address the obstacles currently limiting the commercial application of these cleaning methods.

3.4. BAST FIBRE CHARACTERISTICS

A comprehensive understanding of fibre characteristics (e.g. physical, mechanical, dielectric, degradation, hygroscopic, and surface properties) is required to determine the ideal fibre applications. Fibre properties significantly impact the quality of the resulting bioproducts [74]. Many parameters affect the properties of natural fibres, such as crop cultivation and geographical origin, fibre location in the plant, climate, harvesting time, as well as extraction methods [77]; however, these are beyond the scope of this study. The following sections describe some of the properties of bast fibres including the effects of chemical composition and comparisons between bast fibres.

3.4.1. Physical properties

The physical properties discussed in this section are density, aspect ratio, fibre fineness, and microfibril angle, which all play an important role in determining the mechanical properties of bioproducts. Low density is one of the most attractive properties of bast fibres. Kenaf fibre has a density of 1200 kg/m^3 (Table 2.1). The densities of other bast fibres are approximately 1500 k*g/m*^{3}, comparatively lower than those of synthetic fibres. The density of E-glass fibres, one of the most common synthetic fibres, is approximately 2550 kg/m^3 [36]. The aspect ratio is defined as the proportion of the fibre length to its diameter [78]. High aspect ratio values indicate high strength [36] and are considered to be better for spinning in textile industries. Fibre fineness, also called linear density in the textile industry, describes the positive relationship between the fibre's surface

area and the substances blended with the fibres such as polymers [79]; this is an indicator of interfacial bond strength in composite materials. Fibre fineness is defined as weight per unit length and determined according to the following formula [80]:

$$f = \rho \times \frac{\pi d^2}{4} \qquad (2.1)$$

where: f is the fineness of the fibre in tex (g/km), ρ is the density in kg/m^3, and d is the diameter of fibres in mm.

The density and diameter of common bast fibres reported by Zimniewska et al. [26] were used to compute fibre fineness (Table 2.1). Ramie fibre fineness is greater than other bast fibres and varies widely. Hemp, flax, and kenaf have similar levels of fibre fineness, while Jute fibres have a narrow range of fibre fineness (Table 2.1). The plant population affects fibre fineness. When the plant population was increased from 50 to 350 plants/m^2, the fineness of hemp bundles decreased from 150 to 88 tex, as reported by Khan et al. [83].

Table 3.1. Density, diameter, and fineness of typical bast fibres. Fineness was calculated based on the data from [25] and [36] with permission from Springer.

Bast fibres	Density (kg/m^3)	Diameter (μm)	Fineness (tex)
Hemp	1480	15–30	0.26-1.05
Flax	1500	17–20	0.34-0.47
Kenaf	1200	14–33	0.18-1.03
Jute	1460	14–20	0.22-0.46
Ramie	1510–1550	40–60	1.90-4.40

As explained in Section 2, most of the content of a single fibre resides in the S2 layer. Microfibrils in the S2 layer are wound helically (Figure 3.7). The angle between the single fibre axis and the microfibrils is referred to as the microfibril angle (MFA) [81]. The MFA can vary between and within plants, in a range of 2 to 10°. For hemp and kenaf, MFA varies from 2 to 6.2°

[36] and 2 to 6° respectively [82] and a higher range (between 5 - 10°) has been described for flax [36]. The MFAs for ramie and jute are 7.5° and 8° respectively [36,82]. Chemical composition influences a fibre's MFA. Komuraiah et al. [42] examined several natural fibres including hemp and jute. They reported that a higher cellulose and hemicellulose content decreased the MFA; the MFA increased as the lignin and pectin proportions increased; and wax had a negligible impact on the MFA. The correlation coefficients between MFA and cellulose, hemicellulose, lignin, pectin, and wax were -0.487, -0.94, 0.82, 0.63, and -0.074 respectively.

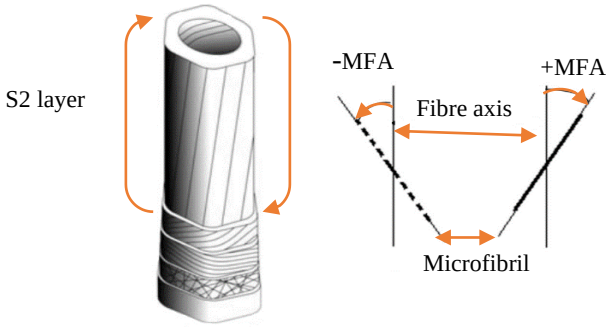

©Figure 3.7. Left side: Microfibril angle; Source: [86] with permission from L. Donalson; Right side: MFA stands for microfibril angle.

3.4.2. Mechanical properties

The mechanical properties of bast fibres affect the performance of its produced products, such as biocomposites. The mechanical properties of bast fibres also affect the performance of machines, which process the fibres, such as decorticators and post-decortication cleaning machines. Therefore, to develop high-performance bioproducts and machines to handle bast fibres, an understanding of the mechanical properties of bast fibres is required. The critical mechanical properties include shear strength, tensile strength, and Young's modulus. In the literature used for this section, the authors did not apply the FACF and instead used a circular CSA for the fibres to

calculate their mechanical properties. Therefore, in this section, “apparent” tensile strength and “apparent” Young’s modulus terms were used.

Direct shear tests were performed to measure the shear strength, internal cohesion and friction coefficients of hemp fibres [61]. Due to the limited size of the shear box (diameter: 52 mm; height: 46 mm), hemp fibres were ground to 1.2-mm particles before the tests. A typical applied load ranging from 94 to 194 N produced a measured shear strength of 92 to 182 N for hemp fibres. The measured internal cohesion and friction coefficients of the hemp fibres were 1.59 and 0.9 kPa respectively. The results provide useful information for improving machine performance when processing hemp fibres.

Tensile tests on retted and unretted hemp fibres have been carried out to determine the tensile properties [83]. The average apparent tensile strength of unretted hemp fibres (average diameter: 0.34 mm) was 358 MPa; retted hemp fibres had an apparent tensile strength of 343 MPa. The corresponding elongations at break were 3.5% and 3.2% respectively for a specimen length of 25 mm. The tensile properties of bast fibres are highly variable and depend on many factors, such as growing conditions and agronomic practices. For example, increasing plant density from 50 to 350 plants/m^2 increased the specific tensile strength of hemp fibres from 22.9 to 44.0 cN/tex [79]. Based on George et al. [40] and Ashby [89], a range of tensile properties for the various bast fibres is shown in Figure 3.8. The apparent tensile strength of several types of bast fibres range from 200 to 1200 MPa, except for flax fibre whose apparent tensile strength reached 1,800 MPa (Figure 3.8.a). Glass fibres have both a higher value and a greater range of apparent tensile strength, found to be 2,000 to 3500 MPa (Figure 3.8.a). In addition to high strength, low weight is also crucial; particularly if bast fibres are to be used in automotive and aerospace applications, as overall weight directly impacts fuel consumption and emissions [36]. Therefore, apparent tensile strength is a

more suitable for assessing the overall performance of fibres. The specific tensile strength is obtained by dividing a fibre's tensile strength by its density. Similar specific tensile strength distributions were seen between the natural fibres (Figure 3.8.b). However, the differences between the specific apparent tensile strengths of glass fibres and bast fibres were smaller than their apparent tensile strengths; furthermore, the specific apparent tensile strength range of flax fibre has some crossover with that of glass fibre. The measured apparent Young's moduli for flax and ramie fibres are comparable to that of a glass fibre, while the other bast fibres have a lower apparent Young's modulus (Figure 3.8.c). The apparent Young's modulus was highly variable among different bast fibres and within a bast fibre, especially in ramie fibres, which varied from 44 to 128 GPa. Fibres with low variability in mechanical properties are more desirable since they are more predictable. The specific Young's modulus was obtained by dividing Young's modulus by the fibre density, the measured specific Young's modulus of the natural fibres was found to be comparable to glass fibres. Among the bast fibres, hemp fibre appears to be superior in its mechanical properties, fibre density, as well as the range of variation for each property.

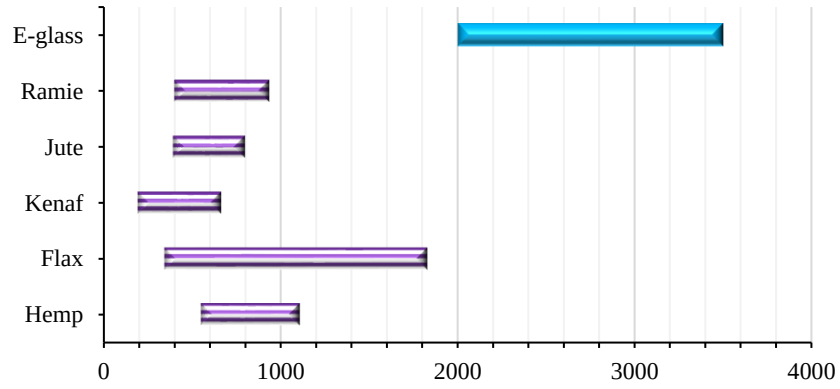

a. Tensile strength (MPa)

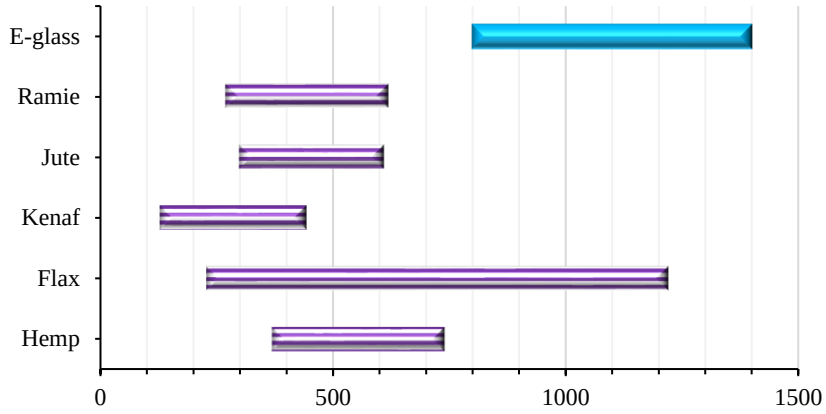

b. Specific tensile strength (MPa/Mg m-3)

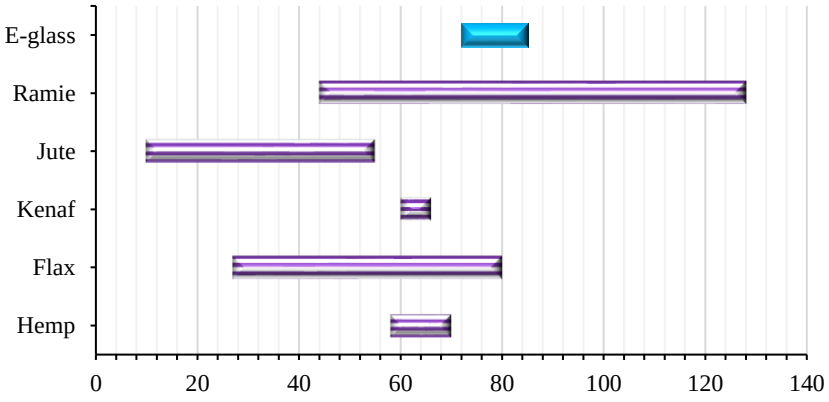

c. Young's modulus (GPa)

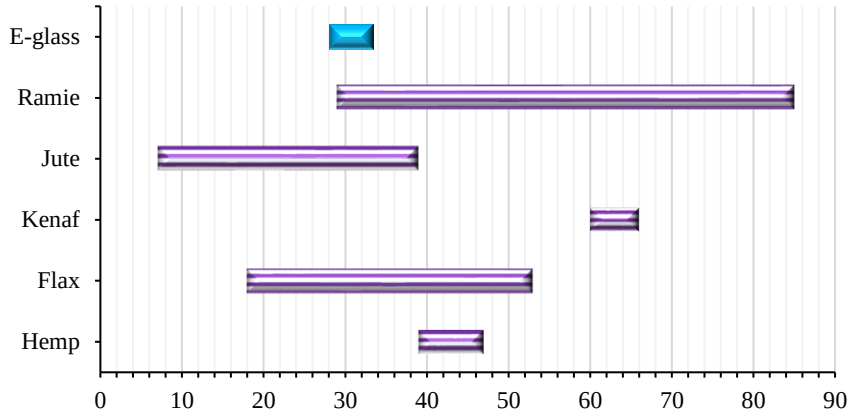

d. Specific Young's modulus (GPa/Mg m-3)

Figure 3.8. Comparing tensile properties of common bast fibres and synthetic fibres. Source: Based on data from [40,89] with permission from Elsevier.

Depending on the application, bast fibres may be treated with different processing conditions. For example, if bast fibres are to be used in composites, their mechanical properties would be affected by high temperature. The impact of high temperature on the tensile behaviour of kenaf fibre bundles has been studied in the literature [85]. The temperature conditions were selected based on composite fabrication conditions: 170°C for 1 hour to represent injection moulding; 180°C for 1 hour to represent compression moulding; and 130°C for 24 hours to represent the highest temperature applied to front-end automotive components. The results demonstrated that high-temperatures increased the fibre's Young's modulus by approximately 5% and tensile strength and failure strain declined by 10% due to decreasing moisture content. Gassan and Bledzki [90] investigated the mechanical behaviour of retted/unretted jute and flax fibres under diverse thermal conditions to find that under 170°C, the tenacity of the fibres remained constant, while at temperatures above 170°C, it changed remarkably.

Regardless of extrinsic factors, two important intrinsic factors affecting the mechanical properties of bast fibres are microfibre angle and chemical composition. Fibres with small angles

are more rigid, stiff, and stable [30,35]. If the fibre orientation is parallel to the load direction, the fibres are rigid and have a correspondingly high tensile strength. The value of the angle changes from one fibre to the next [35]. The relationship between the chemical composition and tensile properties of bast fibres are reflected by their correlation coefficients (Table 3.1) [38]. The correlation coefficient is indicative of the strength of the relationship between chemical composition and other tensile properties (e.g. tensile strength, specific strength, and specific Young's modulus). Cellulose has a noticeable positive influence on tensile strength, specific strength, and specific Young's modulus; nevertheless, there is a negative correlation between cellulose and failure strength. Similar behaviours are observed for the effects of other chemical elements on tensile strength, except for pectin, whose influence here is trivial. There is a direct relationship between the effects of hemicellulose and wax on specific strength and specific Young's modulus. The impact of wax on specific strength is more remarkable than other components. Lignin and pectin correlate negatively with specific Young's modulus but positively for failure strength [87]. In summary, fibres with a small microfibril angle and high cellulose content tend to have the highest tensile strength but also a low tolerance for elongation before breakage.

Table 3.2. The correlation coefficient for chemical compositions of natural fibres vs. tensile properties. Source: Based on data from [38].

	Tensile strength	Specific strength	Specific Young's modulus	Failure strength
Cellulose	+0.596	+0.385	+0.366	-0.183
Hemicellulose	-0.114	+0.501	+0.691	-0.446
Lignin	-0.555	-0.546	-0.355	+0.641
Pectin	-0.065	+0.102	-0.499	+0.391
Wax	-0.144	+0.907	+0.322	-0.439

3.4.3. Dielectric properties

The dielectric properties of natural fibres (e.g. conductivity, resistivity, dielectric constant, dissipation, and loss factors) determine whether they are appropriate for conducting or insulating products (e.g. neural probes or switches). The electrical resistivity is the reciprocal of the electrical conductivity, which represents a material's ability to conduct electricity. Fibres with low resistivity have a higher tendency to flow electric current. The dielectric constant, a function of the polarization degree of the material's composition, denotes a material's ability to store electrical energy once an external electric field is applied. The chemical composition of plant fibres, particularly the presence of hydroxyl groups (OH) in the cellulose, greatly affect their dielectric constant. The dissipation factor, or loss tangent, represents the electrical energy that converts into heat within an insulator. The loss factor expresses the amount of energy lost in transmission and distribution at any given moment [88]. Bora et al. [94] reported that the electrical constants of ramie and jute are 5.18 and 4.46, respectively. Increasing the moisture content increases the electrical conductivity and decreases the electrical resistivity. By increasing the moisture content, the flow of electrical current rises on account of increased non-crystalline regions in the matrix

phase [88,90]. The influences of fibre size, moisture, and water uptake on the dielectric behaviour of plant fibre-based composites have been investigated [91]. The results revealed that composites with same-sized fibres had a high mechanical performance and a smooth flow of electrical discharge. The effect of frequency on the dielectric constant and electrical conductivity of natural fibre reinforced/low density polyethylene (LDPE) composites, glass/LDPE, and carbon black/LDPE composites was also studied [90]. The findings revealed that changing the frequency had a significant impact on the dielectric constant of natural fibre reinforced LDPE composites, owing to the low interfacial polarization of their natural fibres. Furthermore, the electrical conductivity of hydrophilic natural fibre reinforced LDPE was improved due to hydrophilic lignocellulosic fibres and conductive carbon black.

3.4.4. Degradation properties

Determining the degradation behaviour of plant fibres is crucial especially when they are used in composite industries since natural fibres undergo multiple high-temperature processes during composite manufacturing [92]. This property is also of importance when natural fibres are used for insulation, as they must be highly resistant to fire. Thermogravimetric analysis (TGA) is a method employed to determine the thermal characteristics of materials. It is used to evaluate the ability of natural fibres to resist degradation under high temperatures. With TGA, the weight loss of a material can be plotted as a function of temperature. Alternatively, its derivative mass can be plotted as a function of time in any given temperature using derivative thermogravimetric analysis (DTG). Figure 3.9 represents a typical thermogravimetric plot for natural fibres [93]. In low temperatures (100 – 200ºC), fibre mass decreases slightly due to the loss of moisture content. At high temperatures (200 – 400ºC), up to 70% of fibre mass can be lost due to the decomposition of

hemicellulose, cellulose, and lignin, in that order. Hemicellulose is the first chemical components to decompose due to their amorphous structure, and positions within the fibres [94]. In contrast, cellulose is formed from several microfibrils and is responsible for fibre reinforcement. This confers cellulose with relatively high thermal stability when compared to hemicellulose. Cellulose begins to degrade once the hemicellulose is completely decomposed. Lignin is the third component to break down under high thermal conditions. Lignin provides rigid support to fibrous plants and imparts greater thermal stability for fibres than hemicellulose and cellulose. Other components of natural fibres including pectin and wax are the last to degrade [95].

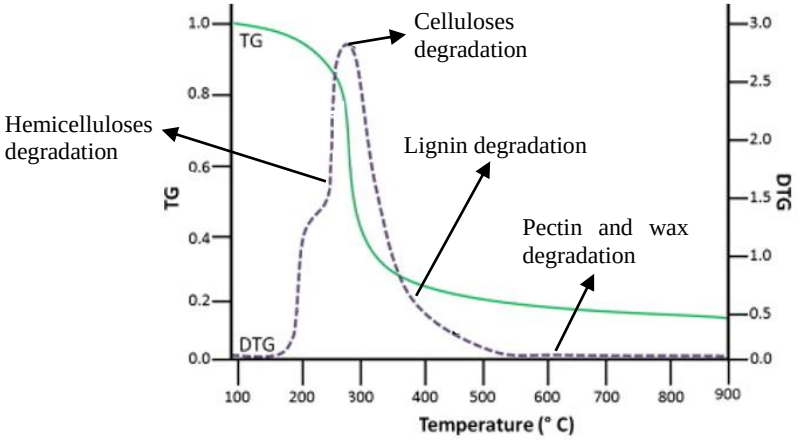

©Figure 3.9. A typical weight loss curve (TG) and derivative curve (DTG) obtained from the TGA analysis for natural fibres. Source: [98] with permission from Elsevier.

Multiple studies have measured the degradation temperature range of the individual chemical components of natural fibres; they found that it is between 200 and 350°C for hemicellulose, and for cellulose and lignin vary approximately from 300 to 500°C [96,97]. According to another investigation, for most natural fibres, around 60% thermal decomposition took place when the temperature was in the 215 to 310°C range [98]. Koronis et al. [104] advocated that in temperatures up to 200°C during composite manufacturing process, natural fibres degrade and shrink on account of their low thermal stability. Overall, the thermal stability of natural fibres is less than synthetic

fibres [100]. Modification of bast fibres is a good way to improve their thermal stability. During the modification process, non-cellulosic components, such as lignin, are removed from bast fibres. Since lignin contains char, which protects fibre-based products from fire, adding an optimised amount of metallic hydroxide during the manufacturing process compensates for the lack of lignin [93].

3.4.5. Hygroscopic properties

From a hygroscopic behaviour perspective, natural fibres absorb or adsorb water until moisture equilibrium is reached, this equilibrium depends on the moisture content of the material and the environment. This property could serve an advantage or disadvantage, depending on the future application. If bast fibres are used to make insulation, particularly in building physics, absorbing moisture is a desirable feature since they act to buffer moisture. However, when bast fibres are used as reinforcements in biocomposites, absorbing moisture would incur adverse effects on the technical performance of the composites. For natural fibres, at 65% humidity and 21°C, the maximum and minimum equilibrium moisture content (EMC) were found to be 12% for jute and 9% for flax, hemp, and ramie [25]. Assarar et al. [106] concluded that flax fibre composites absorb more water than glass fibre composites. Increasing the fibre volume fraction within natural fibre composites increases their moisture absorption [102]. Madsen et al. [108] compared the deformability of composites with different proportions of hemp fibres; they discovered that higher fibre content results in a larger hydro-expansion coefficient. The same result was obtained by Arbelaiz et al. [108] when they evaluated flax fibre bundle composite materials. They also found that the mechanical properties of natural fibre composites decreased with increased moisture absorption [105]. The strength of natural fibre composites drops up to 31% when absorption of

water is increased [106]. Davies and Bruce [112] stated that the Young's modulus for flax fibre decreased by approximately 23% when humidity rose from 30 to 80%. The same pattern was observed by Ho & Ngo [113] for hemp fibres. The results of a study carried out on flax and kenaf demonstrated that increasing the fibre moisture content lead to a noticeable decline in the mechanical properties of flax, while the properties of kenaf remained unaffected [109]. Natural fibre stiffness decreases with increased moisture content because the covalent bonds in the hemicellulose macromolecular network are replaced with hydrogen bonds, resulting in a more flexible and compliant fibre structure [110]. In contrast, increasing relative humidity from 25 to 80% led to a 20% increase in stiffness due to the rearrangement of microfibrils and other molecules which function as reinforcing elements [111]. Moisture absorption of the fibres causes swelling phenomena through micro cracks in the biocomposite matrix, which can potentially induce a capillarity mechanism. The mechanism includes a diffusion process throughout the matrix phase of water molecules along fibre interfaces, which can lead to a debonding of the fibre and the matrix (Figure 3.10) [112].

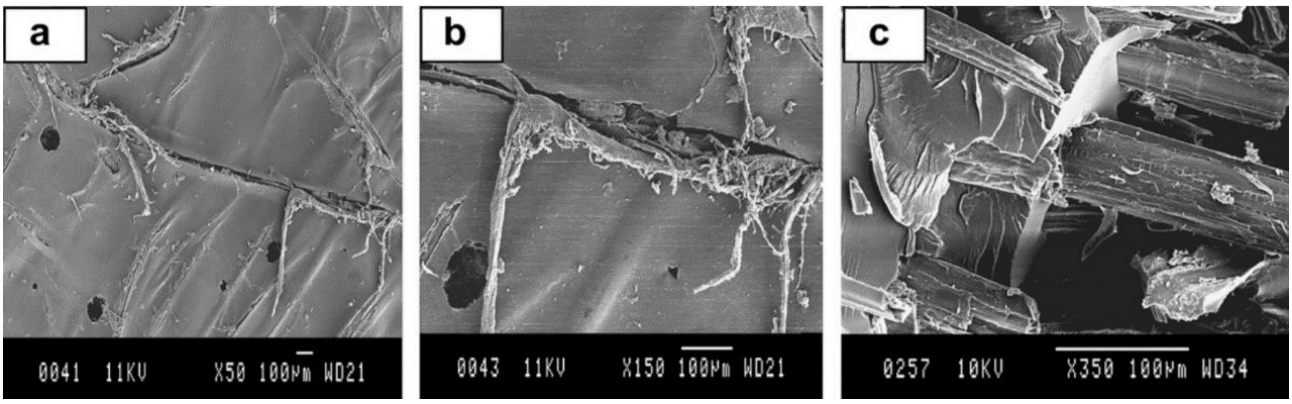

©Figure 3.10. (a) Matrix cracking, (b) Fracture running along the interface, (c) Fibre/matrix deboning due to attack by water molecules. Source: [117] with permission from Elsevier.

The hygroscopic characteristics of natural fibres are determined by their chemical composition. For example, the large number of -OH found in cellulose, and the -OH and acetyl groups ($-C_2H_3O$) in the amorphous structure of hemicellulose [113,114]. Lignin has minimal influence on the hygroscopic behaviour of natural fibre-based materials [114]. Pectin, the main element of the middle lamella, is water-soluble; therefore, fibre bundles uptake more moisture compared to single fibres [110]. Komuraiah et al. [42] found that, while there was a negative correlation between fibre moisture absorption and the percentage of cellulose and pectin in the fibre, there was a positive correlation between moisture absorption and the proportion of hemicellulose, lignin, and wax. The correlation coefficient for cellulose was negligible (-0.197) but it was statistically significant for pectin (-0.538). The coefficients for the other chemical components were: 0.322 for wax and 0.42 for hemicellulose. In conclusion, eliminating the non-cellulose portions of natural fibres is recommended to limit their hygroscopic behaviour when used for composite applications. Further research is needed to determine the effect of pectin.

3.4.6. Surface properties

Surface properties are critical if the fibres are to be used as reinforcements in composite materials. Surface energetics regulate the adhesion between fibres and the matrix phase, in which high surface energy leads to strong adhesion [115]. The surface free energy of natural fibres (γs), which is equivalent to the surface tension of a liquid, is calculated based on the contact angle or using inverse gas chromatography. There is a direct and strong relationship between the surface free energy and thermodynamic work of adhesion (WA). High WA values are desirable as they correlate with practical adhesion [116]. The parameter WA is the work required to divide a single surface into two new surfaces and strongly depends on the contact angle and liquid surface tension [117]. Fowkes [123] stated that the γs includes a dispersive (d) and a polar (p) component ($\gamma_s = \gamma_s^d + \gamma_s^p$). The contact angle is related to the degree of wettability. By increasing the contact angle, the degree of wettability declines [119]. Diverse strategies have been employed to calculate the contact angle, including the sessile drop, Wilhelmy plate, wicking technique, and atomic force microscopy (AFM). In the sessile drop method, a small amount of liquid is positioned on the solid material and the contact angle is computed based on the sessile drop profile [120]. Obtaining the contact angle directly is one distinct advantage of the sessile drop method; however, diversity in the cylindrical geometry of the fibres, which influences the drop shape, prohibits the wide-spread use of this method [121,122]. In the Wilhelmy technique, a solid plate is placed on a liquid perpendicular to the interface, the liquid spreads upwards on the plate and the weight of the lifted liquid is measured. This technique is not well-suited for natural fibres due to their surface irregularity and perimeter variation [123]. The wicking approach, or capillary rise, employs the Lucas-Washburn equation to test and indirectly determine the contact angle of cellulosic materials [124]. A limitation of this strategy is the need to prepare multiple samples for each measurement.

Several researchers have utilised this technique. Shen et al. [130] stated that the dispersive surface tension energy of bamboo and cotton linter was equal to 42.29 and 41.18 mN/m respectively. Another study determined a dispersive energy tension of 18.8 mN/m for unretted sisal [126]. Cantero et al. [132] reported that the dispersive surface tension energy for flax was 32.2 mN/m. Alternatively, AFM can be used to estimate the adhesion force of a spherical particle on a solid surface [128]. The surface tension energy of unretted hemp fibre determined through AFM was equal to 41 mN/m [128]. More recently, Schellbach et al. [134] developed a novel method that they used to measure the contact angle of hemp, jute, ramie, and some other natural fibres. For each type of fibre, two single fibres of similar diameters were placed parallel to each other under an optical stereomicroscope, ensuring that a small spacing was left between the fibres. A syringe was then used to drop a probe liquid into the space between the fibres, prior to imaging. They reported that the advancing contact angles for all the natural fibres examined ranged from 40 to 50°. These values were typically a few degrees smaller for the receding contact angles. The difference between advancing and receding contact angles is called hysteresis and is caused by the surface roughness and/or heterogeneity of the natural fibres [130]. Schellbach et al. [134] also determined that the contact angle hysteresis for fibres with a rough surface varied from 22 to 30°.

Inverse gas chromatography (IGC) uses vapour instead of liquid to determine the surface free energy of natural fibres. IGC is based on the infinite dilution principle, where the injection of a small amount of probe liquid creates adsorption within the linear region of the adsorption isotherm. IGC experiments are executed by using a series of alkane vapours such as decane, nonane, octane, and heptane as probes to measure the dispersive surface free energy [131]. Heng et al. [136] used IGC to determine that the dispersive surface tension energy of hemp and flax was 40.7 and 43.1 mN/m respectively.

The surface properties of natural fibres are affected by both extrinsic factors (e.g. fibre extraction method) and intrinsic factors (e.g. chemical composition). Heng et al. [136] ascertained that flax fibres extracted by dew retting had higher surface energies than those extracted by steam explosion (a method to separate fibres at high temperature and pressure). Applying three biological treatments (e.g. laccase, a combination of xylanase and cellulase, and polygalacturonase) enhanced the surface energy of hemp fibre [132]. The laccase significantly removed lignin; xylanase degraded the hemicellulose around the fibre bundle (thereby causing cracks in the fibre surface); and polygalacturonase treatment eliminated pectin. Micrographs of untreated and treated hemp fibres prepared using scanning electron microscopy are shown in Figure 3.11.

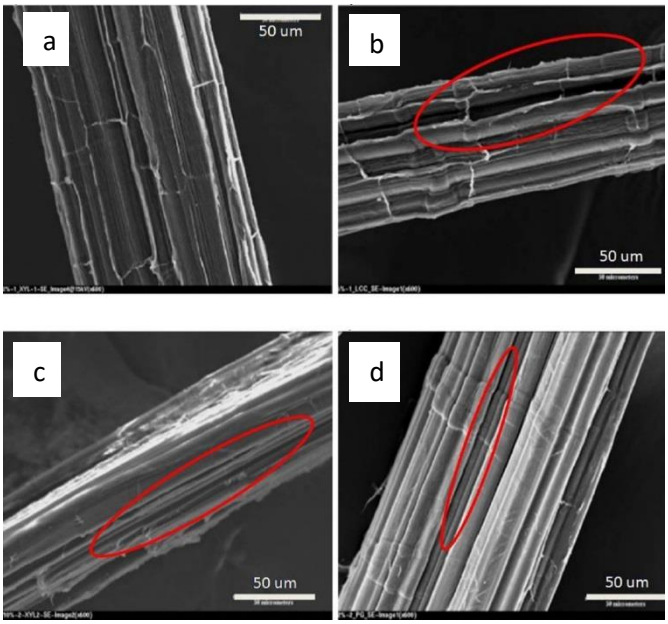

©Figure 3.11. Scaning Electron Microscopy of of hemp fibre before and after applying the biological treatments: (a) control, (b) laccase, (c) xylanase + cellulase and (d) polygalacturonase. The red insets highlighted the effect of each treatment (For interpretation of the references to colour in this figure legend, the reader is referred to the web version of the article). Source: [137] with permission from Elsevier.

3.5. BAST FIBRE APPLICATIONS

Bast fibres have many potential applications due to their technical properties; Figure 3.12 exhibits

an overview of these various applications [133]. Raw fibres can be directly used as insulation, fluid sealing, upholstery, and reinforcement in composite materials. Indirectly, these fibres can be aerodynamically or mechanically incorporated into fleeces and felts, which can be used for thermal insulation or in composite and geotextile applications. The other indirect application of bast fibres is to prepare slivers. Slivers are used either as reinforcement in biocomposites or to prepare yarn. Yarn is used to manufacture fabrics, knitted goods, knotted nets, and ropes; its associated products are listed in Figure 3.12. Fabrics and knitted materials, including felts and fleeces, can also be used for reinforcement in composite materials. The following sections provide a comprehensive review of the three most important applications of bast fibres: insulation, biocomposites, and geotextiles.

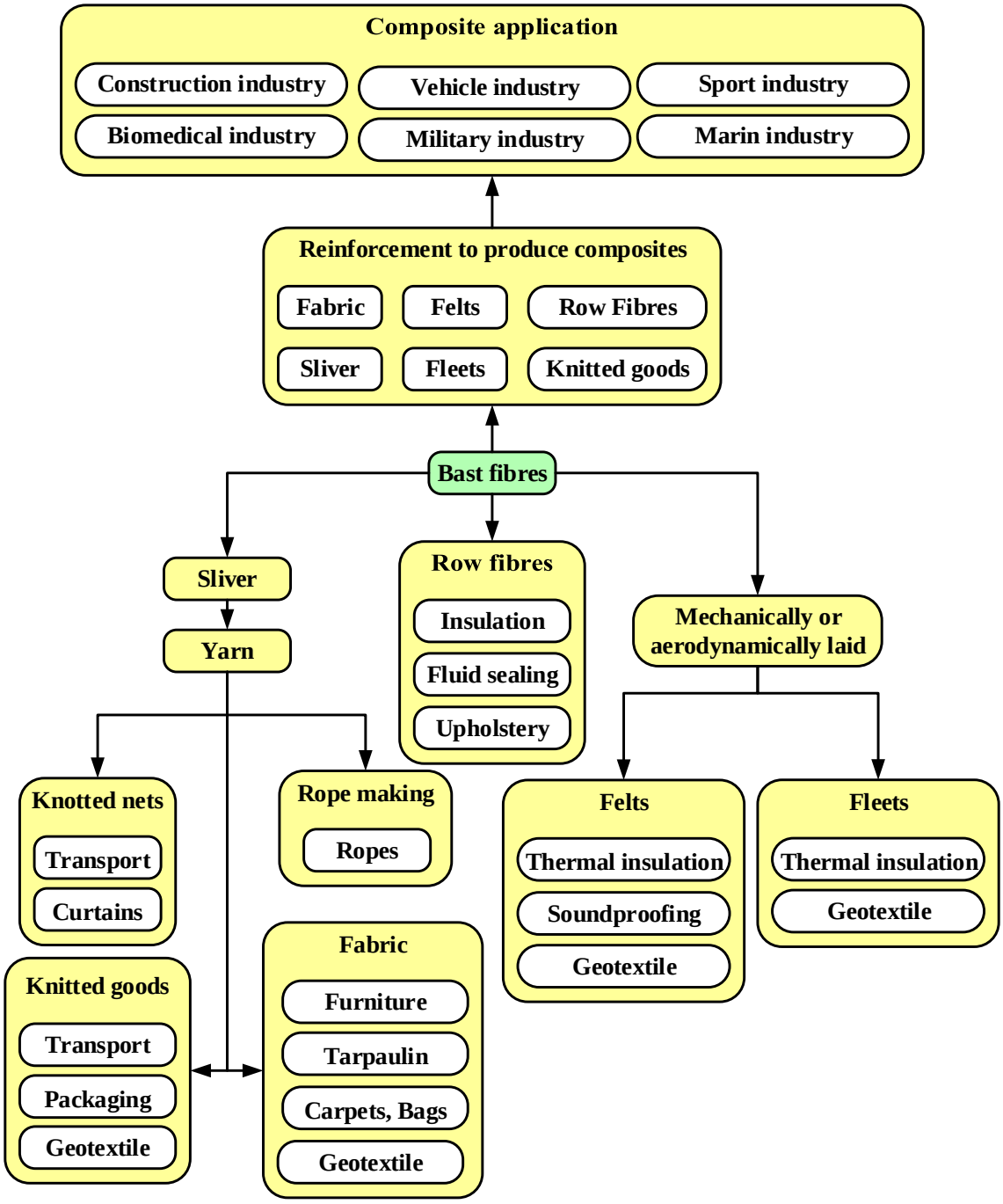

Figure 3.12. Technical applications of bast fibres.

3.5.1. Insulation

Bast fibre-based insulation has acceptable thermal conductivity because the lumens inside of the single fibres render their structure porous and low-density. As a result, considerable amounts of

air occupy the pore spaces. Fire resistance is another key technical property of insulation material. The fire resistance of bast fibres is relatively low. Kokkala [139] demonstrated that the risk of smouldering in cellulose insulation was higher than in glass wool. Adding a mass fraction of certain chemicals can provide flame retardancy to cellulose. The fire resistance of flax insulation was increased by adding 13% mass fraction of boric compounds [135]. Nevertheless, it has been reported that since the apparent density of insulation is high enough, the combustibility is not an important property for insulation [136]. For example, hemp fibre insulation, without any additive, showed typical combustibility levels, comparable to other commonly-used fibres [137].

Many international regulations specify the quality and criteria for insulation, related to their technical properties and some environmental aspects [138]. Bast fibres contain natural microbial flora that are undesirable for insulation materials. Considerable amounts of additives are required to eliminate these microbes [135]. For example, the addition of a bio-binder like starch decreases microbes and the environmental impact of the insulation.

3.5.1.1. Processing techniques

Fleeces and felts are both processed bast fibres that can be used as insulation. The first step in preparing fleeces and felts involves making fibrous webs from bast fibres using horizontal cross-lappers or aerodynamic laying machines. In a horizontal cross-lapper, thin layers of carded fibres are piled up. The drawback of this method is the restricted speed of fibrous web-laying, especially when producing very thick webs. The aerodynamic laying machine was developed to address this concern. However, this method increases the thermal conductivity of the insulation. This increase is explained by the fibres or fibre bundles not being oriented parallel to the insulation surface, but instead being aligned at an angle. Consequently, heat flows through, across, or at an angle to the direction of fibres. Therefore, the orientation of the fibres during processing is of importance.

There is a correlation between the fibre alignment and the thermal conductivity of the final product. If the heat flow is in the same direction as the fibres are aligned, the thermal conductivity is high. Thermal conductivity is lowest when the heat-flow across the fibre length perpendicularly. A comparative study was performed on a glue-bonded flax fibre insulation product with both parallel and perpendicular heat flow. It was found that when the heat flowed parallel to fibre alignment, the thermal conductivity was almost 50% higher than when in the perpendicular orientation [136].

Fleeces are fibrous webs that are bonded with approximately 10 - 15% thermoplastic and hardened to the desired thickness in a thermobonding layer. During thermal processing, thermoplastic helps fibrous webs attach. The ability to make insulation over 100-mm-thick is the main advantage of thermobonding. Another approach to manufacturing fleece is to spray an adhesive during the processing of fibrous webs and then to dry the webs in an oven. Since fleeces are associated with a good compressibility, they suffer from low compressive strength. Nevertheless, because their strength is good enough for self-support and self-adhesion, they can be used as filling or stand wedges between constructions. The main advantages of fleeces include good thermal insulating properties and acoustic sound damping. Hemp and flax fibres are commonly processed into insulating fleece in Europe [136].

Felts, which are thinner than fleeces, are constructed by bonding fibrous webs to fibres using many fine needles. The thickness of the finished product is approximately 25 mm. The thickness can be increased up to 80 mm with felting machines that stitch the fibrous webs from above and below. The main application of felts is in the fabrication of impact sound insulation materials used to reduce sound from people walking on a floor structure. For this purpose, felts require a certain elasticity to return to their initial state after loading. Hemp, flax, and jute fibres have been used to prepare felts [136].

3.5.1.2. Applications

Building applications: The primary application of bast fibre-based insulation is in external walls and ceilings (Figure 3.13). Bioinsulations are also used in lightweight partitions and wall surfaces that consist of panelling and metal studs or wooden posts, known as the frame. The material filling the cavities between the studs can act as auditory or thermal insulators. High-quality sound insulations include a double-wall design with separate panelling. A soft separating layer should be used to make ceiling, floor, and wall connections that prevent sound transmission through the flanking structure. Natural fibres in the fine-fibre felt format are appropriate for cavity damping, while the flanking structures are made from tight-needled felts. Using sound insulation in wooden buildings is another application of natural fibre insulation, for example, footstep insulation, which requires a balance between compressibility and dynamic stiffness. The sound insulation has to be compressed enough to tolerate heavy loads; however, high compressibility results in high dynamic stiffness, which reduces the efficacy of the sound insulation [136]. On the other hand, since floating dry floors are not as bend-resistant as cement floors, the dynamic stiffness should be high enough to weather natural variation. The load-bearing capacity of insulation under extreme conditions, particularly during installation, represents another important factor. The low mechanical strength of the fibres used in insulation leads to a sound bridge under excessive loads. Bast fibres have acceptable mechanical properties and are enough for fabricating acoustic absorbers and sound barriers, where they are combined with synthetic binding fibres.

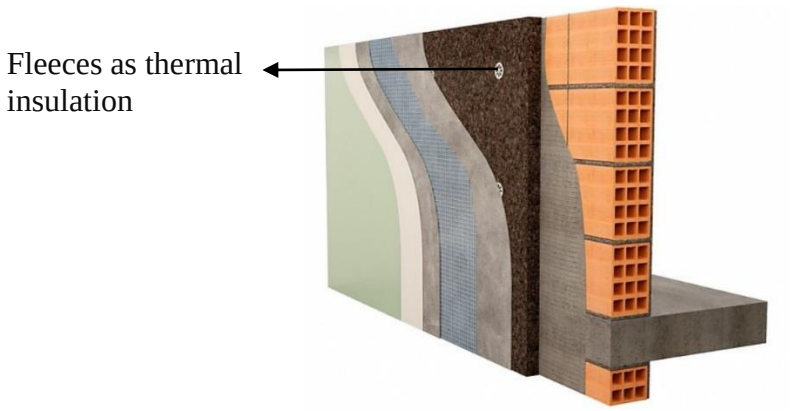

©Figure 3.13. Application of thermal insulation in external walls. Source: [144]

Technical use: Insulation layers have been used in the heat stores of hot water tanks, biomasses, and solar heating systems. Natural fibres as renewable materials and can suitably replace synthetic or mineral-based materials, which are traditionally used to make thermal insulation shells. The thickness of the natural fibres should be adjusted depending on their thermal conductivity. Furthermore, repair and maintenance are easier on products built with natural fibre insulation [137].

3.5.2. Composites

As previously discussed, bast fibres are the most popular type of natural fibres. Compared to glass fibres, one of the most common synthetic fibres, they have high relative specific mechanical properties. According to Fotouh et al. [145], the amount of energy consumed to manufacture biocomposites is lower than for conventional composites. The lower maintenance costs of the processing equipment is another advantage [141]. Bast fibres are combined with polymers to generate composite materials. In the next section, the methods used to manufacture biocomposites are briefly discussed.

3.5.2.1. Processing techniques

From a technical perspective, selecting a suitable manufacturing process is dependent on the type and form of the fibres, the size and complexity of the product, and the speed of production. Summerscales et al. [148] and Ku et al. [149] have reviewed most of the methods used to produce natural fibre composites. A short review of the commonly used methods follows below.

There are a variety of techniques to manufacture bast fibre-reinforced composites depending on the length of the fibres. Fibres are classified as short (less than the critical length defined by Cox shear lag theory) or long (in the limit continuous) with the former acting as fillers and the latter as reinforcements. Long fibres are used to produce fabrics, yarn, or fibre strands used as reinforcement for thermosetting matrices through resin transfer moulding (RTM) [144]. Although thermosetting polymer-based composites boast high technical performances, the RTM process is laborious and relatively wasteful [144]. Therefore, research has focused on using other strategies, including film stacking and compression moulding to develop bast fibre mat-, fabric-, or roving-reinforced thermoplastic composites, which also have the potential to be reprocessed or recycled [145–147]. As outlined in the Insulation section, thermoplastics are used to bond fibrous webs to make felts and fleece that can also act as reinforced phases in composites. However, the main drawbacks of using thermoplastics as matrices is the thermal degradation of fibres during processing and consolidation [148] and the high relative porosity of long bast fibre-reinforced composites [149]. The main reason for high-porosity in long fibre thermoplastic composites is the lack of a proper integration of fibres with melted thermoplastics. Conversely, short bast fibres are dispersed within the matrix using high-speed mixers, single or twin-screw extruders to produce the compounds. These compounds are then processed using extrusion, compression, or injection moulding to manufacture three-dimensional parts [144]. The main challenge in producing such

compounds is the length of the fibres; fibres should be short enough to ensure homogeneous distribution within the matrices [150] yet long enough to provide acceptable mechanical performance. To tackle this challenge, yarn of short bast fibres are pre-impregnated or pre-coated with a thermoplastic matrix under a process called cable-coating or pultrusion, followed by extrusion to produce final composite parts. However, the disadvantage of this method is the increased costs and efforts associated with the manufacturing process [151].

3.5.2.2. Applications

Specific mechanical properties of bast fibres are comparable to those of glass fibres. Biocomposite characteristics help towards identifying appropriate applications. For example, composites with high tensile and low impact strength are suitable for making furniture and boarding. In contrast, composites with more favourable impact properties and higher tensile strength are used when there are more impact stresses. Due to the wide range of biocomposite properties, they can be applied to a multitude of industries, explored in the following section.

Vehicle applications: The automotive industry is one of the pioneering sectors for biocomposite usage, due to the high demand for vehicles that are low-weight and sustainable. The number of plant fibres used to produce biocomposite materials for automotive applications was approximately 60,000 t in 2012 and is projected to reach 80,000 t by 2020 [152]. Hemp fibre thermoplastic and thermoset composites in moulded form constitute a significant percentage of the market in the European automotive sector [153]. The specific benefits of using bast fibres in the automotive industry include acceptable mechanical properties and reduced health risks. Another benefit is the lack of splintering of parts during an accident because of the less abrasive nature of natural fibres and the tendency of the fibres to rupture instead of splinter when released from a fail

structure [36]. More than 50 European vehicle parts manufactured by DaimlerChrysler are made from bio-based materials. Door cladding, floor panels, and seatback linings have been fabricated from hemp and flax fibres. At General Motors, a mixture of kenaf and flax fibres are processed to make package trays and door panels for Opel Vectras and Saturn L300s in the European market. Kenaf fibres were used to manufacture Lexus' package shelves at Toyota [140]. The structural part of the Kestrel, an electric hybrid vehicle designed by Calgary-based Motive Industries, Inc., was successfully made from hemp, kenaf, and flax fibre mats at the Composite Innovation Centre (CIC), MB, Canada. In India, to replace the medium density fibreboard in railcars, natural fibre composites have been evaluated [154]. At Boeing and Airbus, the interior panelling of aeroplanes has also adopted natural fibre composites. Bast fibre composites have also been used in the bicycle industry. Carbon fibres, which have recently become popular in the bike industry, were hybridized with flax fibres to manufacture a bicycle frame with the low cost and renewability of flax fibre and the high technical performance of carbon fibre [155]. Researchers have found that, in addition to the lower costs of the newly-developed frame, its stiffness and strength were similar to or higher than commercially available carbon, titanium, and aluminium frames [155].

Construction applications: The construction industry is another market for biocomposites since they have a lighter mass and, when sourced locally, lower costs. The use of fibre composites in critical load-bearing applications is rare, though they are popularly used for repairing existing structures. They are also used in reinforced concrete in exchange for steel, but they are not suitable for new civil structures. In addition to fulfilling immediate infrastructural and sustainability needs, they increase energy production and reduce construction waste [156]. The European Union has recently placed a premium on decreasing medium-term raw material consumption by 30% and waste production by 40% [157]. Bast fibre composites have been used extensively in rehabilitation

and retrofitting. In 1998, it was estimated that around $900B (CAD) was required for the repair and retrofitting of the infrastructure of the world [156]. Also, in 2000, the estimated cost of repairing and upgrading concrete structures in Australia was around $500M per annum [158]. The conventional materials used to enhance strength and ductility for rehabilitation are concrete and external steel sheets. Concrete is used to encapsulate elements like bridge piers because of its suitability for submerged installations and its ability to form complex shapes [159]. Steel is then applied to improve the strength and stiffness of concrete structures. Recently, the use of fibre composites as the surface layer for the encapsulated element has been increasing. Bast fibres, in the form of fibre bundles, strips, plates, and fabrics, are externally bonded to the structure. The ability to bond well to many substrate materials and their capacity to form complex shapes renders them a suitable alternative in the construction industry [156].

Bast fibres have also been used as reinforcement in structural materials. Laminate composites were manufactured from industrial aluminium sheets sandwiched with ramie fibre epoxy. The results showed that the specific tensile properties of the ramie fibre/aluminium laminate composites were significantly enhanced compared to aluminium composites alone. Furthermore, the developed composites were 33% more cost-effective [160]. The application of flax fabric-reinforced epoxy composite tubes to concrete confinement has been investigated [161]. This study revealed approximately 115% enhancement of the axial compressive strength of the four-layer flax epoxy tube confinement over unconfined concrete. Furthermore, the pre-fabricated flax epoxy composite tube decreased the construction time and protected the encased concrete from harsh environmental conditions.

Biomedical applications: The biomedical sector is another popular application of bast fibres. Biocomposites can be fabricated to meet the requirements of different applications, including

socket prostheses, internal and external fracture fixators, and dental implants to date. Ramie fibre-reinforced epoxy composites have better mechanical performance for developed socket prostheses compared to fibreglass polyester composites [162]. The feasibility of replacing conventional materials with ramie fibre-reinforced epoxy composites towards enhancing the safety and accessibility of prosthetics was investigated in another study [163]. The results demonstrated that the failure load of the ramie fibre-based composites was similar to traditional composites, meeting the ISO 10328 standard. Ramesh [169] found that kenaf fibre-reinforced composites could be used for hard-tissue applications including orthodontic brackets, dental posts, orthodontic archwires, bone plates, external fixators, prosthetic sockets, and neural probes.

Other applications: The military, marine, sport, and electric industries have integrated bast fibre-based composites. Marsyahyo et al. [170] designed a bulletproof panel made from ramie fabric-reinforced composites. In addition to the lighter weight and lower costs compared to conventional products, this panel demonstrated an impressive penetration resistance. Bast fibre composites can be used to make docks, boats, and piers but are not suitable for structural applications in the marine industry. Surfboards, helmets, tennis and paddle racquets, fishing rods, and racing boat sails are some of the sports products that utilize bast fibre composites. Lipstick cases, smartphone cases, and suitcases represent other applications [35]. Recently, there has been interest in using bio-based products in electrical industries. Industrial and household plugs, switches, terminals, connectors, printed circuit boards, panels, as well as insulators constitute the first group of applications for plant fibre-based composites in this sector [166]. The second group of applications includes bio-actuators, finding antennas, biosensors, electronic noses, chemical and electrochemical catalysts, chemical detecting sensors, fuel cells, self-regulating heaters, and photothermal optical recording devices [167].

3.5.3. Geotextiles

Because of recent climate change, natural disasters (e.g. landslides) have become less predictable. Towards decreasing the effects of these phenomena, geotextile engineers have focused on improving ground-based scientific and systematic techniques. Geotextiles, which are made from both synthetic and natural fibres, encompass the use of woven or non-woven fabrics that improve soil structure performance. The primary applications of geotextiles are drainage, aggregate separation, soil reinforcement, liquid segregation, and filtration [96]. Limited Life Geotextiles (LLGs) that are applied when limited product lifetimes are required have become a popular natural fibre-derived textile in civil and agricultural engineering applications. Basal embankment reinforcement and temporary roads over soft land are also examples of civil applications [168]. Repairing cracked road surfaces with naturally-based textiles is another application such that if it became a reality, the market would double in volume, thereby greatly decreasing overall costs [169]. For agricultural applications, these textiles can protect the growth of surface vegetation and provide long-term soil protection. At the same time, they leave fewer undesirable materials on the ground compared to geosynthetics. Other advantages of natural geotextiles which make them suitable for agricultural applications include their ability to preserve soil moisture content, control fluctuations of soil temperature, increase seed germination, increase filtration by decreasing surface sealing, reduce rain drop impact, and improve soil fertility [170]. Natural geotextiles are also promising for protecting the soil after large-scale wildfires, for example, those common to California, USA. To control the erosion and sediment deposition following fires, fibre rolls are regularly placed in a slope interceptor format [169].

Hemp [168], jute [171], flax [172], and kenaf [173] have all been investigated and employed as raw materials in geotextile applications. Although the high cost is an obstacle for market entry of

bast fibres, they have been tested in this industry. For example, hemp, kenaf, and flax fibres used for producing as a growth medium in Europe. Nevertheless, on account of the growing awareness of environmental impact, the market for natural fibre-based geotextiles is increasing where technically applicable [168].

3.6. ENVIRONMENTAL ASPECTS

The environmental aspects of bast fibres are one of the major reasons for their popularity. Figure 3.14 shows the life cycle of bast fibre-based products. Life cycling assessment (LCA) is a typical technique used by material engineers to determine the environmental impact of the different approaches to fibre improvement and the potential uses of these fibres in different applications. LCA outcomes are used to identify the main parameters used to optimize the environmental function of a single product and then is expanded to whole products. The major categories of the LCA technique are ozone depletion, climate change, eutrophication, acidification, global warming, water consumption, energy consumption, and waste production. According to ISO 14040 [179], the key phases of a LCA include: (1) goal and scope definition of the LCA, including the objective of the assessment and the function of the investigation; (2) Life Cycle Inventory analysis (LCI) , including organizing an account of pollutant emissions and consumed resources; (3) Life Cycle Impact Assessment (LCIA) , including classifying and evaluating the environmental effects of the resulting emissions; and (4) Life Cycle Interpretation , including analysis and interpretation of the results and estimation of the uncertainties. Taken together, LCA leads to a decision on whether executing the specific process or producing the specific product is possible or not.

Figure 3.14. Life cycle of bast fibre based products. A: Plant cultivations, B: Plant harvesting, C: Fibre extraction, D: Product manufacturing, E: Product usage, F: End of life.

The results of using LCA to investigate the possibility of growing flax fibres for bioproduct application (e.g. composite materials) indicate that favourable results for environmental issues such as acidification and climate changes are reachable. However, eutrophication is a big challenge [175]. Unfavourable eutrophication results are caused using fertilizers and pesticides during the flax cultivation process. The same results were obtained when LCA was performed to compare hemp/epoxy composite with acrylonitrile butadiene styrene for the manufacturing of automotive side panel components [176]. Alves et al. [182] used the LCA method to compare the environmental performance of jute fibre composites (JFCs) with glass fibre composites (GFCs). They reported that the environmental damage from GFCs was higher on account of their higher weight, which requires higher fuel consummation. Also, a qualitative analysis demonstrated that JFCs were associated with higher economic and social effects but lower technical performance.

Another investigation performed using LCA was conducted to study the environmental impact of both flax and hemp fibre-based paper pulp. The results indicated that the hemp fibre-based products induce more environmental damage than flax fibre-based ones [178].

The environmental aspects of insulation materials are also evaluated using LCA. For example, Ardente et al. [184] determined the environmental impact of kenaf-reinforced polymers insulations. They observed that the environmental impact of using kenaf fibres for insulation board applications was significantly lower than from synthetic fibres.

3.7. SUMMARY

This study reviews the structure, processing, properties, and applications of bast fibres. The crucial points are summarised below.

1. The application of bast fibres in bioproducts has increased on account of environmental concerns and their lower cost.
2. The main component of a single fibre is in its S2 layer, which constitutes approximately 70 - 80% a single fibre's mass and determines the mechanical strength of the fibre.
3. The chemical components of bast fibres are cellulose, hemicellulose, lignin, and pectin. Cellulose supplies the strength, stiffness, and stability of the fibres. Hemicellulose is susceptible to biodegradation, micro-absorption, and thermal degradation. Lignin provides rigidity to plants, and the flexibility of fibrous plants is owed to pectin.
4. Bast fibres are the most popular type of natural fibres because their mechanical properties are comparable to synthetic fibres and they are lighter than synthetic fibres.
5. Two main methods of extracting bast fibres from plants are retting and mechanical extraction. The latter is more environmentally friendly, faster, and cheaper. However,

fibre wrapping around rotating decorticator parts is a major challenge and decorticated fibres often have low fibre purity.

6. Several methods of post-decortication cleaning have been developed to improve fibre purity. However, challenges still exist to solve fibre-tangling problems.
7. The dielectric properties of bast fibres are important for determining if they are suitable for use as conductive or non-conductive biomaterials.
8. The low thermal stability of bast fibres represents an obstacle for application in composite industry because they undergo multiple high-temperature processes during composite manufacturing.
9. If bast fibres are used to make insulation materials, particularly in building physics, hygroscopic behaviour is a desirable feature. Nevertheless, if bast fibres are to be applied to reinforce biocomposites, absorbing moisture could adversely impact their technical performance.
10. From the composite industry point of view, the low surface energy of bast fibres is detrimental since it reduces adhesion of fibres to the matrix phase. Modifying the surface properties of bast fibres represents a promising approach towards improving bast fibre characteristics and increasing their suitability for large industrial-scale use.
11. Bast fibres have many additional applications including insulation, automotive, construction, biomedical, military, marine, sports, electrical, and geotextile.

3.8. FUTURE TRENDS

Environmental changes and the planet’s depleting fossil fuels pose threats to humanity. A big challenge for industries, and a potential competitive edge, is the ability to address such ecological issues. Environmentalists believe that the current environmental industry roles are not strong

enough and should be modified to tackle the big issues facing the world. Replacing synthetic products with bioproducts is promising towards mitigating the concerns outlined above.

Researchers have recently focused on developing bioproducts from natural, renewable, and biodegradable raw materials. Bast fibres, used for thousands of years, are one of the major sources of this natural resource, and they have little negative effect on human health and the environment compared to synthetic fibres. Acquiring enough practical knowledge to efficiently and effectively extract bast fibres from plant stalks adds to their value, decreases the cost of extraction, and motives their large-scale use. Advanced technology needs to be developed in order to increase fibre yields from extraction processes. Bast fibre characteristics should inspire researchers to identify new applications. In addition to fulfilling the common applications of plant fibres, bast fibres can also be used in structural products. Providing acceptable technical and economic conditions for the application of bast fibres in bioproducts, particularly in insulation, automotive, and construction industries will lead to increase job generation, less waste, and decrease environmental impact. Nevertheless, more investigations are needed on product commercialization. Some of the main limitations to the large-scale development of the bast fibre-based products are listed below.

- Lack of harmony among different fibres or even within fibres extracted from one plant.
- Lack of technology that enables extraction of high quality fibres with high yields.
- Lack of sufficient mechanical properties that facilitate use as structural products.
- Lack of effective moisture resistance and interfacial adhesion when used as insulation and composite materials.
- Lack of appropriate processing technology to distribute fibres within polymers in short and long fibre composites.

If the listed restrictions were to be addressed, the technical issues facing bioproducts would be eliminated; this would also help to tackle economic problems. The biorefinery potential of by-products obtained during fibre modification is also another solution to decrease the total costs.

3.9. ACKNOWLEDGMENTS

The authors would like to thank the CIC (Composite Innovation Centre, MB, Canada) and MITACS (Grant number FR20472) for funding this work.

3.10. REFERENCES

[1] Bourmaud A, Morvan C, Bouali A, Placet V, Perré P, Baley C. Relationships between micro-fibrillar angle, mechanical properties and biochemical composition of flax fibres. Ind Crops Prod 2013;44:343–51. https://doi.org/10.1016/j.indcrop.2012.11.031.

[2] Liu M, Fernando D, Meyer AS, Madsen B, Daniel G, Thygesen A. Characterization and biological depectinization of hemp fibres originating from different stem sections. Ind Crops Prod 2015;76:880–91. https://doi.org/10.1016/j.indcrop.2015.07.046.

[3] Terzopoulou ZN, Papageorgiou GZ, Papadopoulou E, Athanassiadou E, Alexopoulou E, Bikiaris DN. Green composites prepared from aliphatic polyesters and bast fibres. Ind Crops Prod 2015;68:60–79. https://doi.org/10.1016/j.indcrop.2014.08.034.

[4] Rowell RM, Young RA, Rowell JK. Paper and composites from agro-based resources. CRC/Lewis Publishers; 1997.

[5] Shah DU, Porter D, Vollrath F. Can silk become an effective reinforcing fibre? A property comparison with flax and glass reinforced composites. Compos Sci Technol 2014;101:173–83. https://doi.org/10.1016/j.compscitech.2014.07.015.

[6] Pickering KLL, Efendy MGGAGA, Le TMM. A review of recent developments in natural fibre composites and their mechanical performance. Compos Part A Appl Sci Manuf 2016;83:98–112. https://doi.org/10.1016/j.compositesa.2015.08.038.

[7] Gowda B. Fibres, rubber, firewood, timber, and bamboo. Bangalore, India, Univerity of Agricultural Sciences; 2007. (no. 560065). 2007.

[8] Pari L, Baraniecki P, Kaniewski R, Scarfone A. Harvesting strategies of bast fibre crops in Europe and in China. Ind Crops Prod 2015;68:90–6. https://doi.org/10.1016/j.indcrop.2014.09.010.

[9] Deyholos MK, Potter S. Engineering bast fibre feedstocks for use in composite materials. Biocatal Agric Biotechnol 2014;3:53–7. https://doi.org/10.1016/j.bcab.2013.09.001.

[10] Kumar S, Kant Singh Mer K, Prasad L, Kumar Patel V. A review on surface modification of bast fibre as reinforcement in polymer composites. Int J Mater Sci Appl 2017;6:77–82. https://doi.org/10.11648/j.ijmsa.20170602.12.

[11] Richardson MO, Madera-Santana TJ, Hague J. Natural fibre composites–the potential for the Asian markets. Prog Rubber, Plast Recycl Technol 1998;14:174 –188.

[12] Shahzad A. Hemp fibre and its composites – a review. J Compos Mater 2012;46:973–86. https://doi.org/10.1177/0021998311413623.

[13] Heywood V. Flowering plants of the world. London: Oxford University Press; 1978.

[14] Catling D, Grayson J. Identification of Vegetable Fibres. Dordrecht (Netherlands): Springer, 1982. Chapter 3, Flax (Unum usitatissimum L.);, n.d., p. 12–7. https://doi.org/10.1007/978-94-011-8070-2_3.

[15] Rival A. Oil Palm. In: Pua E-C, Davey MR, editors. Transgenic Crop. VI, vol. 61, Berlin, Heidelberg: Springer; 2007, p. 59–80. https://doi.org/10.1007/978-3-540-71711-9.

[16] Rowell RM, Stout HP. Jute and kenaf. In: Lewin M, Editor. Handb. fibre Chem., Boca Raton (USA): CRC/Taylor & Francis; 2007: n.d., p. 406–50.

[17] Nosbi N, Akil HM, Ishak ZAM, Bakar AA. Behavior of kenaf fibres after immersion in several water conditions. BioResources 2011;6:950–60. https://doi.org/10.15376/BIORES.6.2.950-960.

[18] Akil H, Zamri MH, Osman MR. The use of kenaf fibres as reinforcements in composites. In: Faruk O, Sain M, editors. Biofibre Reinf. Compos. Mater., Elsevier; 2015, p. 138–61. https://doi.org/10.1533/9781782421276.1.138.

[19] Chawla K. Fibrous materials. Cambridge: Cambridge University Press; 2016. https://doi.org/10.1017/CBO9781139342520.

[20] Khan JA, Khan MA. The use of jute fibres as reinforcements in composites. In: Faruk O, Sain M, editors. Biofibre Reinf. Compos. Mater., Elsevier; 2015, p. 3–34. https://doi.org/10.1533/9781782421276.1.3.

[21] Kundu BC, Basak KC, Sarkar PB. Jute in India. Calcutta (India): Indian Central Jute Committee; 1959. n.d.

[22] Fangueiro R, Textile Institute. Fibrous and composite materials for civil engineering applications. Woodhead Publishing; 2011.

[23] Robinson BB. Ramie fibre production. Washington, D.C. (USA). Department of Agriculture; 1940. (no. 585). 1940.

[24] Ciaramello D, Medina JC, Salgado AL de B. Diameter and lenght of ramie stalks and the content, fineness and strenght of the fibre. Bragantia 1963;22:73–80. https://doi.org/10.1590/S0006-87051963000100007.

[25] Zimniewska M, Wladyka-Przybylak M, Mankowski J. Cellulosic bast fibres, their structure and properties suitable for composite applications. In: Kalia S, Kaith BS, Kaur I, editors. Cellul. fibres bio- nano-polymer Compos., Berlin, Heidelberg: Springer; 2011, p. 97–119. https://doi.org/10.1007/978-3-642-17370-7_4.

[26] Charlet K, Baley C, Morvan C, Jernot JP, Gomina M, Bréard J. Characteristics of Hermès flax fibres as a function of their location in the stem and properties of the derived unidirectional composites. Compos Part A Appl Sci Manuf 2007;38:1912–21. https://doi.org/10.1016/j.compositesa.2007.03.006.

[27] Oza S. A study of surface modification effect of hemp fibres on the bulk properties of hemp-poly (lactic acis) composites: Thermal stability, mechanical, thermomechanical, and biodegradability [dissertation]. Charlotte (NC): The University of North Carolina at Charlotte, 2013.

[28] Gorshkova T, Salnikov V V., Pogodina NM, Chemikosova SB, Yablokova E V., Ulanov A V., et al. Composition and distribution of cell wall phenolic compounds in flax (Linum usitatissimum L.) stem tissues. Ann Bot 2000;85:477–86. https://doi.org/10.1006/anbo.1999.1091.

[29] Zykwinska A, Thibault J-F, Ralet M-C, Thibault J, Ralet M. Competitive binding of pectin and xyloglucan with primary cell wall cellulose. Carbohydr Polym 2008;74:957–61. https://doi.org/10.1016/j.carbpol.2008.05.004.

[30] Baley C. Analysis of the flax fibres tensile behaviour and analysis of the tensile stiffness increase. Compos - Part A Appl Sci Manuf 2002;33:939–48. https://doi.org/10.1016/S1359-

835X(02)00040-4.

[31] Virk AS, Hall W, Summerscales J. Modulus and strength prediction for natural fibre composites. Mater Sci Technol 2012;28:864–71. https://doi.org/10.1179/1743284712Y.0000000022doi.org/10.1179/1743284712Y.0000000022.

[32] Batra SK. Other long vegetable fibres: abaca, banana, sisal, henequen, flax, ramie, hemp, sunn, and coir. In: Lewin M, editor. Handb. fibre Chem. Third, CRC Press; 2006, p. 454–93. https://doi.org/doi.org/10.1201/9781420015270.ch8.

[33] Xanthos M. Functional fillers for plastics. Wiley-VCH; 2006.

[34] Mwaikambo LY. Review of the history, properties and application of plant fibres. African J Sci Technol 2006;7:120-133.

[35] Müssig J, Haag K. The use of flax fibres as reinforcements in composites. In: Faruk O, Sain M, editors. Biofibre Reinf. Compos. Mater., Elsevier; 2015, p. 35–85. https://doi.org/10.1533/9781782421276.1.35.

[36] George M, Chae M, Bressler DC. Composite materials with bast fibres: Structural, technical, and environmental properties. Prog Mater Sci 2016;83:1–23. https://doi.org/10.1016/j.pmatsci.2016.04.002.

[37] Reddy N, Yang Y. Biofibres from agricultural byproducts for industrial applications. Trends Biotechnol 2005;23:22–7. https://doi.org/10.1016/j.tibtech.2004.11.002.

[38] Komuraiah A, Kumar NS, Prasad BD. Chemical composition of natural fibres and its

influence on their mechanical properties. Mech Compos Mater 2014;50:359–76. https://doi.org/10.1007/s11029-014-9422-2.

[39] Taj S, Munawar MA, Khan SU. Natural fibre-reinforced polymer composites. Pakistan Acad Sci J 2007;44:129–44.

[40] Thompson NS. Hemicellulose as a biomass resource. In: Soles E, editor. Wood a Agric. Residues, Elsevier; 1983, p. 101–19. https://doi.org/10.1016/B978-0-12-654560-9.50010-X.

[41] Charlet K, Jernot JP, Eve S, Gomina M, Bréard J. Multi-scale morphological characterisation of flax: From the stem to the fibrils. Carbohydr Polym 2010;82:54–61. https://doi.org/10.1016/j.carbpol.2010.04.022.

[42] Hobson RN, Hepworth DG, Bruce DM. Quality of fibre separated from unretted hemp stems by decortication. J Agric Engng Res 2001;78:153–8. https://doi.org/10.1006.

[43] Chellamani DP, Arnold F. Pineapple-leaf fibres: a critical appreciation of recent developments, 1993.

[44] Henriksson G, Akin DE, Hanlin RT, Rodriguez C, Archibald DD, Rigsby LL, et al. Identification and retting efficiencies of fungi isolated from dew-retted flax in the United States and Europe. Appl Environ Microbiol 1997;63:3950–6.

[45] Walker JCF. Basic wood chemistry and cell wall ultrastructure. In: Walker JCF, Butterfield BG, Harris JM, Langrish, T AG, Uprichard JM, editors. Prim. wood Process., Dordrecht (Netherlands): Springer; 1993, p. 23–67. https://doi.org/10.1007/978-94-015-8110-3_2.

[46] Dhakal H, Zhang Z. The use of hemp fibres as reinforcements in composites. In: Faruk O, Sain M, editors. Biofibre Reinf. Compos. Mater., Elsevier; 2015, p. 86–103.

[47] Morrison III W., Archibald D., Sharma HS., Akin D. Chemical and physical characterization of water- and dew-retted flax fibres. Ind Crops Prod 2000;12:39–46. https://doi.org/10.1016/S0926-6690(99)00044-8.

[48] Keller A, Leupin M, Mediavilla V, Wintermantel E. Influence of the growth stage of industrial hemp on chemical and physical properties of the fibres. Ind Crops Prod 2001;13:35–48. https://doi.org/10.1016/S0926-6690(00)00051-0.

[49] Friedrich Munder F, Christian Furll C. Effective processing of bast Fibre plants and mechanical properties of the fibres. 2004, Ottawa, Canada August 1 - 4, 2004, St. Joseph, MI: American Society of Agricultural and Biological Engineers; 2004, p. 1. https://doi.org/10.13031/2013.16960.

[50] Akin DE, Condon B, Sohn M, Foulk JA, Dodd RB, Rigsby LL. Optimization for enzyme-retting of flax with pectate lyase. Ind Crops Prod 2007;25:136–46. https://doi.org/10.1016/j.indcrop.2006.08.003.

[51] Song KH, Obendorf SK. Chemical and biological retting of kenaf fibres. Text Res J 2006;76:751–6.

[52] Yu H, Yu C. Study on microbe retting of kenaf fibre. Enzyme Microb Technol 2007;40:1806–9. https://doi.org/10.1016/j.enzmictec.2007.02.018.

[53] Evans JD, Akin DE, Foulk JA. Flax-retting by polygalacturonase-containing enzyme

mixtures and effects on fibre properties. J Biotechnol 2002;97:223–31.

[54] Van Sumere CF. Retting of flax with special reference to enzyme retting. In: Sharma HS, Van Sumere C, editors. Biol. Process. flax, Belfast (Northern Ireland): M Publications; 1992, p. 157–98.

[55] Md. Tahir P, Ahmed AB, SaifulAzry SOA, Ahmed Z. Retting process of some bast plant fibres and its effect on fibre quality: A review. BioResources 2011;6:5260–81. https://doi.org/10.15376/biores.6.4.5260-5281.

[56] Paridah MT, Khalina A. Effects of soda retting on the tensile strength of kenaf (Hibiscus cannabnius L.) bast fibres. Kenaf EPU; 2009. n.d.

[57] Armstrong B. Process for decorticating fibrous materials. United State patent US 2747232 A. 1956 May 29., 1956.

[58] Gratton JL, Chen Y. Development of a field-going unit to separate fibre from hemp (cannabis sativa) stalk. Appl Eng Agric 2004;20:139–45. https://doi.org/10.13031/2013.15882.

[59] Furll C, Hempel H. Optimization of a new machine for fibre processing by impact stress. Potsdam-Born (Germany): Institute for Agrartechnic; 2000. n.d.

[60] Thakur S, Chen Y, Morrison J. Separation of Fibre and Shivesfrom Decorticated Flax. Appl Eng Agric 2017;33:113–20. https://doi.org/10.13031/aea.11335.

[61] Sadek MA, Chen Y, LaguÃ C, Landry H, Peng Q, Zhong W. Characterization of the shear properties of hemp fibre and core using discrete element method. Trans ASABE

2011;54:2279–85. https://doi.org/10.13031/2013.40641.

[62] Baker ML. Evaluation of a hammer mill and planetary ball mill for hemp fibre decortication [master's thesis]. Winnipeg (MB): University of Manitoba; 2009. 2009.

[63] Leduc PJ, Hill LG, Kelly DH, Stratton MA. Method for decorticating plant material. United States patent US 5720083 A. 1996 July 19., 1996.

[64] Fang Q, Bölöni I, Haque E, Spillman CK. Comparison of energy efficiency betweena roller mill and a hammer mill. Appl Eng Agric 1997;13:631–5. https://doi.org/10.13031/2013.21636.

[65] Baker ML, Chen Y, Laguë C, Landry H, Peng Q, Zhong W, et al. Hemp fibre decortications using a planetary ball mill. Can Biosyst Eng 2010;52:7–15.

[66] Khan MMR, Y. Chen Y, C. Laguë C, H. Landry H, Q. Peng Q, W. Zhong W. Hemp (Cannabis sativa L.) decortication using the drop weight method. Appl Eng Agric 2013;29:79–87. https://doi.org/10.13031/2013.42521.

[67] Chen Y, Liu J, Gratton J-L. Engineering perspectives of the hemp plant, harvesting and processing. J Ind Hemp 2004;9:23–39. https://doi.org/10.1300/J237v09n02_03.

[68] Guzman L. Modelling of energy requirements for fibre peeling and mechanical processing of hemp [master's thesis]. Winnipeg (MB): University of Manitoba; 2012. University of Manitoba, n.d.

[69] Parvin S, Chen Y, Laguë C, Landry H, Peng Q, Zhong W. Post-decortication cleaning of hemp fibre using selected methods. AES Tech Rev Int Journal, Part C Int J Adv Trends Eng

Mater Their Appl 2013;1:53–65.

[70] Akin DE, Dodd RB, Foulk JA. Pilot plant for processing flax fibre. Ind Crops Prod 2005;21:369–78. https://doi.org/10.1016/j.indcrop.2004.06.001.

[71] Münder F, Fürll C, Hempel H. Advanced decortication technology for unretted bast fibres. J Nat Fibres 2004;1:49–65. https://doi.org/10.1300/J395v01n01_04.

[72] Sadek M. Modelling biofibre (hemp) processing using the Discrete Element Method (DEM) [dissertation]. Winnipeg (MB): University of Manitoba; 2013. 2013.

[73] Pecenka R, Furll C. Simulation of natural fibre cleaning in a comb shaker by means of a geometric-statistical mode. ISHS Acta Hortic 2008:205–11.

[74] Xu B, Pourdeyhimi B, Sobus J. Fibre Cross-Sectional Shape Analysis Using Image Processing Techniques. Text Res J 1993;63:717–30. https://doi.org/10.1177/004051759306301204.

[75] Göktepe F, Göktepe Ö, Süleymanov T. The Effect of the Licker-in Speed on Fibre Properties on Modern Carding Machines with a Triple Licker-in. J Text Inst 2003;94:166–76. https://doi.org/10.1080/00405000308630605.

[76] Parvin S. Separation of fibre and core from decorticated hemp [master's thesis]. Winnipeg (MB): University of Manitoba; 2011. 2011.

[77] Yan L, Chouw N, Jayaraman K. Flax fibre and its composites – A review. Compos Part B Eng 2014;56:296–317. https://doi.org/10.1016/j.compositesb.2013.08.014.

[78] Eder M, Burgert I. Natural fibres - function in nature. In: Müssig J, editor. Ind. Appl. Nat. fibres Struct. Prop. Tech. Appl., Chichester, UK: John Wiley & Sons, Ltd; 2010, p. 23–39.

[79] Khan MM, Chen Y, Belsham T, Laguë C, Landry H, Peng Q, et al. Fineness and tensile properties of hemp (Cannabis sativa L.) fibres. Biosyst Eng 2011;108:9–17. https://doi.org/10.1016/j.biosystemseng.2010.10.004.

[80] Saville BP. Physical testing of textiles. Cambridge, UK: Woodhead Publishing Ltd, CRC Press; 1999.

[81] Donaldson L. Microfibril angle: measurement, variation and relationships – A Review. IAWA J 2008;29:345–86. https://doi.org/10.1163/22941932-90000192.

[82] Mohanty AK, Misra M, Hinrichsen G. Biofibres, biodegradable polymers and biocomposites: An overview. Macromol Mater Eng 2000;276–277:1–24. https://doi.org/10.1002/(SICI)1439-2054(20000301)276:1<1::AID-MAME1>3.0.CO;2-W.

[83] Sadek MA, Guzman L, Chen Y, Laguë C, Landry H. Simulation of tensile tests of hemp fibre using discrete element method. Agric Eng Int CIGR J 2014;16:126–35.

[84] Ashby MF. Materials and the environment : eco-informed material choice. Butterworth-Heinemann; 2012.

[85] Xue Y, Du Y, Elder S, Wang K, Zhang J. Temperature and loading rate effects on tensile properties of kenaf bast fibre bundles and composites. Compos Part B Eng 2009;40:189–96. https://doi.org/10.1016/j.compositesb.2008.11.009.

[86] Gassan J, Bledzki AK. Thermal degradation of flax and jute fibres. J Appl Polym Sci 2001;82:1417–22. https://doi.org/10.1002/app.1979.

[87] Rowell RM, Han JS, Rowell JS. Characterization and factors effecting fibre properties. Nat Polym an Agrofibres Compos 2000:115–34.

[88] George G, Joseph K, Nagarajan ER, Tomlal Jose E, George KC. Dielectric behaviour of PP/jute yarn commingled composites: Effect of fibre content, chemical treatments, temperature and moisture. Compos Part A 2013;47:12–21. https://doi.org/10.1016/j.compositesa.2012.11.009.

[89] Bora MN, Baruah GC, Talukdar C. Studies on the dielectric properties of some natural (plant) and synthetic fibres in audio frequency range and their DC conductivity at elevated temperature. Thermochim Acta 1993;2:435–43.

[90] Paul A, Thomas S. Electrical properties of natural-fibre-reinforced low density polyethylene composites: A comparison with carbon black and glass-fibre-filled low density polyethylene composites. J Appl Polym Sci 1997;63:247–66. https://doi.org/10.1002/(SICI)1097-4628(19970110)63:2<247::AID-APP12>3.0.CO;2-#.

[91] Kechaou B, Salvia M, Fakhfakh Z, Juvé D, Boufi S, Kallel A, et al. Electron beam irradiation in natural fibres reinforced polymers (NFRP). Nucl Instruments Methods Phys Res Sect B Beam Interact with Mater Atoms 2008;266:4742–8. https://doi.org/10.1016/j.nimb.2008.06.028.

[92] Yusriah L, Sapuan SM, Zainudin ES, Mariatti M. Characterization of physical, mechanical, thermal and morphological properties of agro-waste betel nut (Areca catechu) husk fibre. J

Clean Prod 2014;72:174–80. https://doi.org/10.1016/j.jclepro.2014.02.025.

[93] Azwa ZN, Yousif BF, Manalo AC, Karunasena W. A review on the degradability of polymeric composites based on natural fibres. Mater Des 2013;47:424–42. https://doi.org/10.1016/j.matdes.2012.11.025.

[94] Yang H, Yan R, Chen H, Lee DH, Zheng C. Characteristics of hemicellulose, cellulose and lignin pyrolysis. Fuel 2007;86:1781–8. https://doi.org/10.1016/j.fuel.2006.12.013.

[95] Parker SP, Howard JN. McGraw-hill concise encylopedia of science and technology. Appl Opt 1989;28:2730.

[96] Methacanon P, Weerawatsophon U, Sumransin N, Prahsarn C, Bergado DT. Properties and potential application of the selected natural fibres as limited life geotextiles. Carbohydr Polym 2010;82:1090–6. https://doi.org/10.1016/j.carbpol.2010.06.036.

[97] Lee S-H, Wang S. Biodegradable polymers/bamboo fibre biocomposite with bio-based coupling agent. Compos Part A Appl Sci Manuf 2006;37:80–91. https://doi.org/10.1016/j.compositesa.2005.04.015.

[98] Yao F, Wu Q, Lei Y, Guo W, Xu Y. Thermal decomposition kinetics of natural fibres: Activation energy with dynamic thermogravimetric analysis. Polym Degrad Stab 2008;93:90–8. https://doi.org/10.1016/j.polymdegradstab.2007.10.012.

[99] Koronis G, Silva A, Fontul M. Green composites: A review of adequate materials for automotive applications. Compos Part B Eng 2013;44:120–7. https://doi.org/10.1016/j.compositesb.2012.07.004.

[100] Azwa ZN, Yousif BF. Thermal degradation study of kenaf fibre/epoxy composites using thermogravimetric analysis. Malaysian Postgrad. Conf., 2013, p. 256–64.

[101] Assarar M, Scida D, El Mahi A, Poilâne C, Ayad R. Influence of water ageing on mechanical properties and damage events of two reinforced composite materials: Flax–fibres and glass–fibres. Mater Des 2011;32:788–95. https://doi.org/10.1016/j.matdes.2010.07.024.

[102] Fotouh A. Characterization and modelling of natural-fibres-reinforced composites (moisture absorption kinetics, monotonic behaviour and cyclic behaviour). 2014.

[103] Madsen B, Hoffmeyer P, Lilholt H. Hemp yarn reinforced composites – III. Moisture content and dimensional changes. Compos Part A Appl Sci Manuf 2012;43:2151–60. https://doi.org/10.1016/j.compositesa.2012.07.010.

[104] Arbelaiz A, Fernández B, Ramos JA, Retegi A, Llano-Ponte R, Mondragon I. Mechanical properties of short flax fibre bundle/polypropylene composites: Influence of matrix/fibre modification, fibre content, water uptake and recycling. Compos Sci Technol 2005;65:1582–92. https://doi.org/10.1016/j.compscitech.2005.01.008.

[105] Panthapulakkal S, Sain M. Studies on the water absorption properties of short hemp--glass fibre hybrid polypropylene composites. J Compos Mater 2007;41:1871–83. https://doi.org/10.1177/0021998307069900.

[106] Dittenber DB, GangaRao HVS. Critical review of recent publications on use of natural composites in infrastructure. Compos Part A Appl Sci Manuf 2012;43:1419–29. https://doi.org/10.1016/j.compositesa.2011.11.019.

[107] Davies GC, Bruce DM. Effect of environmental relative humidity and damage on the tensile properties of flax and nettle fibres. Text Res J 1998;68:623–9. https://doi.org/10.1177/004051759806800901.

[108] Ho TN, Ngo AD. Influence of temperature and humidity on the tensile strength and stiffness of hemp and coir fibres. 5th Int. Can. - Compos. Conf., UBC, Vancouver: 2005.

[109] Symington MC, Banks WM, West OD, Pethrick RA. Tensile testing of cellulose based natural fibres for structural composite applications. J Compos Mater 2009;43:1083–108. https://doi.org/10.1177/0021998308097740.

[110] Célino A, Fréour S, Jacquemin F, Casari P, Mensitieri G. The hygroscopic behavior of plant fibres: a review. Front Chem 2013;1:43. https://doi.org/10.3389/fchem.2013.00043.

[111] Placet V, Cisse O, Boubakar ML. Influence of environmental relative humidity on the tensile and rotational behaviour of hemp fibres. J Mater Sci 2012;47:3435–46. https://doi.org/10.1007/s10853-011-6191-3.

[112] Dhakal H, Zhang Z, Richardson M. Effect of water absorption on the mechanical properties of hemp fibre reinforced unsaturated polyester composites. Compos Sci Technol 2007;67:1674–83. https://doi.org/10.1016/j.compscitech.2006.06.019.

[113] Li X, Tabil LG, Panigrahi S. Chemical treatments of natural fibre for use in natural fibre-reinforced composites: A review. J Polym Environ 2007;15:25–33. https://doi.org/10.1007/s10924-006-0042-3.

[114] Wallenberger FT, Weston NE. Natural fibres, plastics and composites. New York (NY):

Springer; 2003.

[115] Sreekala MS, Kumaran MG, Joseph S, Jacob M, Thomas S. Oil palm fibre reinforced phenol formaldehyde composites: influence of fibre surface modifications on the mechanical performance. Appl Compos Mater 2000;7:295–329. https://doi.org/10.1023/A:1026534006291.

[116] Wu S. Polymer interface and adhesion. New York (NY): M. Dekker; 1982.

[117] Young T. An essay on the cohesion of fluids. Philos Trans R Soc London 1805;95:65–87. https://doi.org/10.1098/rstl.1805.0005.

[118] Fowkes FM. Attractive forces at interfaces. Ind Eng Chem 1964;56:40–52. https://doi.org/10.1021/ie50660a008.

[119] Yuan Y, Lee TR. Contact angle and wetting properties. In: Bracco G, Holst B, editors. Surf. Sci. Tech., vol. 51, Berlin: Springer; 2013, p. 3–34. https://doi.org/10.1007/978-3-642-34243-1_1.

[120] Drelich J. Guidelines to measurements of reproducible contact angles using a sessile-drop technique. Surf Innov 2013;1:248–54. https://doi.org/10.1680/si.13.00010.

[121] McHale G, Newton M. Global geometry and the equilibrium shapes of liquid drops on fibres. Colloids Surfaces A Physicochem Eng Asp 2002;206:79–86. https://doi.org/10.1016/S0927-7757(02)00081-X.

[122] Carroll B. The accurate measurement of contact angle, phase contact areas, drop volume, and Laplace excess pressure in drop-on-fibre systems. J Colloid Interface Sci 1976;57:488–

95. https://doi.org/10.1016/0021-9797(76)90227-7.

[123] Fuentes CA, Tran LQN, Dupont-Gillain C, Vanderlinden W, De Feyter S, Van Vuure AW, et al. Wetting behaviour and surface properties of technical bamboo fibres. Colloids Surfaces A Physicochem Eng Asp 2011;380:89–99. https://doi.org/10.1016/j.colsurfa.2011.02.032.

[124] Hubbe MA, Gardner DJ, Shen W. Contact angles and wettability of cellulosic surfaces: A review of proposed mechanisms and test strategies. BioResources 2015;10:8657–749.

[125] Shen Q, Liu D-S, Gao Y, Chen Y. Surface properties of bamboo fibre and a comparison with cotton linter fibres. Colloids Surfaces B Biointerfaces 2004;35:193–5. https://doi.org/10.1016/j.colsurfb.2004.04.002.

[126] Rong MZ, Zhang MQ, Liu Y, Yan HM, Yang GC, Zeng HM. Interfacial interaction in sisal/epoxy composites and its influence on impact performance. Polym Compos 2002;23:182–92. https://doi.org/10.1002/pc.10424.

[127] Cantero G, Arbelaiz A, Llano-Ponte R, Mondragon III. Effects of fibre treatment on wettability and mechanical behaviour of flax/polypropylene composites. Compos Sci Technol 2003;63:1247–54. https://doi.org/10.1016/S0266-3538(03)00094-0.

[128] Pietak A, Korte S, Tan E, Downard A, Staiger MP. Atomic force microscopy characterization of the surface wettability of natural fibres. Appl Surf Sci 2007;253:3627–35. https://doi.org/10.1016/j.apsusc.2006.07.082.

[129] Schellbach SL, Monteiro SN, Drelich JW. A novel method for contact angle measurements

on natural fibres. Mater Lett 2016;164:599–604. https://doi.org/10.1016/j.matlet.2015.11.039.

[130] Long J, Hyder MN, Huang RYM, Chen P. Thermodynamic modelling of contact angles on rough, heterogeneous surfaces. Adv Colloid Interface Sci 2005;118:173–90. https://doi.org/10.1016/j.cis.2005.07.004.

[131] Heng JYY, Pearse DF, Thielmann F, Lampke T, Bismarck A, Heng JYY. Methods to determine surface energies of natural fibres: a review. Compos Interfaces 2007;14:581–604.

[132] George M, Mussone PG, Bressler DC. Surface and thermal characterization of natural fibres treated with enzymes. Ind Crops Prod 2014;53:365–73. https://doi.org/10.1016/j.indcrop.2013.12.037.

[133] Graupner N, Mussing J. Technical applications of natural fibres: An overview. In: Mussing J, editor. Ind. Appl. Nat. fibres Struct. Prop. Tech. Appl., Bremen (Germany): John Wiley and Sons, Ltd; 2010, p. 63–72. https://doi.org/10.1002/9780470660324.

[134] Kokkala M. Fire tests on loose-fill insulation materials. Espoo: Technical Research Centre of Finland; 1987. n.d.

[135] Kymaïaïnen H-R, Sjoerg A-M. Flax an hemp fibres as raw materials for thermal insulations. Build Environ 2008;43:1261–9. https://doi.org/10.1016/j.buildenv.2007.03.006.

[136] Neubauer F. Insulation materilas based on natural fibres. In: Mussing J, editor. Ind. Appl. Nat. fibres Struct. Prop. Tech. Appl., Bremen (Germany): John Wiley & Sons, Ltd; 2010, p. 481–508.

[137] Neubauer F. Hemp as building material for energy efficient wooden houses. Austria: Technical University Graz; 2002. (Report no: 28615). n.d.

[138] Papadopoulos AM. State of the art in thermal insulation materials and aims for future developments. Energy Build 2005;37:77–86. https://doi.org/10.1016/j.enbuild.2004.05.006.

[139] Fotouh A, Wolodko JD, Lipsett MG. A review of aspects affecting performance and modelling of short-natural-fibre-reinforced polymers under monotonic and cyclic loading conditions. Polym Compos 2015;36:397–409. https://doi.org/10.1002/pc.22955.

[140] Holbery J, Houston D. Natural-fibre-reinforced polymer composites in automotive applications. JOM 2006;58:80–6. https://doi.org/10.1007/s11837-006-0234-2.

[141] Hargitai H, Rácz I, Anandjiwala R. Development of hemp fibre – PP nonwoven composites. Macromol Symp 2006;239:201–8. https://doi.org/10.1002/masy.200690097.

[142] Summerscales J, Dissanayake N, Virk A, Hall W. A review of bast fibres and their composites. Part 2 – Composites. Compos Part A Appl Sci Manuf 2010;41:1336–44. https://doi.org/10.1016/j.compositesa.2010.05.020.

[143] Ku H, Wang H, Pattarachaiyakoop N, Trada M. A review on the tensile properties of natural fibre reinforced polymer composites. Compos Part B Eng 2011;42:856–73. https://doi.org/10.1016/j.compositesb.2011.01.010.

[144] Fortea-Verdejo M, Bumbaris E, Burgstaller C, Bismarck A, Lee KY. Plant fibre-reinforced polymers: where do we stand in terms of tensile properties? Int Mater Rev 2017;62:441–

64. https://doi.org/10.1080/09506608.2016.1271089.

[145] Garkhail SK, Heijenrath RWH, Peijs T. Mechanical properties of natural-fibre-mat-reinforced thermoplastics based on flax fibres and polypropylene. Appl Compos Mater 2000;7:351–72. https://doi.org/10.1023/A:1026590124038.

[146] Oksman K. Mechanical properties of natural fibre mat reinforced thermoplastic. Appl Compos Mater 2000;7:403–14. https://doi.org/10.1023/A:1026546426764.

[147] Faruk O, Bledzki AK, Fink H-P, Sain M. Progress report on natural fibre reinforced composites. Macromol Mater Eng 2014;299:9–26. https://doi.org/10.1002/mame.201300008.

[148] Wielage B, Lampke T, Marx G, Nestler K, Starke D. Thermogravimetric and differential scanning calorimetric analysis of natural fibres and polypropylene. Thermochim Acta 1999;337:169–77. https://doi.org/10.1016/S0040-6031(99)00161-6.

[149] Madsen B, Lilholt H. Physical and mechanical properties of unidirectional plant fibre composites—an evaluation of the influence of porosity. Compos Sci Technol 2003;63:1265–72. https://doi.org/10.1016/S0266-3538(03)00097-6.

[150] Kazemi Najafi S. Use of recycled plastics in wood plastic composites - A review. Waste Manag 2013;33:1898–905. https://doi.org/10.1016/j.wasman.2013.05.017.

[151] Ganster J, Fink HP, Pinnow M. High-tenacity man-made cellulose fibre reinforced thermoplastics - Injection moulding compounds with polypropylene and alternative matrices. Compos Part A Appl Sci Manuf 2006;37:1796–804.

https://doi.org/10.1016/j.compositesa.2005.09.005.

[152] Carus M, Eder A, Dammer L, Korte H, Scholz L, Essel R, et al. Wood-Plastic composites (WPC) and natural fibre composites (NFC): European and global markets 2012 and future trends in automotive and construction. Plast Addit Compd 2015;4:18–21.

[153] Karus M, Kaup M. Natural fibres in the European automotive industry. J Ind Hemp 2002;7:119–31. https://doi.org/10.1300/J237v07n01_10.

[154] Pickering KL. Properties and performance of natural-fibre composites. CRC Press; 2008.

[155] Amiri A, Krosbakken T, Schoen W, Theisen D, Ulven CA. Design and manufacturing of a hybrid flax/carbon fibre composite bicycle frame. Proc Inst Mech Eng Part P J Sport Eng Technol 2018;232:28–38. https://doi.org/10.1177/1754337117716237.

[156] Humphreys MF. The Use of Polymer Composites in Construction. Int. Conf. Smart Sustain. Built Environ., 2003, p. 1–10.

[157] Pacheco-Torgal F, Jalali S. Cementitious building materials reinforced with vegetable fibres: A review. Constr Build Mater 2011;25:575–81. https://doi.org/10.1016/j.conbuildmat.2010.07.024.

[158] Development of design rules for retrofitting by adhesive bonding or bolting either FRP or steel plates to RC beams or slabs in bridges and buildings. Compos Part A Appl Sci Manuf 2001;32:1345–55. https://doi.org/10.1016/S1359-835X(01)00089-6.

[159] Shayan A. The asset management of a long bridge structure affected by alkali-silica reaction. Int. Conf. Alkali-Aggregate React. Concr. 10th, 1996, Melbourne, Victoria, Aust.,

AARC Australia; 1996, p. 1025–32.

[160] Shihong L, Benlian Z, Qiyun Z, Xianrong B. A new kind of super-hybrid composite material for civil use - ramie fibre/Al. Composites 1994;25:225–8. https://doi.org/10.1016/0010-4361(94)90020-5.

[161] Yan L, Chouw N. Behavior and analytical modelling of natural flax fibre-reinforced polymer tube confined plain concrete and coir fibre-reinforced concrete. J Compos Mater 2013;47:2133–48. https://doi.org/10.1177/0021998312454691.

[162] Irawan AP, Soemardi TP, Widjajalaksmi K, Reksoprodjo AHS. Tensile and flexural strength of ramie fibre reinforced epoxy composites for socket prosthesis application. Int J Mech Mater Eng 2011;6:46–50.

[163] Campbell AI, Sexton S, Schaschke CJ, Kinsman H, McLaughlin B, Boyle M. Prosthetic limb sockets from plant-based composite materials. Prosthet Orthot Int 2012;36:181–9. https://doi.org/10.1177/0309364611434568.

[164] Ramesh M. Kenaf (Hibiscus cannabinus L.) fibre based bio-materials: A review on processing and properties. Prog Mater Sci 2016;7879:1–92. https://doi.org/10.1016/j.pmatsci.2015.11.001.

[165] Marsyahyo E, Jamasri, Heru Santoso Budi Rochardjo HSB, Soekrisno. Preliminary investigation on bulletproof panels made from ramie fibre reinforced composites for NIJ level II, IIA, and IV. J Ind Text 2009;39:13–26. https://doi.org/10.1177/1528083708098913.

[166] Pathania D, Singh D. A review on electrical properties of fibre reinforced polymer composites. Int J Theor Appl Sci 2009;1:34–7.

[167] AL-Oqla FM, Sapuan SM, Anwer T, Jawaid M, Hoque ME. Natural fibre reinforced conductive polymer composites as functional materials: A review. Synth Met 2015;206:42–54. https://doi.org/10.1016/j.synthmet.2015.04.014.

[168] W.Sarsby R. Use of 'Limited Life Geotextiles' (LLGs) for basal reinforcement of embankments built on soft clay. Geotext Geomembranes 2007;25:302–10. https://doi.org/10.1016/J.GEOTEXMEM.2007.02.010.

[169] Leson G, Harding M V., Dippon K. Natural fibres in geotextiles for soil protection and erosion control. In: Mussig J, editor. Ind. Appl. Nat. fibres, John Wiley & Sons, Ltd; 2010, p. 509–22.

[170] Sutherland RA, Ziegler AD. Effectiveness of coir-based rolled erosion control systems in reducing sediment transport from hillslopes ARTICLE IN PRESS. Appl Geogr 2007;27:150–64. https://doi.org/10.1016/j.apgeog.2007.07.011.

[171] Ranganathan SR. Development and potential of jute geotextiles. Geotext Geomembranes 1994;13:421–33. https://doi.org/10.1016/0266-1144(94)90006-X.

[172] Rawal A, Anandjiwala R. Comparative study between needlepunched nonwoven geotextile structures made from flax and polyester fibres. Geotext Geomembranes 2007;25:61–5. https://doi.org/10.1016/j.geotexmem.2006.08.001.

[173] English B. Geotextiles—A specific application of biofibres. Proc. a Semin. Res. Ind. Appl.

non food Crop., Copenhagen, Denmark: 1995, p. 79–86.

[174] Xu X, Jayaraman K, Morin C, Pecqueux N. Life cycle assessment of wood-fibre-reinforced polypropylene composites. J Mater Process Technol 2008;198:168–77. https://doi.org/10.1016/J.JMATPROTEC.2007.06.087.

[175] Le Duigou A, Davies P, Baley C. Environmental impact analysis of the production of flax fibres to be used as composite material reinforcement. J Biobased Mater Bioenergy 2011;5:153–65. https://doi.org/10.1166/jbmb.2011.1116.

[176] Wötzel K, Wirth R, Flake M. Life cycle studies on hemp fibre reinforced components and ABS for automotive parts. Die Angew Makromol Chemie 1999;272:121–7. https://doi.org/10.1002/(SICI)1522-9505(19991201)272:1<121::AID-APMC121>3.0.CO;2-T.

[177] Alves C, Silva AJ, Reis LG, Freitas M, Rodrigues LB, Alves DE. Ecodesign of automotive components making use of natural jute fibre composites. J Clean Prod 2010;18:313–27.

[178] González-García S, Hospido A, Feijoo G, Moreira MT. Life cycle assessment of raw materials for non-wood pulp mills: Hemp and flax. Resour Conserv Recycl 2010;54:923–30.

[179] Ardente F, Beccali M, Cellura M, Mistretta M. Building energy performance: a LCA case study of kenaf-fibres insulation board. Energy Build 2008;40:1–10.

Chapter 4: Characterization of Two Alternative Plant Fibres: Canola and Sweet Clover Fibres

4.1. ABSTRACT

Identifying sustainable resources of natural fibres is essential due to high demand for industrial applications such as automotive and biomedical materials. Two alternative fibres obtained from canola and sweet clover stalks were characterized for their properties using energy dispersive X-ray spectroscopy (EDS), fourier transform infrared spectroscopy (FTIR), X-ray diffraction (XRD), thermogravimetric analysis (TGA), contact angle, and tensile test. Hemp and flax fibres, both in use as industrial fibres, were also characterized as conventional fibres. Results showed that all the fibres had the same chemical elements, chemical bonds, and crystallinity index. The thermal stability of the alternative fibres was close to the conventional fibres. The alternative fibres had contact angles less than 90º showing high surface energy. The alternative fibres are suitable where low Young's modulus and tensile strength are required. In contrast, the conventional fibres are suitable where more stiffness and higher strength are required.

4.2. INTRODUCTION

Replacing synthetic based fibres with natural fibre products has been considerably increased due to growing ecological, economic and social awareness, as well as the governmental emphasis on the environmental effects and sustainability. Bast fibres, one type of natural fibre, have been found suitable for use in many industries such as automotive, sport, marine, construction, and biomedical application. Therefore, introducing and optimizing performance of these alternative materials associated with acceptable characteristics are essential to meet this increasing demand. Some of

the alternative fibres already introduced are buriti fibre [1], okra fibre [2], artichoke fibre [3], ferula fibre [4], borassus fibre [5], conium maculatum fibre [6], and coccinia grandis.L fibre [7]. However, there are still many other alternative natural fibres to explore.

In this study, the possibility of using two alternatives natural fibres including canola (*Brassica Napus*) and sweet clover (*Melilotus*) was investigated. The reason to select canola fibres was because Canada is one of the leading countries in the world to produce canola seeds, with a total area harvested of canola in 2017 of 9.27 Mega hectares [8]. After the seeds are harvested, regrettably, almost all canola stalks remain in the field as wastes. Using the canola biomass not only increases the value added of planting canola seeds, but also potentially provides a renewable composite reinforcement. Wild sweet clover plant can also be found Canada wide. This plant is drought resistant, and it can be grown at very northerly latitudes, and it is compatible with saline land [9].

Most commonly used techniques to characterize fibres are microstructural, thermal, surface, and mechanical analyses. The microstructure of the fibres affects their physical and mechanical properties which is used to predict the performance of the developed bio-products. The thermal behavior of natural fibres is of importance since they undergo several high temperature processes during the bio-products manufacturing process. Besides, applying high temperature on the lignocellulosic fibres results in undesirable properties of the final products. Contact angle, which is a good indicator of surface energy of the fibres, is also a good scale of interfacial shear strength (IFSS) controlling the performance of the developed bio-products. Mechanical properties of natural fibres strongly control the mechanical properties of the bio-products [10].

The objective of this investigation was to study the possibility of using canola and sweet clover fibres for industrial purposes by characterizing their microstructural, thermal, surface, and

mechanical properties. The characteristics included energy dispersive X-ray spectroscopy (EDS), fourier transform infrared spectroscopy (FTIR), X-ray diffraction (XRD), thermogravimetric analysis (TGA), contact angle, and tensile properties.

4.3. MATERIALS AND METHODS

4.3.1. Types of plant fibres

Canola (1861 variety) and sweet clover (wild variety) stalks as well as hemp (Alyssa variety), and flax (sorrel variety) stalks were hand-harvested from various locations in Manitoba, Canada. Fibres were hand peeled, air-dried, and stored in paper bags for further analysis. Figure 4.1 shows all of the extracted fibres.

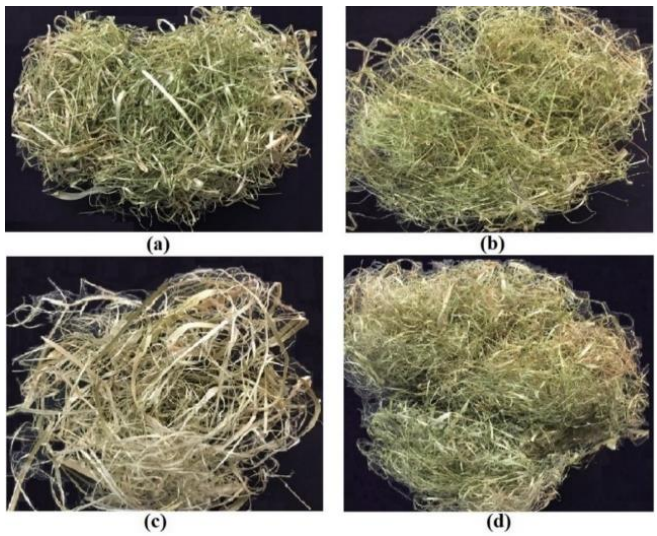

Figure 4.1. (a) Canola fibre, (b) Sweet clover fibre, (c) hemp fibre, and (d) flax fibre

4.3.2. Fibre characterization

4.3.2.1. Microstructural characterization

The microstructural properties of the obtained fibres were studied using energy dispersive X-ray spectroscopy (EDS), Fourier transform-infrared spectroscopy (FTIR), and X-ray diffraction (XRD) tests illustrated as follows.

The EDS is an analytical approach to measure the percentage of different elements such as C and O along with Na, Al, Si, Mg on the fibre surface. However, EDS unable to identify H, which shows the main constituents of natural fibres. A FEI Nova NanoSEM 450 was used to take scanning electron microscopy images to do the EDS analysis. The accelerating voltage of the instrument was set between 10 and 15 kV, spot size was adjusted to 30 µm, and the working distance was kept on 10 mm. The pictures were taken at scanning speed of 4 to obtain a higher quality image. From each type of fibre, three samples were selected, the distribution of the elements was measured four times, and the average values were reported.

The FTIR tests in attenuated total reflection mode were performed to identify the chemical functional groups and the types of bonds in the fibres. A fibre sample was placed against a diamond, and then the infrared beam interacted with the sample at the interface. An evanescent wave penetrated the sample to a shallow depth, while the radiation underwent total internal reflection at the crystal surface, and the absorption of this component produced the infrared spectrum [12]. The IR spectrum of the samples was recorded in the 4000-650 cm^{-1} region with 32 scans and a resolution of 4 cm^{-1}. The number of replications for each type of fibre was four.

The crystallinity index of the studied fibres was determined using XRD analysis. A Bruker D8 DaVinci diffractometer with a CuKα radiation was used to measure the crystallinity index of the samples. After the sample was prepared and placed into the machine, the X-ray detector rotated

over a range of 2Θ values from 10° to 50° at a scanning speed of 0.03 mm/s, a current of 40 mA and voltage of 40 mV.

4.3.2.2. Thermal characterization

Thermal behavior of the samples was analyzed using a Perkin Elmer TGA 7 Thermogravimetric Analyzer. The samples were placed in an alumina pan and heated from room temperature to 600 ºC at a rate of 2 ºC min^{-1} while maintaining a static argon flow of 150 mL/min. The TG graph was plotted in the percentage of mass loss of the fibre at various temperatures. A DTG graph was also generated for the rate of change in weight at various temperatures by using the first derivative values of the mass losses.

4.3.2.3. Contact angle measurement

To measure the contact angle of the fibres, a 700 Sigma One Attension tensiometer (Biolin Scientific) was employed. Prior to doing the tests, all samples were dried for 3 h at 80 ºC. The Washburn capillary rise method was selected to estimate the contact angle. Since the edge of the fibres were not spherical, the first 0.1 mm of each sample was ignored to decrease errors. The immersion speed for both advancing (penetration of the fibre into water) and receding (recession of the fibre from water) was set to 5 mm/min, and the contact angle was measured.

4.3.2.4. Mechanical characterization

Tensile properties of the samples were measured according to ASTM Standard D3822 [13]. A Lloyd LS5 electromechanical testing system (Ametek Inc., FL, USA) was used. The Lloyd system consisted of a frame with a moveable crosshead, a load cell attached to the crosshead, a pair of clamps, a drive system for the crosshead, and a controller software. The bottom clamp was a

stationary grip attached directly to the base of the frame, while the top clamp was connected to the load cell (5 kN capacity) which itself was connected to the crosshead.

To measure tensile properties of the fibres, their cross section area was needed. The cross section area of plant fibres are closer to rectangular than circular [14]. From each fibre type, 20 fibre samples were randomly chosen. They were cut to 25-mm long specimens. Prior to the tensile tests, the width and thickness of the specimens were measured. In the measurement, a fibre was attached to two aluminum cube blocks covered by a double-coated carbon conductive tape (Ted Pella, Inc.). Nine measurements along approximately a 10-mm of the middle section of the fibre were performed. For the tensile test, a fibre specimen was attached to a thin cardboard frame using a fabric adhesive which was secured using the clamps [15]. After cutting the sides of the cardboard frame and setting a 2 N preload to remove any slack, the drive system moved the crosshead up at a loading rate of 25 mm/min until the fibre specimen failed. The Lloyd machine's Nexygen software recorded the tensile load and machine extension for each test and calculated the tensile properties.

4.4. RESULTS AND DISCUSSION

4.4.1. Microstructure analysis

The EDS analysis of the studied fibres demonstrated that the main compositional elements of the canola and sweet clover fibres, like flax and hemp fibre, were carbon and oxygen (Figure 4.2) showing the expected results of lignocellulosic fibres [8,16]. Low percentage of carbon element is desirable since it shows low non-cellulosic materials. The lowest percentage of carbon, regarding both weight and atomic basis, was related to hemp, followed by sweet clover, canola, and highest

in flax fibre. Magnesium and potassium were the other elements found in all of the fibres, but canola fibre was the only one containing sodium.

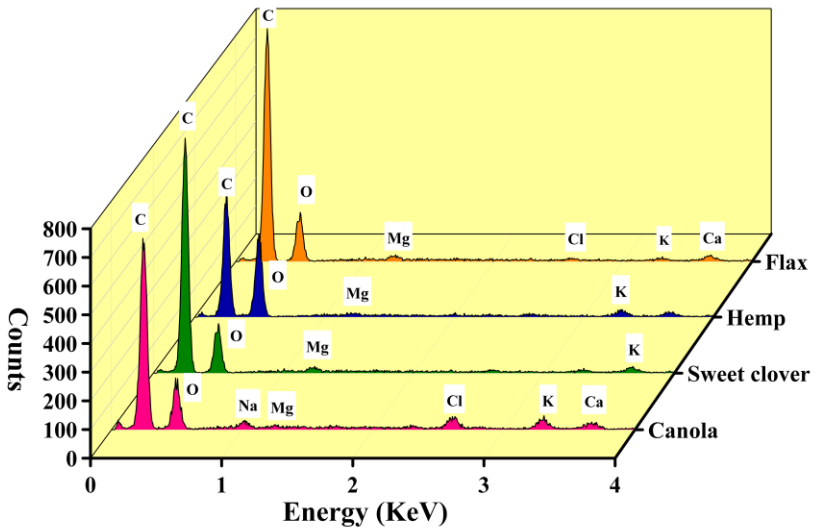

Figure 4.2. The chemical element of the studied fibres

Figure 4.3 demonstrates that the trend of ATR–FTIR spectrum of the new fibres (e.g. canola and sweet clover) were almost similar to the popular plant fibres (e.g. hemp and flax), proving that all of them have the same chemical bonds. The absorbance bonds at around 3400 to 3200 cm^{-1} were due to O-H stretching via vibration as well as hydrogen bond of the O-H stretching vibration in cellulose, hemicellulose, lignin, and pectin [5,17]. The C-H stretching vibration of the general organic material such as wax produced a peak at around 2900 cm^{-1} [12]. The absorbance peaks at around 2840 cm^{-1} could be explained by the C-H stretching vibration from CH and CH_2 in all chemical components of the fibres [17]. The peaks at around 1735 cm^{-1} were associated to the C=O ester bond from pectin [12] and the peak centered around 1600 cm^{-1} represents O-H stretching group in the absorbed water [18]. The absorbance at around 1595 and 1505 cm^{-1} arose from C=C stretching of aromatic ring of the lignin [3,19]. The absorbance peaks at around 1475 cm^{-1} were attributed to CH_2 symmetric bending in cellulose, lignin, hemicellulose, and pectin [19,20]. The

vibration of C-H and C-O groups of the aromatic ring at absorbance around 1365 and 1315 cm^{-1} were because of polysaccharides [21,22]. The C-O stretching vibration of the acetyl group in lignin produced a peak at around 1235 cm^{-1} [22,23]. The absorbance at around 1155 cm^{-1} and 1105 cm^{-1} was respectively the characteristics bonds for C-C ring and C-O-C glycosidic ether of the polysaccharide components which were largely cellulose [12]. The b-glycosidic linkages between the monosaccharides of cellulose and hemicellulose generated intense peaks at around 900 cm^{-1} [3,19].

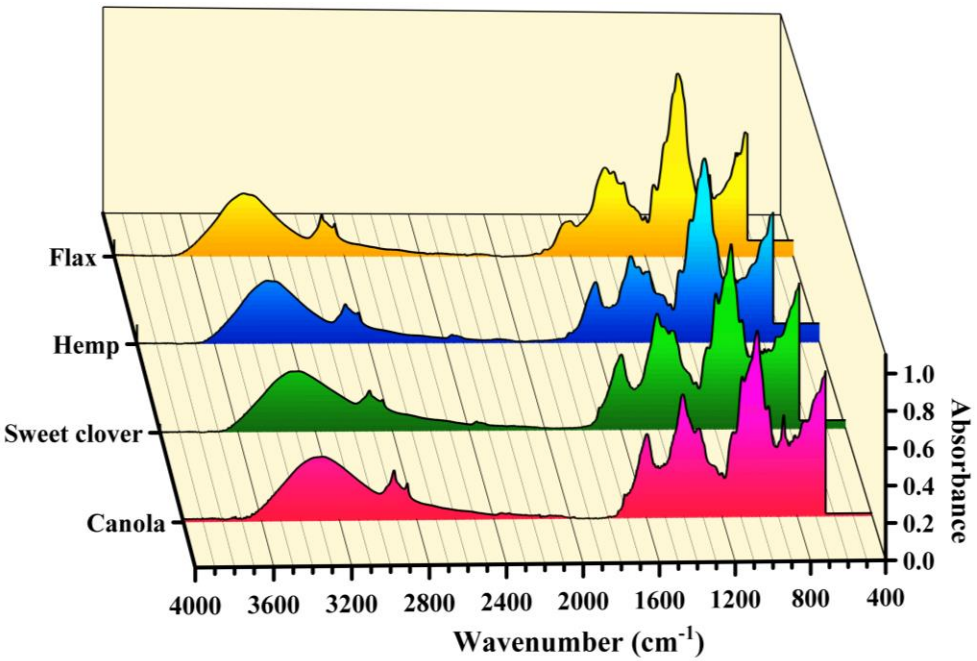

Figure 4.3. The average FTIR spectrum of the studied fibres

Crystallinity index, which is one of the most important structural parameters, strongly affects mechanical properties of the natural fibres such that natural fibres with high crystallinity index have greater stiffness. Figure 4.4 shows the X-ray diffraction graph of the investigated fibres. The two main reflections at $18^{o}<2\Theta<20^{o}$ and $22^{o}<2\Theta<24^{o}$ corresponds to the amorphous and crystalline part in the fibre respectively.

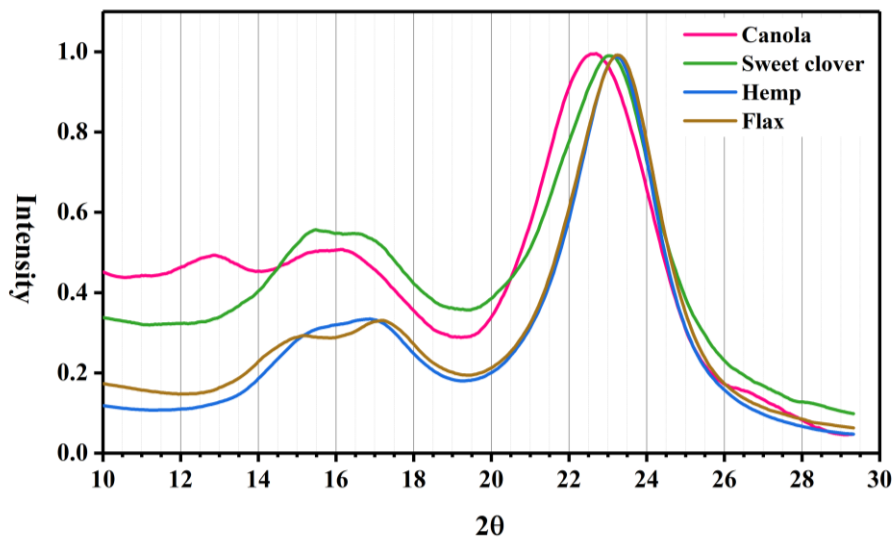

Figure 4.4. X-ray diffraction curves for the studied fibres

From qualitative standpoint, the intensity of crystalline parts of the fibres was almost similar but the amorphous parts of the new fibres were higher than the common fibres. It could be concluded that the structure of hemp and flax fibres was more crystalline compared to the canola and sweet clover fibres. To compare the fibres from a quantitative standpoint, the crystallinity index was calculated using equation (4.1) [24].

$$CI = \frac{I_{002} - I_{amp}}{I_{002}} \times 100 \qquad (4.1)$$

where I_{002} is the intensity of peak around crystalline phase, and I_{amp} is the intensity of peak around amorphous phase. The results showed the crystallinity index of the canola and sweet clover fibres were 71% and 62%, respectively, which were higher than the alternative plant fibres including 52.27% for Sansevieria ehrenbergii fibre [24], 60% for Sansevieria cylindrica fibre [25], and 68% for A. officinalis L. fibre [26]. The crystallinity index of the hemp (82%) and flax (80%) fibres were the highest but in the same range with what was found in the literatures [6,27,28].

4.4.2. Thermal analysis

The TG and DTG curves of the investigated fibres showed that thermal behavior of the new lignocellulosic fibres was similar to the hemp and flax fibres (Figure 4.5). The initial peaks in the DTG graph located between 30 to 100 ºC were due to the vaporization of moisture in the fibre. Hemicellulose was the first chemical composition to decompose because of their amorphous structure and positions within the fibres. For the studied fibres, the range for hemicellulose decomposition was from 218.63 ºC to 305.2 ºC. The initial degradation temperature where hemicelluloses started decomposing, referring to the thermal stability of the fibres, for canola and sweet clover fibres was 219.78 ºC and 219.2 ºC, respectively. These values were close to the initial degradation temperature of flax (218.63 ºC) and hemp fibre (237.55 ºC). It is clear that canola and sweet clover fibres had similar thermal stability to hemp, flax, and those of other natural fibres such as buriti fibre (150 ºC) [2], okra fibre (220 ºC) [3], and artichoke fibre (230 ºC) [4]. Cellulose was the second chemical composition starting to decompose. The reason for higher thermal stability of cellulose compared to hemicellulose was several microfibrils, which are responsible for fibre reinforcement, located at the structure of cellulose. The range where cellulose of the studied fibres was decomposed varied from 292.17 ºC to 413 ºC. The maximum degradation temperature showing decomposition of cellulose for the canola, sweet clover, hemp, and flax were 331 ºC, 354.51 ºC, 333.86 ºC, and 348.78 ºC, respectively. Lignin provides rigid support to the fibres and supplies higher thermal stability to the fibres than hemicellulose and cellulose. Lignin decomposed from very low temperature to 600 ºC due to its complex composition structure of aromatic rings with various branches [11]. The small peaks at temperatures ranged from 460 ºC to 520 ºC were because of oxidative degradation of the charred residue. Residues of 31%, 28%, 26%,

and 29% at 600 °C for canola, sweet clover, hemp, and flax fibres, respectively, were probably owing to the non-oxidizing atmosphere used in the experiment [2].

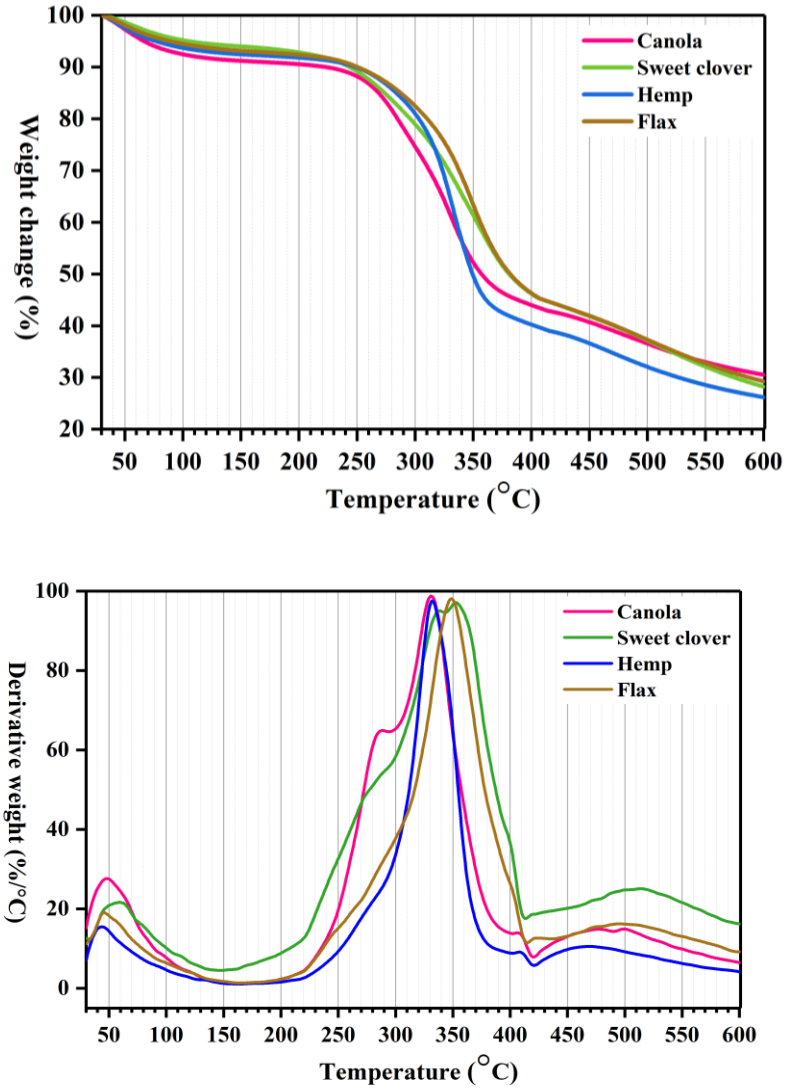

Figure 4.5. The weight loss curve (TG) and derivative curve (DTG) obtained from the TGA analysis for the studied fibres

4.4.3. Contact angle analysis

The advancing and receding angles of the examined fibres were measured. There was a difference between advancing and receding angle in which advancing angles for all fibres were greater than receding angles. The reasons for this hysteresis (e.g. differences between advancing and receding

angles) were the geometric and chemical heterogeneity, or small scale roughness, of the samples' surface. Table 4.1 shows the advancing and receding angles of the studied fibres. The contact angles for canola and sweet clover fibres, regardless of advancing or receding, were less than 90º, similar to hemp and flax fibres. A contact angle less than 90° is desirable as it shows high surface energy and high wettability meaning that the matrix will spread over a large area of fibres and high IFSS is achievable. However, contact angles greater than 90º show minimum tendency of the matrix to contact with fibres which is undesirable. The minimum advancing and receding angle (e.g. the most favorable) were for sweet clover and canola fibre, 71.63º and 29.36º, respectively, while the flax fibre had the maximum angle for both advancing (81.42º) and receding (64.96º). The highest hysteresis value was for canola fibres which was desirable since it showed high adhesion of matrices to the canola fibres. The reason for different values of contact angle were due to different structural arrangements of the chemical components of a single fibre of the studied fibres. A single fibre is constituted from primary and secondary walls. The primary wall is made of hemicellulose, pectin compounds, and glycoproteins. The secondary wall is a three-layer structure (S1, S2, and S3) which are made from cellulose, hemicellulose, and lignin. Therefore, the polarity of different fibres may vary due to varying chemical components in each section of the fibre network [10].

Table 4.1. Contact angle of the studied fibres.

Fibre	Advancing angle	Receding angle
Canola	79.17	29.36
Sweet clover	71.63	52.13
Flax	81.42	64.96
Hemp	77.36	59.89

4.4.4. Mechanical analysis

Typical stress-strain curves for all of the plant fibres are shown in Figure 4.6. For all of the fibres, stress increased to the peak value and then suddenly dropped to zero. Most samples failed at maximum strength and behaved like brittle materials. Other studies also proved that natural fibres behave like a brittle material [4,25,26].

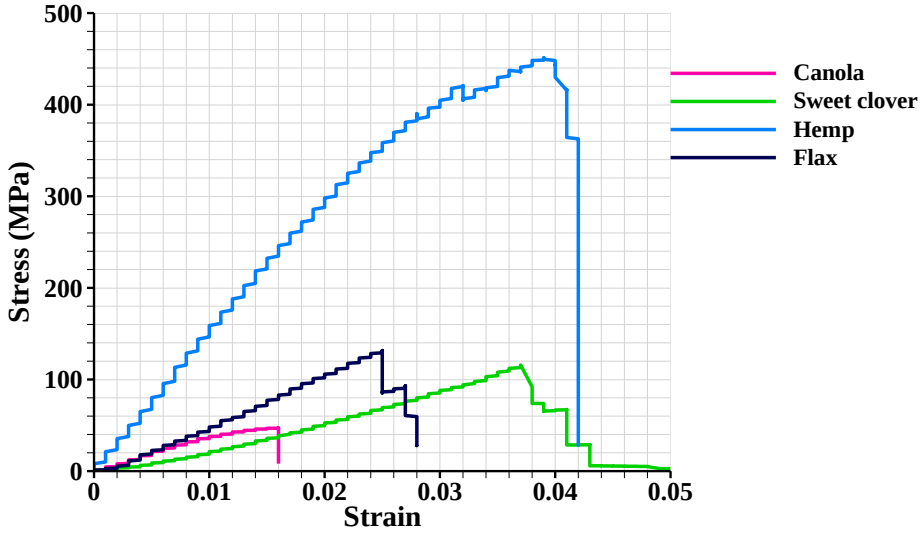

Figure 4.6. The stress-strain curves for the investigated plant fibres

There was a high scatter in the tensile properties of the fibres even within one specific fibre (Figure 4.7). This variation was due to three main factors including plant characteristics (i.e. growing condition, agronomic practices, harvesting time, fibre extraction method, and the presence of defects), cross section area measurements, and test parameters/conditions [27].

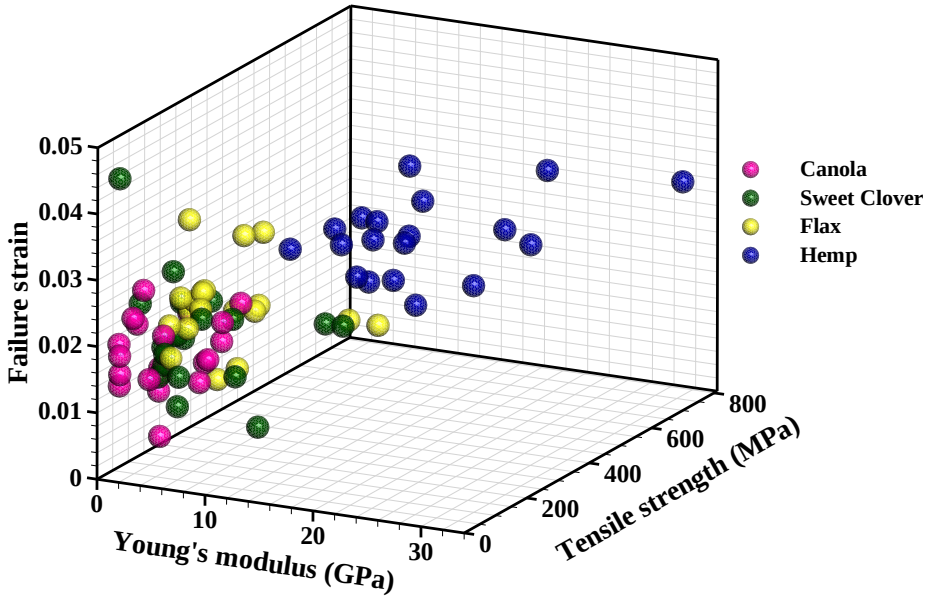

Figure 4.7. Failure strain, tensile strength, and Young's modulus of the studied fibre bundles.

Where there is a large variation among data, the two-parameter Weibull distribution is used to statistically analyze the reliability of the data. Several researchers used Weibull cumulative distribution to determine the reliability of mechanical performance of natural fibres [3,4,28–30]. The results of Weibull distribution analysis showed a reasonable approximation of the experimental data for both tensile strength and Young's modulus.

Table 4.1. shows statistical parameters obtained after analyzing the data. The shape parameter which is also known as Weibull modulus shows the variability of the data, and a higher value is more desirable. For both tensile strength and Young's modulus, the hemp fibres had the lowest variability in data (e.g. highest shape parameter), but the highest variability (e.g. lowest shape parameter) for tensile strength was related to the canola fibres, while the highest variability for Young's modulus was for the sweet clover fibres (Table 4.2). The scale parameter which is also known as Weibull characteristic is the 63.2 percentile of the data. It has the same trend as the average tensile strength and Young's modulus. The hemp fibre was the strongest and stiffest. The scale parameter for the tensile strength and Young's modulus of the hemp fibre bundle were 456.26

MPa and 19.36 GPa, respectively. In contrast, canola fibre bundle was the weakest in which the scale parameter for tensile strength was 57.45 MPa. The flax fibre bundle was the most flexible with a scale parameter of 9.39 GPa for Young's modulus (Table 4.1). The scale parameter for tensile strength of hemp and flax fibres were significantly higher than canola and sweet clover demonstrating that hemp and flax fibres are suitable to be used as reinforcement in structural materials, but canola and sweet clovers are appropriate for other applications where low elastic modulus and normal tensile strength are required.

Table 4.2. Weibull distribution parameters for mechanical properties of the studied plant fibres.

		Canola	Sweet clover	Flax	Hemp
Tensile strength (MPa)	Shape parameter	1.57	2.34	2.43	3.32
	Scale parameter	57.45	71.26	141.23	456.26
	Mean	51.61	63.14	125.24	409.40
	Standard deviation	33.64	28.71	54.79	135.85
Young's modulus (GPa)	Shape parameter	1.93	1.62	2.30	3.34
	Scale parameter	5.57	8.52	9.39	19.36
	Mean	4.94	7.63	8.32	17.38
	Standard deviation	2.66	4.82	3.83	5.73

The mechanical properties of the canola and sweet clover fibres are comparable to those of other natural fibres recently introduced as potential reinforcement in composites. For example, tensile strength and Young's modulus of abaca, alfa, coir, cotton, jute, and sisal fibres were respectively 12, 350, 140.5, 500, 325, 460 MPa, and 41, 22, 6, 8, 37.5, 15.5 GPa [31].

4.5. CONCLUSIONS

The microstructural, thermal, surface, and mechanical properties of the two alternative lignocellulosic fibres (e.g. canola and sweet clover) were compared with two popular lignocellulosic fibres (e.g. hemp and flax). The following conclusions were drawn:

- The microstructural analysis showed that the alternative fibres had the same microstructure as the conventional ones. The main chemical elements, chemical bonds, and crystallinity index of the alternative fibres were highly similar.
- When heated, the behavior of all the fibres were the same. The thermal stability of the alternative fibres was high enough to be used for developing commercial bio-products.
- Surface analysis demonstrated that the contact angles of the new fibres were less than 90 ° showing high surface energy and high wettability which leads to high IFSS.
- The results of tensile tests showed that canola and sweet clover fibres were associated with low Young's modulus and acceptable tensile strength, while hemp and flax fibres were associated with high stiffness and high strength.

One of the potential applications of canola and sweet clover fibres is biomedical industry to develop cancellous bone, tendon, and ligament; where the low stiffness and acceptable tensile strength is desirable. Another potential application of these alternative fibres is artificial flower industry. Further research is still required in this regard.

4.6. ACKNOWLEDGMENT

This work was supported by Natural Sciences and Engineering Research Council of Canada (NSERC).

4.7. REFERENCES

[1] da Silva Santos R, de Souza AA, De Paoli M-A, de Souza CML. Cardanol–formaldehyde thermoset composites reinforced with buriti fibres: Preparation and characterization. Compos Part A Appl Sci Manuf 2010;41:1123–9. https://doi.org/10.1016/J.COMPOSITESA.2010.04.010.

[2] De Rosa IM, Kenny JM, Puglia D, Santulli C, Sarasini F. Morphological, thermal and mechanical characterization of okra (Abelmoschus esculentus) fibres as potential reinforcement in polymer composites. Compos Sci Technol 2010;70:116–22. https://doi.org/10.1016/J.COMPSCITECH.2009.09.013.

[3] Fiore V, Valenza A, Di Bella G. Artichoke (Cynara cardunculus L.) fibres as potential reinforcement of composite structures. Compos Sci Technol 2011;71:1138–44. https://doi.org/10.1016/j.compscitech.2011.04.003.

[4] Seki Y, Sarikanat M, Sever K, Durmuşkahya C. Extraction and properties of Ferula communis (chakshir) fibres as novel reinforcement for composites materials. Compos Part B Eng 2013;44:517–23. https://doi.org/10.1016/J.COMPOSITESB.2012.03.013.

[5] Obi Reddy K, Uma Maheswari C, Shukla M, Song JI, Varada Rajulu A. Tensile and structural characterization of alkali treated Borassus fruit fine fibres. Compos Part B Eng 2013;44:433–8. https://doi.org/10.1016/j.compositesb.2012.04.075.

[6] Kılınç AÇ, Köktaş S, Seki Y, Atagür M, Dalmış R, Erdoğan ÜH, et al. Extraction and investigation of lightweight and porous natural fibre from Conium maculatum as a potential reinforcement for composite materials in transportation. Compos Part B Eng 2018;140:1–8. https://doi.org/10.1016/j.compositesb.2017.11.059.

[7] Senthamaraikannan P, Kathiresan M. Characterization of raw and alkali treated new natural cellulosic fibre from Coccinia grandis.L. Carbohydr Polym 2018;186:332–43. https://doi.org/10.1016/j.carbpol.2018.01.072.

[8] Statistics Canada. Table 001-0010 - Estimated areas, yield, production and average farm price of principal field crops, in metric units, annual, CANSIM. 2017.

[9] Rigal M, Rigal L, Vilarem G, Vandenbossche V. Sweet Clovers, a Source of Fibres Adapted for Growth on Wet and Saline Soils. J Nat Fibres 2016;13:410–22. https://doi.org/10.1080/15440478.2015.1029202.

[10] Sadrmanesh V, Chen Y. Bast fibres: structure, processing, properties, and applications. Int Mater Rev 2018;64:381–406. https://doi.org/10.1080/09506608.2018.1501171.

[11] Garside P, Wyeth P. Identification of Cellulosic Fibres by FTIR Spectroscopy - Thread and Single Fibre Analysis by Attenuated Total Reflectance. Stud Conserv 2003;48:269–75. https://doi.org/10.1179/sic.2003.48.4.269.

[12] ASTM. Standard Test Method for Tensile Properties of Single Textile Fibres. ASTM Int USA 2015:1–10. https://doi.org/10.1520/D3822.

[13] Sadrmanesh V, Chen Y. Simulation of tensile behavior of plant fibres using the Discrete Element Method (DEM). Compos Part A Appl Sci Manuf 2018;114:196–203. https://doi.org/10.1016/J.COMPOSITESA.2018.08.023.

[14] Sadek MA, Guzman L, Chen Y, Laguë C, Landry H. Simulation of tensile tests of hemp fibre using discrete element method. Agric Eng Int CIGR J 2014;16:126–35.

[15] Manimaran P, Senthamaraikannan P, Sanjay MR, Marichelvam MK, Jawaid M. Study on

characterization of Furcraea foetida new natural fibre as composite reinforcement for lightweight applications. Carbohydr Polym 2018;181:650–8. https://doi.org/10.1016/J.CARBPOL.2017.11.099.

[16] Yang H, Yan R, Chen H, Lee DH, Zheng C. Characteristics of hemicellulose, cellulose and lignin pyrolysis. Fuel 2007;86:1781–8. https://doi.org/10.1016/j.fuel.2006.12.013.

[17] Olsson A-M, Salmén L. The association of water to cellulose and hemicellulose in paper examined by FTIR spectroscopy. Carbohydr Res 2004;339:813–8. https://doi.org/10.1016/J.CARRES.2004.01.005.

[18] Konczewicz W, Zimniewska M, Valera MA. The selection of a retting method for the extraction of bast fibres as response to challenges in composite reinforcement. Text Res J 2018;88:2104–19. https://doi.org/10.1177/0040517517716902.

[19] Sgriccia N, Hawley MC, Misra M. Characterization of natural fibre surfaces and natural fibre composites. Compos Part A Appl Sci Manuf 2008;39:1632–7. https://doi.org/10.1016/j.compositesa.2008.07.007.

[20] Le Troedec M, Sedan D, Peyratout C, Bonnet JP, Smith A, Guinebretiere R, et al. Influence of various chemical treatments on the composition and structure of hemp fibres. Compos Part A Appl Sci Manuf 2008;39:514–22. https://doi.org/10.1016/J.COMPOSITESA.2007.12.001.

[21] Fiore V, Scalici T, Nicoletti F, Vitale G, Prestipino M, Valenza A. A new eco-friendly chemical treatment of natural fibres: Effect of sodium bicarbonate on properties of sisal fibre and its epoxy composites. Compos Part B Eng 2016;85:150–60. https://doi.org/10.1016/j.compositesb.2015.09.028.

[22] Li Y, Pickering KL. Hemp fibre reinforced composites using chelator and enzyme treatments. Compos Sci Technol 2008;68:3293–8. https://doi.org/10.1016/j.compscitech.2008.08.022.

[23] Segal L, Creely JJ, Martin AE, Conrad CM. An empirical method for estimating the degree of crystalline of native cellulose using the X-Ray Diffractometer. Text Res J 1959;29:786–94. https://doi.org/10.1177/004051755902901003.

[24] Sathishkumar TP, Navaneethakrishnan P, Shankar S, Rajasekar R. Characterization of new cellulose sansevieria ehrenbergii fibres for polymer composites. Compos Interfaces 2013;20:575–93. https://doi.org/10.1080/15685543.2013.816652.

[25] Sreenivasan VS, Somasundaram S, Ravindran D, Manikandan V, Narayanasamy R. Microstructural, physico-chemical and mechanical characterisation of Sansevieria cylindrica fibres-An exploratory investigation 2010. https://doi.org/10.1016/j.matdes.2010.06.004.

[26] Sarikanat M, Seki Y, Sever K, Durmus ßkahya C. Determination of properties of Althaea officinalis L. (Marshmallow) fibres as a potential plant fibre in polymeric composite materials 2013. https://doi.org/10.1016/j.compositesb.2013.09.041.

[27] Efendy MGA, Pickering KL. Comparison of harakeke with hemp fibre as a potential reinforcement in composites. Compos PART A 2014;67:259–67. https://doi.org/10.1016/j.compositesa.2014.08.023.

[28] Sathishkumar TP, Navaneethakrishnan P, Shankar S, Rajasekar R, Rajini N. Characterization of natural fibre and composites - A review. J Reinf Plast Compos 2013;32:1457–76. https://doi.org/10.1177/0731684413495322.

[29] Fiore V, Scalici T, Valenza A. Characterization of a new natural fibre from Arundo donax L. as potential reinforcement of polymer composites. Carbohydr Polym 2014;106:77–83. https://doi.org/10.1016/j.carbpol.2014.02.016.

[30] Xue Y, Du Y, Elder S, Wang K, Zhang J. Temperature and loading rate effects on tensile properties of kenaf bast fibre bundles and composites. Compos Part B Eng 2009;40:189–96. https://doi.org/10.1016/j.compositesb.2008.11.009.

[31] Liu D, Han G, Huang J, Zhang Y. Composition and structure study of natural Nelumbo nucifera fibre. Carbohydr Polym 2009;75:39–43. https://doi.org/10.1016/J.CARBPOL.2008.06.003.

[32] Weibull W. A Statistical Theory of the Strength of Materials. A.B. Gunnar Tisells; 1939.

[33] Andersons J, SPARNINS E, JOFFE R, WALLSTROM L. Strength distribution of elementary flax fibres. Compos Sci Technol 2005;65:693–702. https://doi.org/10.1016/j.compscitech.2004.10.001.

[34] Orue A, Jauregi A, Unsuain U, Labidi J, Eceiza A, Arbelaiz A. The effect of alkaline and silane treatments on mechanical properties and breakage of sisal fibres and poly(lactic acid)/sisal fibre composites. Compos PART A 2016;84:186–95. https://doi.org/10.1016/j.compositesa.2016.01.021.

[35] Komuraiah A, Kumar NS, Prasad BD. Chemical composition of natural fibres and its influence on their mechanical properties. Mech Compos Mater 2014;50:359–76. https://doi.org/10.1007/s11029-014-9422-2.

Chapter 5: Simulation of Tensile Behavior of Plant Fibres Using the Discrete Element Method (DEM)

5.1. ABSTRACT

Tensile behavior of plant fibres significantly affect mechanical performance of the fibre reinforced composites. A numerical model was developed to simulate the tensile behavior of a plant fibre using the Discrete Element Method (DEM). The model fibre was constructed with spherical particles bonded together. The model outputs were tensile strength (σ_{macro}) and Young's modulus (E_{macro}) of fibre. Tensile tests were conducted to measure these two properties of hemp fibre to calibrate model micro-parameters. Simulation results showed that the most influential micro-parameters were micro-strength of the bond (σ_{micro}) and Young's modulus of particles (E_{micro}). The following relationships were found: σ_{micro} = 1.89 σ_{macro} and E_{micro}= 0.99 E_{macro}. Using the tensile test data of hemp fibre, the calibrated values were 721.81 MPa for σ_{micro} and 19.50 GPa for E_{micro}. With the results from this study, the micro-parameters can be determined for DE modelling of any plant fibres, such as flax and Jute.

5.2. INTRODUCTION

Natural fibres have gained popularity to be used in bioproducts such as natural fibre reinforced composites because of the concerns for the environment and depleting fossil fuels which arise from using synthetic fibres. Besides being biodegradable, natural fibres also have other attractive properties, such as high mechanical strength relative to the low density. Among approximately 2000 species of natural fibre plants, a few of them provides around 90% of the natural fibres in the world [1]. Hemp is one of them. Natural fibres extracted from plant stalk are in bundle forms. A

fibre bundle consists of individual single fibres connected by middle lamella (Figure 5.1), providing the mechanical strength to the fibre. There is a small channel inside a single fibre called lumen. The channel, which is filled with proteins and pectin, contributes little to the strength of natural fibres.

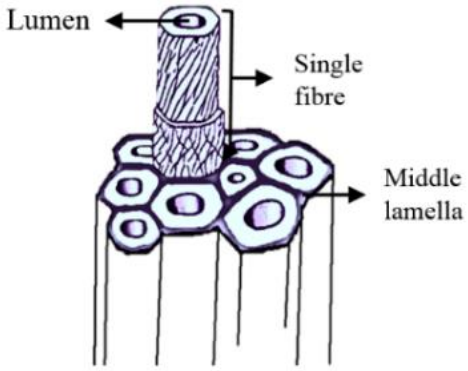

©Figure 5.1. A fibre bundle. Source [2]: permission from National Programme on Technology Enhanced Learning with modification.

When tensile loads are applied to natural fibre based products such as continuous fibre reinforced composites, particularly along the fibre direction, a primary concern is rapture of fibre boundles in the matrix. This failure of fibre bundles significantly decreases the mechanical performance of the bioproducts. Therefore, information on tensile strengths of fibre bundles is critical for making high strength bioproducts. Tensile properties of natural fibres including tensile strength and Young's modulus have been documented using experimental studies. Tensile strength of hemp fibres varied from 244 to 900 MPa [2–4], which were close to those of flax fibre (345 to 950 MPa) [5]. The values reported for Young's modulus of hemp fibre ranged from 8.6-35 GPa [2,4]. The variability in tensile properties is attributable to many factors, including growing condition and agronomic practices. For example, the specific tensile strength of hemp fibres increased from 22.9 to 44.0 cN/tex when plant density increased from 50 to 350 plants/m^2 [6]. Retting condition is expected to have some effects. However, similar tensile strengths have been

reported for retted hemp (343 MPa) and unretted hemp (358 MPa) [3]. Another affecting factor is related to the cross section area of natural fibres. When the cross section area of hemp fibres was envisioned as circular the reported tensile strength and Young's modulus were respectively 277 MPa and 9.5 GPa while when it was considered as rectangular they were 244 MPa and 8.6 GPa [4].

Traditional experimental methods to analyze tensile behaviors of natural fibres are time consuming and requires special equipment (such as Instron and universal machines) that may not always available. Thus, researchers have taken modelling approach to simulate tensile behaviors of natural fibres. The Discrete Element Modelling (DEM) introduced by Cundall (1974) can simulate dynamic behaviors of continues and discontinues solid materials [8]. This method can also be used to simulate tensile behaviors of material. For example, Khattak and Khattab (2013) developed a 2D DEM model to analyze tensile behavior of synthetic fibre reinforcement composites. Roux et al. (2015) used a DEM model to simulate the rapture response of muscle tendon complex. In simulating tensile tests of high-carbon steel using the DEM, Chen et al. (2016) found a correlation between DEM input parameters and mechanical parameters of the steel. These studies have demonstrated that the DEM was a promising tool to simulate varieties of materials under tensile loads. However, there has been only one DEM model developed to predict the tensile behavior of hemp fibres [3]. In this existing model, the total number of particles used to construct a fibre was 15 only. This few numbers of particles are insufficient to reflect the structural failure of a hemp fibre bundle under a tensile load. Furthermore, calibration of DEM input parameters of natural fibres was not been thoroughly investigated.

Calibration of model parameters is one of the major challenges of using the DEM. The main difficulties are that many parameters are required as model inputs, model parameters (referred as

to micro-parameters) are not measurable, and they are not directly related to properties of the material (referred to macro-parameters) that is simulated. The most common method that has been used is the reverse calibration procedure in which micro-parameters are adjusted until the macro-parameters match experimental results [12]. Using this method for calibrations, rests are required. If the relationships between micro-parameters and macro-parameter are developed, one can use the relationship for predictions without the need of doing tests.

Therefore, the main objectives of this study were to (1) measure tensile properties of hemp fibre, (2) develop a model using the DEM to simulate a plant fibre under tensile loads, (3) estimate the combination effects of micro-parameters on macro-properties, and (4) establish relationships between the DEM input micro-parameters and output macro-properties, which is essential for future simulations of micro-dynamics of plant fibre using the DEM models.

5.3. TENSILE EXPERIMENT

5.3.1. Fibre bundle description

In this investigation, hemp (*Cannabis sativa*) fibre, which is the most popular types of plant fibres, was used for tensile tests. It was obtained from a previous study conducted by Hermann (2008). The hemp was grown in Parkland Region of Western Manitoba, Canada. The plant population density was 100 plants/m^2. Plants, randomly chosen in the field, were harvested by hand at the beginning of September when 95% of the mature seed present was hard. Hemp stems, 200-mm long, were cut in the middle of the plants, and 650-850 mm from the soil surface. To obtain fibres from those stems, water retting was used by placing the stems in a container for 7 to 10 days in water at 36° C and 6.8 pH. Then stems were rinsed in tap water and placed in drying racks, next to

heater fans, for four days. After that, fibre bundles were detached from the dried stems using a reciprocating blade-type breaker/decorticator. The final fibres are shown in Figure 5.2.

Figure 5.2. Hemp fibre samples used for tensile tests.

5.3.2. Fibre bundle dimension measurements

To determine the tensile strength of a fibre, the cross-section area of the fibre is required. Thus, dimensions of the cross-sections of fibre were measured. A total of 30 fibres were randomly picked up from the fibres shown in Figure 5.2. Through an optical microscope (Wild Heerbrugg AG model, Gais, Switzerland) (Figure 5.3), it was observed that the cross-section of the fibre was close to a rectangular. For measurement, a fibre was glued on two aluminum cube blocks covered by a double-coated carbon conductive tape (Ted Pella, Inc.). The fibre was placed under the microscope, which was connected to a computer to measure the width and thickness. For each dimension, nine readings were taken along approximately a 10-mm of the middle section of the fibre, and the average width or thickness of the nine readings was reported.

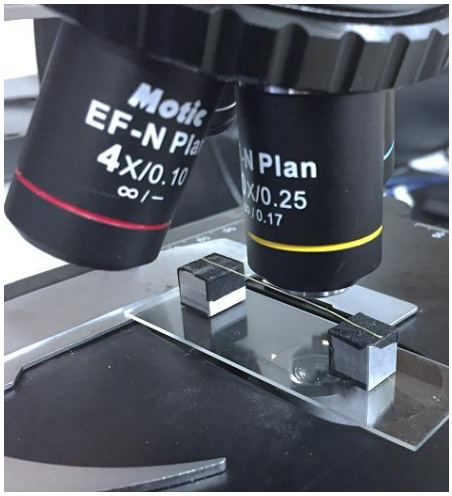

Figure 5.3. Setup for measuring the thickness and width of a fibre using an optical microscope.

5.3.3. Tensile experiment

A 5 kN Instron (Ametek Instruments, LS model, USA) was used for the experiment on tensile properties of fibres. The Instron comprised of a frame, a drive system, a controller, a load cell, and two grips to hold specimen. The Instron was controlled via EXYGEN*Plus* software, which allowed the user to define input parameters and record the data.

To prepare for tensile tests, fibre sample was attached to a clipboard frame using permanent fabric adhesive (Figure 5.4.a). This was to prevent fibre sample from slipping off the clamps of the Instron during pulling. The "window" of the clipboard gave an effective fibre length of 10 mm. The prepared fibre samples were assigned to a number from 1 to 30 for randomly performing the tests. They were then kept in an environmental chamber for three days at 21˚C and 65 % relative humidity to reach an equilibrium condition [14].

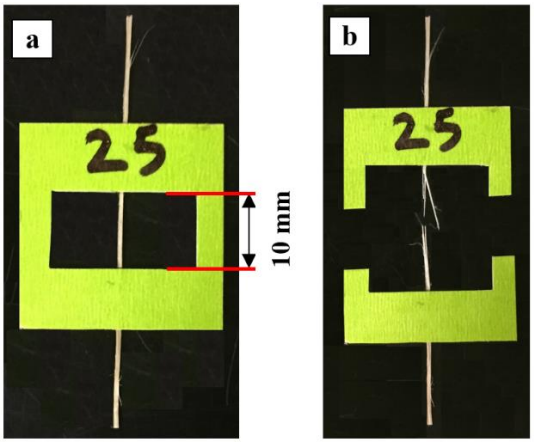

Figure 5.4. A hemp fibre sample attached to a clipboard: (a) before test; (b) after test.

In a test, the clipboard with a fibre sample was fit between the grips of the Instron. Before loading, the sides of the clipboard were cut and then, the mobile grip was moved up at 2 mm⁄min to apply a tension load to the fibre sample. The test stopped when the fibre broke (Figure 5.4.b). In seven out of 30 fibre samples, the glue failed to keep the fibre attached to the clipboard frame during the loading. Thus, 23 tests were successfully performed. All the tests followed the procedure recommended by ASTM Standard D3822 [15]. From each test, the cross-section area of the fibre was input in the computer and the computer generated a stress-strain curve as well as tensile strength and Young's modulus of the fibre.

5.3.4. Results from the experiment

5.3.4.1. Measured fibre cross-section dimensions

On the average of 23 fibre samples, the cross section of the fibre had a thickness of 164±88 μm and a width of 583±174 μm. The high standard deviation values indicated that the cross-section dimensions of the hemp fibre were highly variable. The much smaller mean value of thickness than the width showed that the cross-section of fibre bundles was a thin rectangular. Assuming a round cross-section for hemp fibre bundle in some literature studies [16,17] would result in large

discrepancies in estimating the cross-sectional area of fibre sample and in turn the tensile properties of the fibre. Scanning Electronic Microscopic images also demonstrated that the cross section of hemp fibre bundles is more polygonal than circular [4]. Rectangle is a simple case of polygons.

5.3.4.2. Measured tensile properties

Test results of 23 fibre samples gave various shapes of stress-strain curves. However, they could be classified into two general types: sudden failure and gradual failure. In the sudden failure type, stress increased linearly to the peak value and then suddenly dropped to zero (Figure 5.5.a). The sudden drop in stress meant that the specimen was completely broke. This behavior was similar to a brittle material. In the gradual failure type, the stress increased non-linearly to the peak value and then there was a sudden drop in stress but was not dropped to zero (Figure 5.5.b), implying that some of the single fibres in the fibre bundle were not broken and still carried some loads.

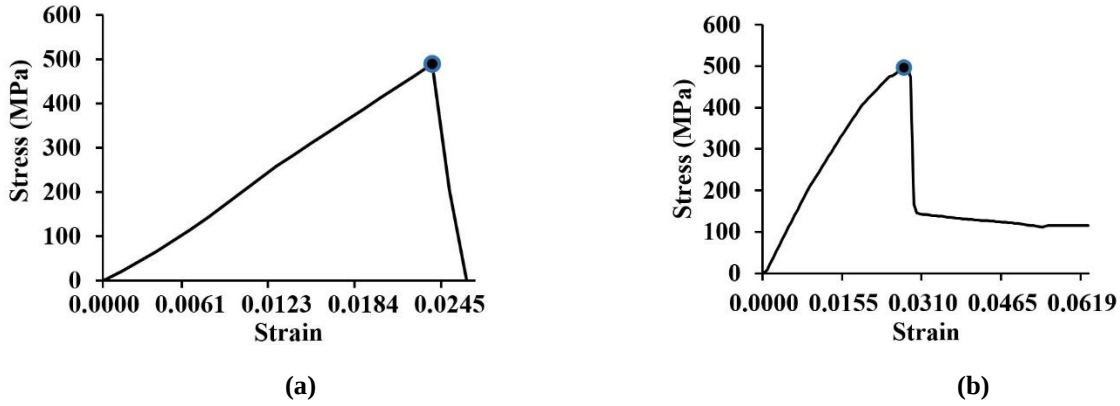

Figure 5.5. Typical results of stress-strain curves from the experiment: (a) sudden failure; (b) gradual failure; the dot on the curves stands for the maximum stresses.

For both types of stress-stain curves, the peak stress could be easily identified as shown in Figs. 5a, b. The tensile strength and Yang's modulus of the fibre sample were automatically generated by the Instron computer system. With all results from 23 stress-strain curves from the experiment, the average tensile strength of fibre samples was 381.95±163.55 MPa. This was in the range

reported for tensile strength of hemp fibres which varied from 244 to 900 MPa [2–4]. The value of measured Young's modulus, 19.70±8.07 GPa, was within the range of 8.6-35 GPa which was reported by other researchers for hemp fibres [2,4]. As outlined in the introduction, the reason for this variability can refer to the growing condition, agronomic practices, and retting condition. Furthermore, considering cross section area as rectangular or circular affects the values of tensile properties.

5.4. DEM MODELLING OF FIBRE TENSILE TEST

PFC^{3D} (Particle Flow Code in Three Dimensions) (Itasca Consulting Group, Minieapolis, MN) was used to model fibre under a tension load. *PFC*^{3D} is a software that employs the DEM to simulate mechanical and dynamic behavior of solid materials. The modelling process in this study included constructing a model fibre, loading the model fibre with tension, monitoring tensile properties of the model fibre, and calibrating model parameters for different types of plant fibres.

5.4.1. Model fibre

The model fibre was formed as an assembly of discrete particles (spheres) with a rectangular cross-section (Figure 5.6.a). These particles were bonded together, so that the particles assembly became a solid material, like a real plant fibre. The model fibre could have any dimensions. In this case, the dimensions of the model fibre were the average dimensions of the real fibres used in the experiment. The effective length (L) of the model fibre was 10 mm, plus additional 1 mm at each end as "grips" for applying tensile loads to the model fibre. The grips contained the same size of particles and the same type of bonds as the model fibre. In simulating a tensile test, the particles in the grips were assigned a velocity along the axial direction of the fibre, which applied a tensile load to the model fibre, causing the breakage of the model fibre (Figure 5.6.a), illustrated by the

detachment of particles (Figure 5.6.b). Bonds between particles were defined using the linear parallel bond (LPB) model implemented in *PFC*^{3D}. Bonds could be envisioned as a cylindrical piece of cement-like material deposited between two contacting particles, providing structural support to the particle assembly. This supporting role of bonds can be illustrated by the "fabric" of bonds in the model fibre as shown in Figure 5.6.c. The well-connected bonds within the particle assembly indicated a good structural representation of a fibre. The breakage of the model fibre was actually the breakage of the bonds within the model fibre.

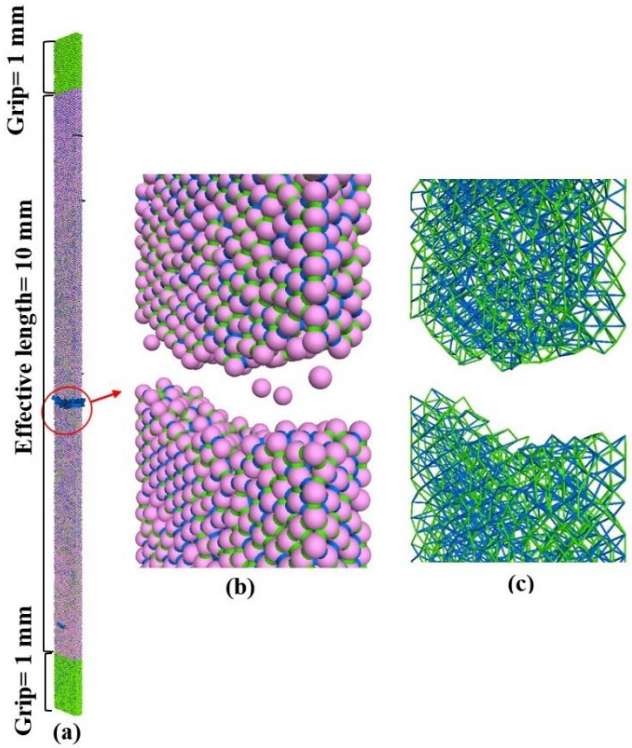

Figure 5.6. Model fibre and tensile failure: (a) entire model fibre with grips at the ends; (b) enlarged particles and bonds; (c) bond structure (particles not shown).

The number of particles and bonds in the model fibre determined the microstructure of the model fibre, which in turn affected the crack propagation in the model fibre under loads. In this study, a particle diameter (D) of 40 μm was set that was as small as the computing time allowed. A minimum bond gap (G) was chosen to ensure that bonded contacts existed between particles in

the model fibre all time. The particle density (ρ), according to the value reported for hemp fibre [19], was set to 1,480 kg⁄m^3. The final number of particles in the model fibre varied with the porosity of the particle assembly. For example, with an arbitrary porosity (n) of 0.34, the particle assembly had 22,650 particles and 80,413 bonds, which gave a well-structured model fibre. The parameters of the model fibre are summarized in Table 5.1.

Table 5.1. Parameters of the model fibre.

Parameter	Symbol	Value
Sample width (μm)	W	583
Sample thickness (μm)	T	164
Sample length (mm)	L	10
Bond gap (μm)	G	0.0
Particle radius (μm)	D	40
Particle density (kg⁄m^3)	ρ	1,480

5.4.2. Micro-properties of the model

In *PFC^{3D}*, particles and bonds are defined by their micro-parameters. The micro-parameters of particles include normal and shear stiffness (k_n and k_s), and particle friction coefficient (μ). The micro-parameters of bonds include normal stiffness ($\bar{k}_n$), shear stiffness ($\bar{k}_s$), bond radius multiplier (λ), tensile strength (σ_{micro}), and shear strength (τ_{micro}) that was determined by:

$$\tau_{micro} = \bar{c} - \sigma_{micro} \tan(\bar{\varphi}) \qquad (5.1)$$

where $\bar{c}$ is cohesion, and $\bar{\varphi}$ is friction angle.

The k_n and $\bar{k}_n$ could be computed using the following equations [18]:

$$k_n = \frac{E_c \bar{A}}{R_A + R_B} \qquad (5.2)$$

$$\bar{k}_n = \frac{\bar{E}_c}{R_A + R_B} \qquad (5.3)$$

where R_A and R_B are the radius of two particles connected together, $\bar{A}$ is the cross section area of the bond, E_c is Young's modulus at particle-particle contact, and $\bar{E}_c$ is Young's modulus of the

bond. To reduce the number of micro-parameters, ratio of k_n/k_s or $\bar{k}_n/\bar{k}_s$ was considered as one micro-parameter, and the two ratios were assumed to be equal: $\bar{k}_n/\bar{k}_s = k_n/k_s$. To further simplify, it was assumed the particle-particle contact is equal to the bond Young's modulus, namely micro Young's modulus:

$$E_c = \bar{E}_c = E_{micro} \qquad (5.4)$$

After these assumptions, the input micro-parameters required for the model were reduced to k_n/k_s, E_{micro}, μ, σ_{micro}, $\bar{c}$, and $\bar{\varphi}$.

5.4.3. Monitoring of macro-properties

Similar to the experiment, stress and strain of the model fibre were monitored in the simulation. To load the model fibre, opposite velocities were specified to the particles in the grips at the two ends of the model fibre. The strain of the model fibre was computed by monitoring the displacement of two "gage" particles located in the grips [18]. During the loading process, the sum of the displacements of the two gage particles divided by the initial length of the model fibre gave the axial strain of the model fibre.

Mechanically, stress is a continuum quantity that does not exist in discrete particles. However, *PFC*^{3D} implemented a technique to obtain "contact stress" in a "measurement region" specified by the user. For this, the contact force and particle displacement are calculated within the region first. They are then converted to a continuum stress using the following equation [18]:

$$\sigma_c = 1/V \sum_{c=1}^{N} F^{(c)} \otimes L^{(c)} \qquad (5.5)$$

where σ_c is average contact stress within the measurement region, V is the volume of a measurement region, N is the number of contacts that lies in the region or on its boundary, c is the

contact number, $F^{(c)}$ is the contact force vector, $L(c)$ is the branch vector joining the centroids of the two particles in contact, and $\otimes$ denotes outer product.

The contact stress from Eq. (5.5) does not have the same definition as the "tensile stress" (load divided by cross-sectional area). Contact stress with the particle assembly is a tensor and the direction is not fixed. However, given the fact that the external load on the model fibre is in the z axis only, the dominant directions of the particle contact forces in the model fibre were expected to be along the z axis as well. Further examination of the contact force distribution in the model fibre proved this as shown in Figure 5.7. Although various directions of the contact forces were seen, most of them were towards the z axis. Therefore, the contact stress was used to approximate the tensile stress. The same assumption has been used by Itasca Consulting Group (2014) in tensile test simulation of a rock.

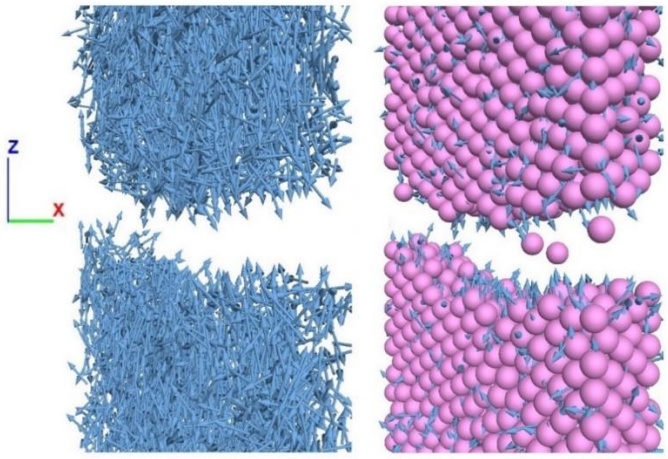

Figure 5.7. The direction of contact forces at the failure location.

Five spherical measurement regions were used to obtain the tensile stress of the model fibre. The spheres were 2 mm apart, evenly distributed along the model fibre (Figure 5.8.a). The enlarged measurement sphere in 1.1 scale is shown in Figure 5.8.b. The contact stress within each sphere was recorded and the average over the five spheres was reported as the tensile stress of the model fibre.

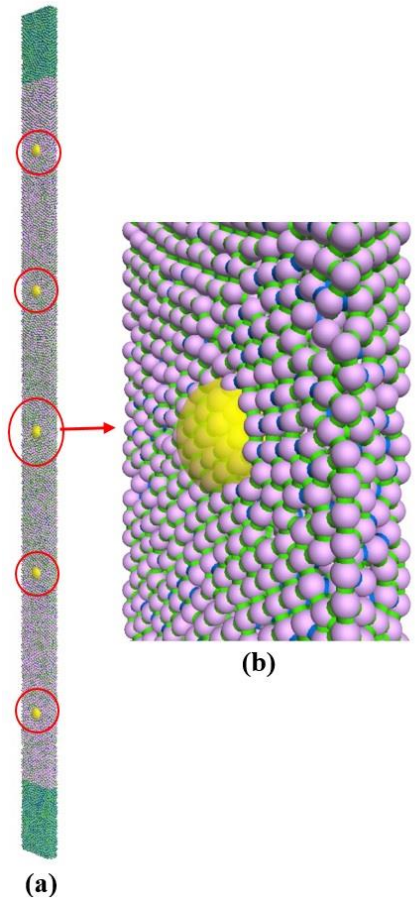

Figure 5.8. Stress measurement in simulations: (a) measurement sphere distribution on the model fibre; (b) an enlarged measurement sphere.

Figure 5.9 shows typical stress-strain curves under different loading velocities. The tensile stress was linearly increased with the strain, and then suddenly dropped to zero, when the model fibre failed. This brittle behavior was similar to that observed in the experiment shown in Figure 5.4.a. Another observation was that there were little variations in stress-strain curves when the loading velocity was altered in the simulation. The stress-strain curves for a range of loading velocity from 0.05 to 1.0 m/s all overlapped together, and there was negligible change in the maximum stress as well. Thus, it was not necessary for the simulation to use the experimental loading velocity, 3.33×10^{-5} m/s (2 mm/min) that was very low, requiring an unpractically long time

for model computing. Given these results, the loading velocity of 0.5 m/s was selected as it met the quasi-static condition and the computing time was affordable.

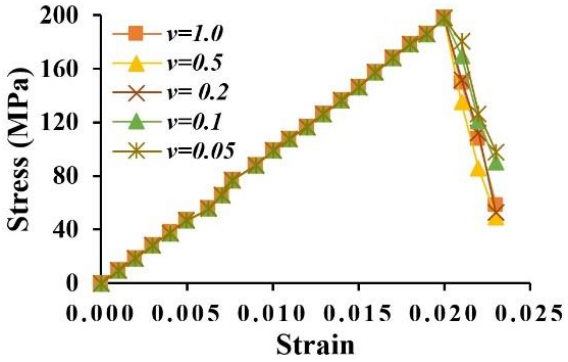

Figure 5.9. Simulated stress-strain curves under different loading velocities (v, m/s).

5.4.4. The combination effect of micro-parameters on macro-parameters

For investigating the combined effect of micro-parameters on macro-parameters, the recommendations from Yang et al. (2006) were followed. They defined several dimensionless parameters and used the Buckingham π-theorem which stated that those dimensionless parameters governed the failure and elastic response of a specimen. In their DEM model, Yang et al. (2006) proposed that the stress response was the function of five dimensionless parameters as:

$$\sigma_{macro} = \sigma_{micro}\Psi\left(\mu, \frac{k_n}{k_s}, n, \frac{E_{micro}}{\sigma_{micro}}, \frac{\tau_{micro}}{\sigma_{micro}}\right) \quad (5.6)$$

and the elastic response was a function of two dimensionless parameters as:

$$E_{macro} = E_{micro}\Phi\left(\frac{k_n}{k_s}, n\right) \quad (5.7)$$

Other dimensionless parameters Yang et al. (2006) mentioned were *R/L* and $v/\sqrt{k_n/\rho}$ which were not included in the above equations as *R/L* was very small (0.002) and $v/\sqrt{k_n/\rho}$ was not critical in the quasi-static loading in this study.

First the following preliminary values were chosen according to the literature: k_n/k_s = 2.5; μ = 0.5; $\bar{c}$ = 100 MPa; $\bar{\varphi}$ = 45°; σ_{micro} = 400 MPa; and E_{micro} = 10 GPa. Before running the simulation,

it was important to consider that in PFC^{3D}, bond breakage occurs when the external tensile stress and shear strength of the bond at a time step are greater than the σ_{micro} and τ_{micro} respectively. Effects of τ_{micro} means effects of $\bar{c}$ and $\bar{\varphi}$ based on Eq. (5.1). Simulations were performed to examine effects of $\bar{\varphi}$ or $\bar{c}$ on the output stress, σ_{macro}. Results showed that changing $\bar{\varphi}$ had little effects on σ_{macro} (results not shown). Thus, $\bar{\varphi}$ was kept as 45º. However, σ_{macro} increased with $\bar{c}$ rapidly first, and then became constant, which means that when the value of $\bar{c}$ or τ_{micro} is large enough, it will not affect the model output. When applying the bond model to tensile test, the value of the τ_{micro} should be made high enough to ensure that if any bond breaks, it is the result of failure in tension strength, not in shear strength [8]. High value of τ_{micro} means high values of $\bar{c}$. Given these facts, 10,000 MPa was chosen for $\bar{c}$ (Figure 5.10). Therefore, the effect of τ_{micro} / σ_{macro} was disregarded in Eq. (5.6).

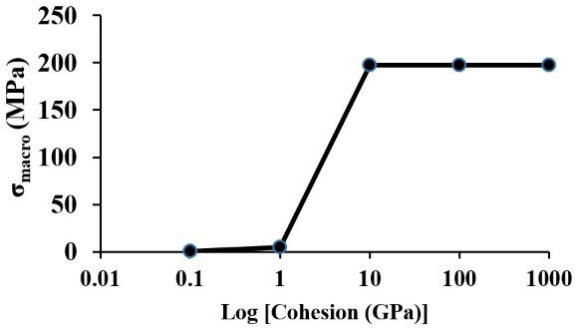

Figure 5.10. Effect of cohesion on macro-tensile strength (σ_{macro}).

Then, with the new value for $\bar{c}$ (10,000 MPa), the model was run with different range of microproperties to estimate the combination effects of micro-parameters on macro-properties. The range for all microproperties were as follows: 300 MPa $\leq \sigma_{micro} \leq$ 600 MPa, $0 \leq \mu \leq 1$, $1 \leq k_n/k_s \leq 5$, $0.3 \leq n \leq 0.4$, $12.5 \leq E_{micro}/\sigma_{micro} \leq 62.5$, and 5 GPa $\leq E_{macro} \leq$ 25 GPa.

According to Eq. (5.6), σ_{macro} would be potentially affected by σ_{micro}, μ, k_n/k_s, n, E_{micro}/σ_{micro}. Figure 5.11 shows the effect of changing σ_{micro} and μ on the average simulated σ_{macro}. The simulated σ_{macro} was not sensitive to μ but considerably affected by σ_{micro}.

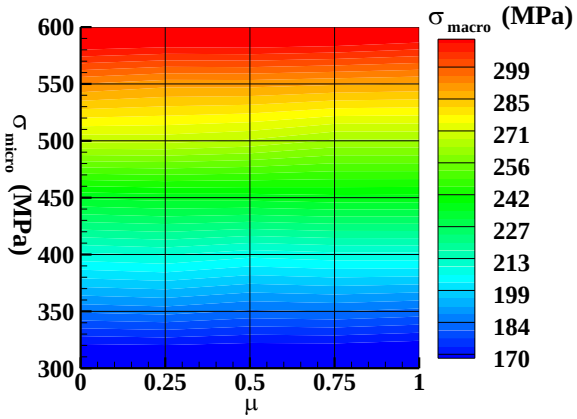

Figure 5.11. Simulated tensile strength (σ_{macro}) for different particle friction coefficients (μ) and micro tensile strength (σ_{micro}).

Changing μ between 0 and 1 caused a 0.84% decrease in the simulated σ_{macro} while increasing σ_{micro} from 300 to 600 MPa increased σ_{macro} by 102%. The influence of k_n/k_s, n, and E_{micro}/σ_{micro} is demonstrated in Figure 5.12. By increasing both k_n/k_s and n, the σ_{macro} decreased at all levels of E_{micro}/σ_{micro}. Furthermore, at all levels of k_n/k_s, when n increased from 0.3 to 0.4, the simulated σ_{macro} decreased, whereas increasing E_{micro}/σ_{micro}, the simulated σ_{macro} remained in very narrow ranges. At all values of n, changing E_{micro}/σ_{micro} did not also affect σ_{macro} while σ_{macro} significantly declined at increasing k_n/k_s. By increasing k_n/ks from 1 to 5, n from 0.30 to 0.40, and E_{micro}/σ_{micro} from 12.5 to 62.5, the average value of σ_{macro} declined by 25.5%, 27.73%, and 3.39% respectively. It could be inferred that σ_{micro} was the most influential factor to the σ_{macro}.

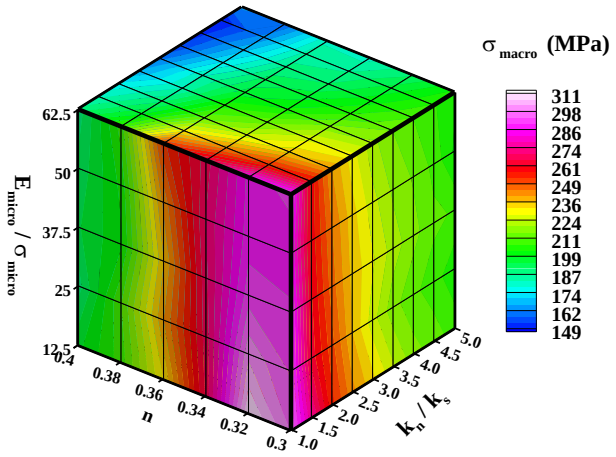

Figure 5.12. Simulated tensile strength (σ_{macro}) for different ratios of micro Young's modulus to micro tensile strength (E_{micro}/σ_{micro}), particle porosities (n), and different normal to shear stiffness ratio (k_n/k_s).

Based on the Eq. (5.7), E_{micro}, k_n/k_s, and n affect E_{macro}. Figure 5.13 depicts the effects of varying these microproperties on the E_{macro}. The highest value of E_{macro} was when E_{micro} was at the highest level, n, and k_n/k_s were at the lowest levels. For all values of k_n/k_s, varying n from 0.3 to 0.4 resulted in a decreasing trend for E_{macro} but a significantly increasing trend was observed for E_{macro} when E_{micro} changed from 5 to 25 GPa. The same trend repeated for E_{macro} at all levels of n once k_n/k_s and E_{micro} increased. Furthermore, the resultant E_{macro} decreased by increasing k_n/k_s and n for all values of E_{micro}. It was found that by increasing k_n/ks from 1 to 5 and n from 0.30 to 0.40, the value of E_{macro} decreased by 45.5% and 50.5%, respectively. Also, there was a 372% increase in the E_{macro} when E_{micro} varied from 5 to 25 GPa. The results showed the model was more sensitive to E_{micro} compared to k_n/k_s and n.

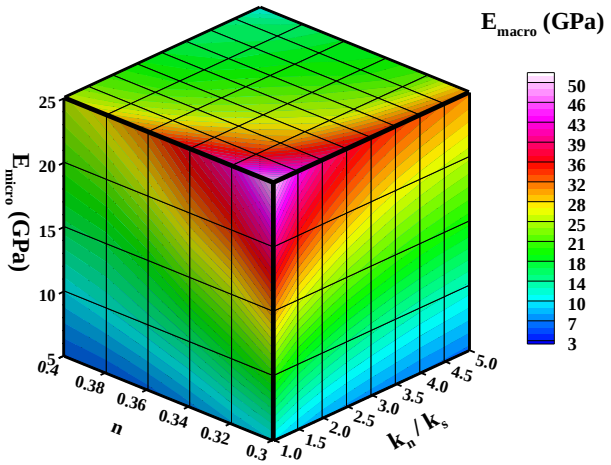

Figure 5.13. Simulated Young's modulus (E_{macro}) for different ratios of micro Young's modulus (E_{micro}), particle porosities (n), and different normal to shear stiffness ratio (k_n/k_s).

5.4.5. Calibration of the DEM micro-parameters

From the previous section, it was found that the most influential micro-parameters on the output σ_{macro} and E_{macro} were respectively σ_{micro} and E_{micro}. Therefore, recalling the preliminary values including n=0.34, k_n/k_s = 2.5 [21] μ = 0.5, $\bar{\varphi}$ = 45°; new value of $\bar{c}$ = 10,000 MPa, σ_{micro} = 400 MPa, and E_{micro} = 10 GPa, the model was run to find relationships between σ_{micro} and σ_{macro} and between E_{micro} and E_{macro}.

When the model was run for a range of σ_{micro} from 300 to 600 MPa, σ_{macro} increased in a linear fashion (Figure 5.14.a). The results fit the following relationship with R^2 = 0.99:

$$\sigma_{micro} = 1.89\ \sigma_{macro} \qquad (5.8)$$

Varying E_{micro} from 5 to 25 GPa, the resultant E_{macro} rapidly increased from 4.98 to 25.31 GPa (Figure 5.14.b). The relationship was perfectly linear with a determination coefficient (R^2) of 0.99, as shown in Eq. (5.9).

$$E_{micro} = 0.99\ E_{macro} \qquad (5.9)$$

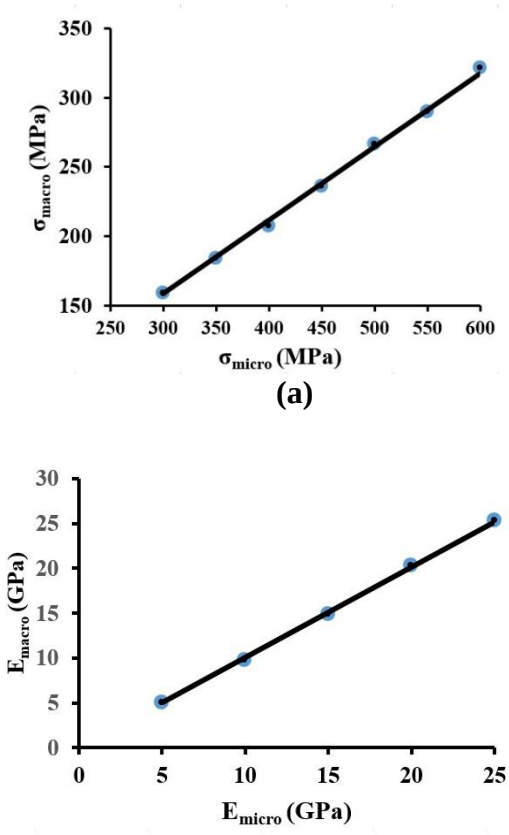

Figure 5.14. Relationships obtained from simulations: (a) between micro-strength (σ_{micro}) and macro-strength (σ_{macro}); (b) between micro-Young's modulus (E_{micro}) and macro-Young's modulus (E_{macro}).

The DEM input micro-parameters suitable for simulating tensile behavior of plant fibres are presented in Table 5.2. Based on the above simulations, the critical micro-parameters affecting the material behaviors included cohesion for reaching a high value of shear strength for parallel bonds, and normal to shear stiffness ratio for having an appropriate failure location. The critical micro-parameters affecting the model outputs were the micro-tensile strength of bonds and micro-Young's modulus of particles. Their relationships to the perspective macro-properties were proposed, and they were expected to be applicable to any plant fibres, besides hemp fibres. If measured values are available, these two micro-parameters of the model can be determined using the relationships (5.8) and (5.9). It should be noticed that the model had limitation that when the

maximum tensile strength was higher than 1020 MPa, the bond breakage behavior should be checked to ensure that all of the bonds are broken due to failing in tension. The suitable micro-parameters are summarized in Table 5.2.

Table 5.2. Modified DEM input parameters to simulate tensile test on the natural fibre bundle.

Parameter	Symbol	Value
Particle contact modulus (GPa)	E_C	0.99 E_{macro}
Particle stiffness ratio	k_n/k_s	2.5
Particle friction coefficient	μ	0.5
Parallel-bond radius multiplier	$\bar{\lambda}$	1.0
Parallel-bond modulus (GPa)	$\bar{E}_c$	0.99 E_{macro}
Parallel-bond stiffness ratio	$\bar{k}_n/\bar{k}_s$	2.5
Parallel-bond tensile strength (MPa)	σ_{micro}	1.89 σ_{macro}
Parallel-bond cohesion strength (MPa)	$\bar{c}$	10,000
Parallel-bond friction angle (degree)	$\bar{\varphi}$	45

5.4.6. Applications of the relationships for plant fibres

For the hemp fibre in this study, the two critical micro-parameters can be determined using Eqs. (5.8) and (5.9). Using the experimental value of tensile strength of 381.91 MPa to replace σ_{micro} in Eq. (5.8), it gave a σ_{macro} of 721.81 MPa for the hemp fibre tested. Similarly, with Young's modulus obtained from the experiment (19.70 GPa), the E_{macro} in Eq. (5.9) was 19.50 GPa. These values were the calibrated values for the hemp fibre model. These two micro-parameters can be used to determine dynamic attributes of hemp fibre using the DEM.

Similarly, Eqs (5.8) and (5.9) can be used to determine the micro-parameters for other plant fibres, if tensile property data are available. Literature data on Young's modulus and tensile strength of 11 other plant fibres were collected and they are listed in Table 5.3. The results of their micro-parameters are also listed in Table 5.3. Pineapple, kenaf, and abaca had the highest micro and macro Young's modulus, and coir and cotton had the lowest micro and macro Young's

modulus. The lowest micro and macro tensile strength were for pineapple, kenaf, and banana and the lowest value was abaca.

Table 5.3. Micro-parameters predicted using experimental data from the literature [23].

Fibre	Literature data		Micro-parameter	
	E (GPa)	σ (MPa)	E_{micro} (GPa)	σ_{micro} (MPa)
Abaca	41	12	40.59	22.68
Alfa	22	350	21.78	661.50
Bamboo	27	575	26.73	1086.75
Banana	29	721.5	28.71	1363.64
Coir	6.0	140.5	5.94	265.55
Cotton	8.0	500	7.92	945.00
Flax	60	700	59.4	1323.00
Hemp	19.70	381.91	19.50	721.81
Jute	37.5	325	37.13	614.25
Kenaf	41	743	40.59	1404.27
Pineapple	71	1020	70.29	1927.80
Sisal	15.5	460	15.34	869.40

5.5. CONCLUSIONS

In this study, tests and discrete element modelling were performed to investigate the tensile behaviors of plant fibre. The following conclusions were drawn:

1. The model fibre should contain enough numbers of particles and bonds to have a well-structured discrete particle assembly to represent the solid nature of a plant fibre.
2. Loading rate of the model did not significantly affect the model output of stress-strain curve.
3. The most critical micro-parameters of the model were micro-Young's modulus of particles and micro-strength (tensile) of bonds. Their relationships with the model outputs (macro-Young's modulus and macro-strength) were linear.
4. With the tensile test results from hemp fibre, the calibrated values were 19.50 GPa for the micro-Young's modulus of particle and 721.81 MPa for micro-strength (tensile) of bond.

Similarly, these two micro-parameters could be determined for other plant fibres, such as flax, jute, and kenaf fibres.

This study focused on the determination of micro-parameters and their relationships with the macro-properties in discrete element modelling of plant fibre under tensile loads. The next step will be to use these micro-parameters to simulate micro-dynamics of plant fibre using the DEM.

5.6. ACKNOWLEDGMENT

This work was supported by Natural Sciences and Engineering Research Council of Canada (NSERC). The authors would like to thank Anndrea Marie Hermann for providing hemp fibre bundles, Dr. Mushiur Rahman and Dr. Stefan Cenkowski for providing the fibre testing systems, and Hamid Reza Fazeli for helping in data visualization.

5.7. REFERENCES

[1] Gowda B. Fibres, rubber, firewood, timber, and bamboo. Bangalore, India, Univerity of Agricultural Sciences; 2007. (no. 560065). 2007.

[2] George M, Chae M, Bressler DC. Composite materials with bast fibres: Structural, technical, and environmental properties. Prog Mater Sci 2016;83:1–23. doi:10.1016/j.pmatsci.2016.04.002.

[3] Sadek MA, Guzman L, Chen Y, Laguë C, Landry H. Simulation of tensile tests of hemp fibre using discrete element method. Agric Eng Int CIGR J 2014;16:126–35.

[4] Shahzad A. A Study in Physical and Mechanical Properties of Hemp Fibres. Adv Mater Sci Eng 2013;2013:1–9. doi:http://dx.doi.org/10.1155/2013/325085.

[5] Lee K-Y, Delille A, Bismarck A. Greener Surface Treatments of Natural Fibres for the Production of Renewable Composite Materials. Cellul. Fibres Bio- Nano-Polymer Compos., Berlin, Heidelberg: Springer Berlin Heidelberg; 2011, p. 155–78. doi:10.1007/978-3-642-17370-7_6.

[6] Khan MM, Chen Y, Belsham T, Laguë C, Landry H, Peng Q, et al. Fineness and tensile properties of hemp (Cannabis sativa L.) fibres. Biosyst Eng 2011;108:9–17. doi:10.1016/j.biosystemseng.2010.10.004.

[7] Cundall PA. A computer model for rock-mass behaviour using interactive graphics for the input and output of geometric data. Rep AD/A-001 1974;602.

[8] Yang D, Sheng Y, Ye J, Tan Y. Discrete element modelling of the microbond test of fibre reinforced composite. Comput Mater Sci 2010;49:253–9. doi:10.1016/j.commatsci.2010.05.003.

[9] Khattak MJ, Khattab A. Modelling Tensile Response of Fibre-Reinforced Polymer Composites Using Discrete Element Method. Polym Compos 2013;34:877–86. doi:10.1002/pc.

[10] Roux A, Haen T-X, Lecompte J, Iordanoff I, Laporte S. Rupture of the muscle-tendon complex in tensile test. Comparison between experimentations and discrete element modelling. Comput Methods Biomech Biomed Engin 2015;18:2046–7. doi:10.1080/10255842.2015.1069616.

[11] Chen G, Schott DL, Lodewijks G. Tensile test simulation of high-carbon steel by discrete element method. Eng Comput 2016;33:1224–45. doi:10.1108/EC-03-2015-0064.

[12] Coetzee CJ. Review: Calibration of the discrete element method. Powder Technol 2017;310:104–42. doi:10.1016/j.powtec.2017.01.015.

[13] Hermann AM. The effect of plant population density and harvest timing on agronomic fibre yield and quality characteristics of industrial hemp (cannabis) cultivar alyssa, grown in the Parkland Region of Manitoba, Canada. University of Manitoba, 2008.

[14] CGSB. Conditioning Textile Materials for Testing. Canadian General Standards Board and Standards Council of Canada.CAN/CGSB-4.2 no. 2-M88.; 2001.

[15] ASTM D3822-14. Standard Test Method for Tensile Properties of Single Textile Fibres. ASTM Int USA 2015:1–10. doi:10.1520/D3822.

[16] Khan MMR, Y. Chen Y, C. Laguë C, H. Landry H, Q. Peng Q, W. Zhong W. Hemp (Cannabis sativa L.) decortication using the drop weight method. Appl Eng Agric 2013;29:79–87. doi:10.13031/2013.42521.

[17] Thakur S, Chen Y, Morrison J. Separation of Fibre and Shivesfrom Decorticated Flax. Appl Eng Agric 2017;33:113–20. doi:10.13031/aea.11335.

[18] Itasca Consulting Group. PFC- Particle Flow Code, Version 5.0, Minneapolis, MN 2014.

[19] Li X, Tabil LG, Panigrahi S. Chemical treatments of natural fibre for use in natural fibre-reinforced composites: A review. J Polym Environ 2007;15:25–33. doi:10.1007/s10924-006-0042-3.

[20] Yang B, Jiao Y, Lei S. A study on the effects of microparameters on macroproperties for specimens created by bonded particles. Eng Comput 2006;23:607–31. doi:10.1108/02644400610680333.

[21] Potyondy DO, Cundall PA. A bonded-particle model for rock. Int J Rock Mech Min Sci 2004;41:1329–64. doi:10.1016/j.ijrmms.2004.09.011.

[22] Bast fibres [Internet]. India: National Programme on Technology Enhanced Learning; [cited 2017 March 10]. Available from: http://nptel.ac.in/courses/116102026/8 n.d. http://nptel.ac.in/courses/116102026/8.

[23] Komuraiah A, Kumar NS, Prasad BD. Chemical composition of natural fibres and its influence on their mechanical properties. Mech Compos Mater 2014;50:359–76. doi:10.1007/s11029-014-9422-2.

Chapter 6: Developing a Decision-Making Model to Identify the Most Influential Parameters Affecting Mechanical Extraction of Bast Fibres

---

6.1. ABSTRACT

Bast fibres, renewable resources used as reinforcement to develop sustainable products, are extracted from plant stalk in a process called decortication. Proper selection of critical parameters affecting decorticators' performance is required for optimization of the process. An analytical hierarchy process (AHP) was developed, according to expert feedback and experimental tests, to identify the most influential parameters affecting mechanical extraction of bast fibres. The experimental tests were done using a research-scale decorticator to find the relationship among the factors determining the quantity and quality of the fibres, and the influencing parameters. The potential inflectional parameters identified by experts were retting condition of the stalks, feed size, the number of passes through the rollers and finisher of the decorticator, 3-comb and 6-comb shaker, and stalk diameter variation. The results of the AHP model demonstrated that among seven potential parameters, the retting condition of the stalks was the most effective parameter constituting 20.4% of the total, followed by the proportion of the number of pass of stalks through the rollers (19.4%), and the feed size (18.3%). In contrast, stalk diameter variation and 3-comb shaker had the least effect on the quality and quantity of the fibres (4.4 % and 10.7%, respectively).

6.2. INTRODUCTION

Due to public awareness and economic considerations, developing sustainable products is of great interest. Natural fibres have already been identified as reinforcement for polymeric matrices in

place of synthetic fibres, especially glass fibres [1]. Among natural fibres, bast fibres are the most suitable and economic because of their high specific tensile strength and stiffness [2–4]. Furthermore, these types of materials have been used in many industrial applications, including insulation, automotive, construction, biomedical, marine, sports, electrical, and geotextile [5]. One of the biggest challenges in the plant fibre industry is the extraction process of plant fibres, which is classified into retting and mechanical extraction. Retting generates the highest purity fibre when performed properly but is time-consuming and produces large amounts of wastewater. In contrast, mechanical extraction is more environmentally friendly, fast, simple, and generates high quantity of fibres, however, it adversely affects the mechanical properties of the extracted fibres [5,6]. Mechanical extraction of bast fibre is commonly completed in two stages: decortication and post-decortication cleaning. In the decortication process, plant stalks are subjected to compressive, shear, and impact forces. This results in detaching fibre bundles from the other parts of the plant, which are called the "core" in this document. The machines used to decorticate bast fibres, include crushing rollers [7], cutter head [8], hammer mills [9], ball mills [10], and drop weight [11]. After decortication, the detached fibres are still mixed with the core. The aim of the post-decortication cleaning is to separate the fibre bundles from the core. The cleaning process significantly enhances the purity of the fibre, and therefore improves the market value [12]. Different methods used for post-decortication cleaning, includes scutching [13], sieving using particle size difference [14], carding and sorting technique [12,15], cleaning using density difference [16], and pneumatic method [12,15].

The performance of a decorticator is controlled by several potential parameters. Selecting the parameters that have the highest effect on the decortication process is beneficial to modify the current decorticators used in industries. Depending on the decorticator and stalk condition, some

parameters may improve fibre's quality while reducing the quantity, and vice versa. This is a multi-criterion decision-making problem (MCDM) where suitable decisions must be made to prioritize the most influential parameters [17]. One of the most widely used decision making tools in MCDM is Analytic Hierarchy Process (AHP). Most models use statistical parameters to evaluate model accuracy levels [18,19]. However, the performance and accuracy of decision-making models, such as the AHP, are not necessarily evaluated based on those statistical parameters. Because its easy to understand and use [20], the AHP has been applied in various research areas, including political, economic, social, and engineering management. The AHP is used to rank the productiveness of choices that have conflicting objectives [21]. AL-Oqla et al. (2015) prioritized different natural fibre types to fabricate a reinforced polymer composite for sustainable automotive industry using an AHP model. In another work, Al-Oqla et al. (2015) developed an AHP model to determine the most suitable polymer matrix for manufacturing natural fibre composites.

Despite some investigations which have been done to select appropriate natural fibre, and matrix to develop natural fibre composites, no work was found that prioritized the most influential parameters which affect the plant fibre extraction processing. Thus, this study focused on identifying the parameters affecting mechanical extraction of bast fibres by developing an AHP model. To achieve this purpose, the model was developed in three steps: (1) modelling the problem as a hierarchy, (2) comparing between the criteria (factors) and the parameters (decision options), and (3) ranking the parameters regarding the measured criteria in the hierarchy with respect to the main goal.

6.3. MODELLING THE PROBLEM AS A HIERARCHY

In this stage, the problem was decomposed into a sub-problem consisting of the objective, criteria

which were divided into suitable level of detail (e.g. sub-criteria), and alternatives (decision options). The objective of the current study, which was to identify the most influential alternatives affecting the performance of the decorticator, was structured at the first hierarchy. The second and third levels of hierarchy were the controlling criteria and sub-criteria, respectively. The criteria and sub-criteria were selected carefully to guarantee that a well illustrative structure of the AHP model, that expressed fair judgment and resulted in confident decision-making, was adopted. For this purpose, an expertise team was created. The main selected criteria were fibre quantity and fibre quality. The quantity of the fibres was evaluated using two factors: core removal (C_R) and fibre fraction (F_F). The C_R represented the percentage of removed core in each run. A higher C_R showed a decortication process that was more effective. The F_F represented the amount of fibre that could be potentially captured after decortication. The process was effective when there was a high value of F_F. The factors considered to evaluate the quality of the fibres were the score of Environmental Scanning Electron Microscopy images (ESEM), fibre diameter (d), tensile strength (σ), Young's modulus (E_M), and elongation at break (δ). The ESEM images were used to inspect the fibres regarding the number and direction of the cracks, as well as the number and diameter of the holes created on the extracted fibres. Small fibre diameter resulted in a high surface area of contact between fibre and matrix, low porosity, and desirable technical properties [24]. Fibres with high σ, E_M, and δ remarkably enhance mechanical properties of the fibre-reinforced composites. Table 6.1 indicates the specified criteria and sub-criteria.

Table 6.1. Main and sub-criteria used in building the decision-making model.

Main Criteria	Sub-criteria	Symbol
Fibre quantity	Core removal	C_R
	Fibre fraction	F_F
Fibre quality	ESEM image score	s
	Fibre diameter	d
	Tensile strength	σ
	Young's modulus	E_M
	Elongation at break	δ

The lowest level of the hierarchy was allocated to the alternatives. The alternatives were the parameters which had potential impact on the quantity and quality of the extracted fibres. These parameters, identified by experts, were related to the stalk condition and decortication machine introduced later in this document. Figure 6.1 shows the hierarchy structure of the model.

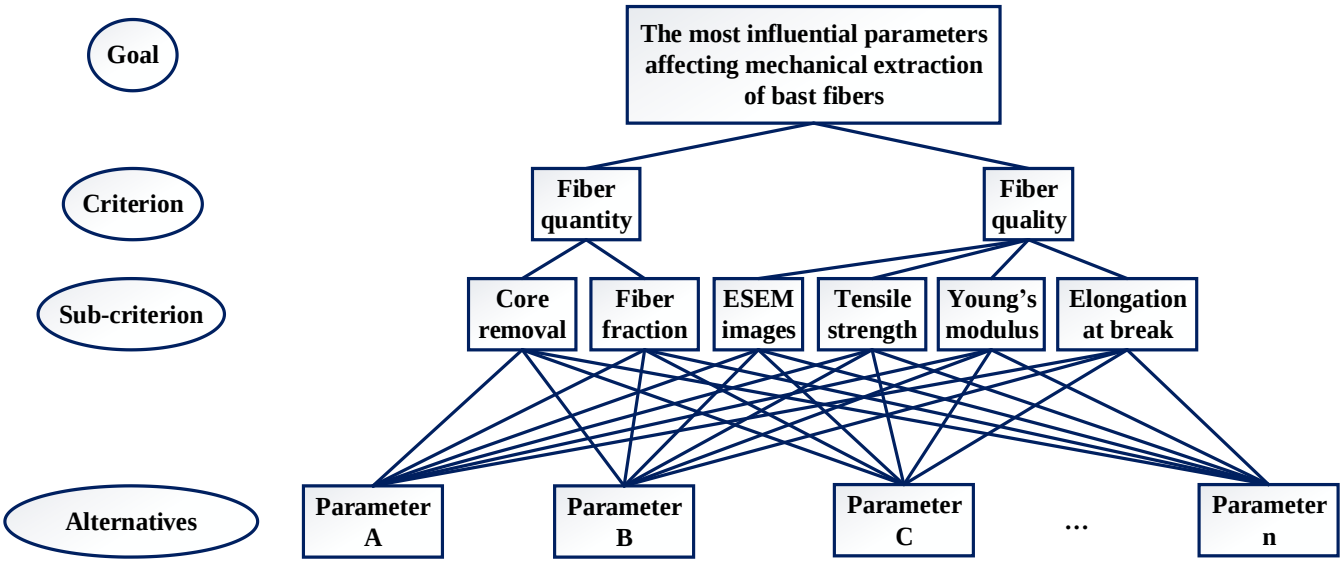

Figure 6.1. The hierarchy structure of the proposed model

6.4. PAIRWISE COMPARISON

6.4.1. Modelling the criteria pairwise comparison

The next step was to develop a set of matrices to represent pairwise comparisons for all levels of the hierarchy. Each sub-factor in the lower level was controlled by its main factor in the higher

level of the hierarchy. The relative importance of each sub-factor within the corresponding level was done with respect to their effect on the controlling factor above. For example, the fibre quality and fibre quantity were compared with each other with respect to the main objective. Correspondingly, the C_R and F_F were compared with each other with respect to the fibre quantity. Such comparisons resulted in a $n \times n$ judgment matrix, as shown in Eq. 6.1.

$$A = \begin{bmatrix} a_{11} & \cdots & a_{1n} \\ \vdots & \ddots & \vdots \\ a_{n1} & \cdots & a_{nn} \end{bmatrix} \qquad (6.1)$$

where n is the size of the pairwise comparison matrix. The number of comparison is equal to $n(n - 1)/2$. According to Saaty (1980), the completed matrix should follow the transitivity and reciprocity rules (Eq. 6.2 and Eq. 6.3, respectively).

$$a_{ij} = a_{ik} \, . \, a_{kj} \qquad (6.2)$$

$$a_{ij} = {}^{1}/_{a_{ji}} \qquad (6.3)$$

A questionnaire was distributed among twenty-four carefully selected experts in the area of natural fibre processing and natural fibre composites, to compare the outlined criteria using Saaty's 1 to 9 scale [26]. Then, the judgment matrix was formed. The value of 1 was allocated to the matrix when a factor was compared with itself. To take the highest advantage of the experts' knowledge, verbal assistance was used. For example, regarding the fibre quantity main criteria, the question that was asked was: "how much more important is the core removal relative to fibre fraction from the fibre quantity standpoint?". Among all the experts asked, eleven returned the completed questionnaire. Before using the collected data to decide, the experts' knowledge was validated using an inconsistency test, which measured the logical inconsistencies of the expert judgment. According to Saaty (1980), a consistency ratio smaller or equal to 10% is acceptable. To calculate

this ratio, the below steps were followed [25]: (1) the whole column of matrix A was normalized by dividing each element of the matrix by the sum of its column, (2) then, the priority vector was developed by taking the average of the resultant rows to reach the corresponding weights of each criteria, (3) and the consistency vector was computed by multiplying matrix A by the priority vector, and then dividing the resultant vector by the priority vector, (4) the largest eigenvalue value (λ_{max}) was obtained by taking average of the elements of the consistency vector, (5) consistency index (I_C) was computed using Eq. (6.4), and finally (6) consistency ratio (R) was obtained using Eq. (6.5).

$$I_c = \frac{\lambda_{max} - n}{n-1} \tag{6.4}$$

where *n* is the matrix size

$$R = \frac{I_c}{I_R} \tag{6.5}$$

where I_R is random index which is equal to 0, 0, 0.58, 0.90, 1.12, 1.24, 1.32, 1.41, 1.45, 1.49, 1.51, 1.58 when the size of the pairwise comparison *n* is 1, 2, 3, 4, 5, 6, 7, 8, 9, 10, 11, 12, respectively. Therefore, the inconsistency test was applied on all the responses, and the R for experts' judgments was calculated. It was found that the maximum consistency ratio was less than or equal to 0.04, which was less than 0.1 and therefore acceptable. Hence, each pairwise comparison matrix resulted in eleven consistent responses.

6.4.2. Modelling the alternative pairwise comparison

An experiment was designed to find a relationship among the alternatives regarding the sub-criterion in the model. Among all bast fibrous plants, hemp was selected since it is one of the most popular plants. Hemp stalks were processed using a research-scale agricultural straw decortication line described as follows.

6.4.2.1. Description of the decortication machine

The decorticator developed by CzTech manufacturer (Čelákovice, Czech Republic) and located in the Composite Innovation Center (CIC), MB, Canada consisted of: six belt conveyors, feeding rollers, a 3-comb shaker located on a timber slot conveyor, a finisher, a 6-comb shaker located on another timber slot conveyor, dust collectors, and control systems (Figure 6.2). The first conveyor belt transported the feed stalk into the feeding rollers, consisting of two bottom rollers and one upper roller. Then, the crushed stalks were fed into the 3-comb shaker through the second conveyor belt. The 3-comb shaker formed by three parallel oscillating combs with downward protruding needles was located after the grooved steel roller to separate the fibres from the crushed stalks. The timber slot conveyor with upward protruding needles helped to pull the crushed material through the shaker. The speed of the slat conveyor was adjusted to be lower or equal to the speed of the subsequent third conveyor belt. This ensured that an even layer of material fed into the finisher. The function of the finisher was to maneuver and crimp the material, to further remove cores. The finisher consisted of three grooved steel rollers: two bottom rollers and one upper roller. After the materials were passed through the finisher, the fourth conveyor belt transferred them to the 6-comb shaker consisting of six parallel combs with downward protruding needles. The structure of the second slat conveyor located under the 6-comb shaker was the same as the first slat conveyor. The short fibre and cores by-products from the two shakers were deposited on the two lower conveyors and were collected as wastes below, and between the 3-comb shaker and finisher.

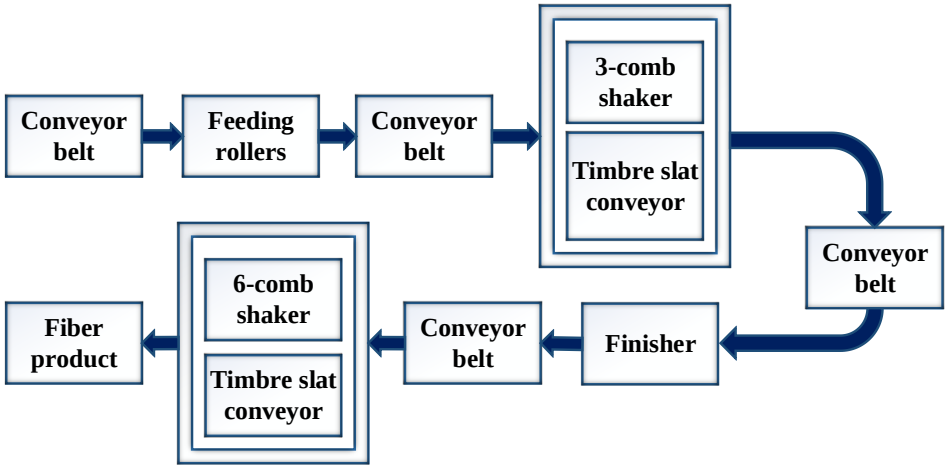

Figure 6.2. Decortication line used in this investigation.

As mentioned earlier, the alternatives identified by experts were related to the stalk condition and machine parameters. Here, the parameters related to stalk conditions were the retting condition and diameter variation of the stalk. The machine parameters included feed size, number of passes through the rollers, number of passes through the finisher, 3-comb shaker, and 6-comb shaker.

6.4.2.2. Experimental design

The experimental design which was based on standard practice for conducting ruggedness tests described in ASTM E-1169 standard [27] was developed to find a relationship among the identified alternatives with regard to the sub-criteria. The Plackett-Burman design from the Standard was used to obtain estimate effect of each alternative. To achieve this goal, the selected alternatives were assigned two values, “low” and “high” (Table 6.2).

Table 6.2. Ruggedness test alternatives, description, and levels for decortication

Alternatives	Variable	Unit	Low level (-1)	High level (+1)
A	Retting condition	No/Yes	No	Yes
B	Feed size	Circumference	Small	Large
C	Number of passes through the rollers	---	1	4
D	Number of passes through the finisher	---	0	2
E	3-comb shaker	Inactive/Active	Inactive	Active
F	6-comb shaker	Inactive/Active	Inactive	Active
G	Stalk diameter variation	---	High variation	Low variation

The ruggedness testing method evaluated the impact of the alternatives in only 8 tests illustrated in Table 6.3. The treatment number one, for example, shows that hemp stalks were retted (A=+1), had a large feed size (B=+1), passed through the feeding rollers for four times (C=+1), did not pass through the finisher (D=-1), passed through the 3-comb shaker (E=+1), did not pass through the 6-combs shaker (F=-1), and had a large stem diameter variation (G=-1). To avoid effects of day-to-day temperature and humidity variations within the processing facility, all tests were done in less than two consecutive days, following an additional day used to prepare all sets.

Table 6.3. Description of the treatments used in this experiment

Treatment	Run #	A	B	C	D	E	F	G
Initial, balanced design								
1	1	+1	+1	+1	-1	+1	-1	-1
2	5	-1	+1	+1	+1	-1	+1	-1
3	3	-1	-1	+1	+1	+1	-1	+1
4	6	+1	-1	-1	+1	+1	+1	-1
5	7	-1	+1	-1	-1	+1	+1	+1
6	2	+1	-1	+1	-1	-1	+1	+1
7	4	+1	+1	-1	+1	-1	-1	+1
8	8	-1	-1	-1	-1	-1	-1	-1

A: retting condition, B: Bundle feed size, C: Number of pass through the roller, D: Number of pass through the finisher, E: 3-comb shaker, F: 6-combs shaker, G: diameter variation. See Table 6.2 for more detail information of each alternative.

6.4.2.3. Experiment procedures

Hemp stalk, Joey variety, was obtained from a farm located in Roseisle, MB, Canada. The crop was seeded on May 21, 2017 with a seed rate of 22.5 kg/ha. The crop matured in the beginning of September, and the seed parts of the crop were harvested by a combine and the stalks were then swathed. For the unretted treatment (A=-1), stalks were handpicked immediately after swathing. For the retted treatment (A=+1), stalks were left in the field to be naturally retted and collected after 33 days. All stalks were stored indoors after collection. At the time of decortication tests, the average moisture content of the stalk was 2.71% (dry basis).

For the stalk diameter variation (G), the retted and non-retted stalks were first visually separated by diameter into three different categories: small, medium, and large. The small and large

diameters were then combined to create samples for the high stalk diameter variation (G=-1) treatment, and the medium diameters were for the low stalk diameter variation (G=+1) treatment. To quantify the variation in diameter, 100 stalks from each treatment were randomly picked and the diameter of each stalk was measured at approximately 100 mm from the bottom of the stalk. The results showed that the stalk for the high diameter variation had an average diameter of 812 mm with a coefficient of variation of 0.42, and the stalk for the low diameter variation treatment had an average diameter of 841 mm with a coefficient of variation of 0.18.

To prepare small and large feed sizes (B), initial bundles (535±15 mm in circumference) were made from both high and low diameter variation samples. For the small feed size treatment (B=-1), the initial bundles were split into six even sub-bundles. For the large feed size treatment (B=+1), the initial bundles were split into two even sub-bundles. All bundles were weighed before being fed into the decorticator. For each treatment, the separated sub-bundles were fed to the decorticator, based on the feed size design shown in Table 6.2, and then the outputs were combined at the end. For instance, in treatment 3, which was the small feed size, six even sub-bundles were decorticated separately in six runs, and the outputs of six runs were recombined for measurements.

For the alternatives, C and D, the number of passes through the rollers or finishers were controlled manually. For the alternatives, E and F, the 3-comb shaker or 6-comb shaker was activated and inactivated accordingly. For example, in treatment 3 shown in Table 6.3, the 3-comb shaker was activated, and the 6-comb shaker was inactivated, the stalks were passed through the first set of rollers for four times, but instead of passing through the 3-comb shaker, they were passed through the finisher. After that, they were passed through the 3-comb shaker.

Before running a test, the machine alternatives were set for the run according to the alternative levels (Table 6.3), and the weighed stalk was then fed into the decorticator. During the

decortication, the wastes were core and fines, which fell to the floor. The decorticator output was mixtures of fibre and core as shown in Figure 6.3.a. Further measurements on the quantity and quality of the product are described in the following sections.

(a)

(b)

(c)

Figure 6.3. The decortication output (a), clean fibre (b), and (c) clean core.

6.4.2.4. Measurements

To determine the effectiveness of the decortication process, the quantity and quality of the extracted fibres were evaluated through the measurements described in the following sections.

Core removal (CR): After each of 8 test runs, the decorticator output was weighed immediately to record the mass (mo). With the initial mass (mi) of hemp material fed into the decorticator, the CR

(%) was determined as

$$C_R = \frac{m_i - m_o}{m_i} 100 \qquad (6.6)$$

Fibre fraction (FF): To determine the F_F in the decorticator output, the fibres and cores were separated by hand. Due to the time-consuming process for the 8 large samples, approximately 20% of the decortication product of each run was randomly taken for the separation. Subsequently, the selected portion was manually separated into clean fibre (Figure 6.3b) and core (Figure 6.3c). They were then dried for 72 h at 60 °C and weighed for the mass dried fibre (m_f) and the dried core (m_c). The F_F was calculated as

$$F_F = \frac{m_f}{m_f + m_c} 100 \qquad (6.7)$$

Environmental Scanning Electron Microscopy (ESEM): A variable pressure field emission scanning electron microscope (FEI Quanta 650 FEG) was used to determine the morphology of the fibres. The alignment of the ESEM were set as follows: the accelerating voltage was maintained between 8-10 kV, spot size of 30, and the working distance was kept at 10 mm. The pictures were taken at a slow scanning speed (Scan 4) to obtain a higher quality image. In order to quantify the quality of the ESEM images, selected worldwide experts in the field of natural fibres were asked to classify the images' quality into five groups including 'very low', 'low', 'moderate', 'high', and 'very high', which respectively corresponded to 0, 25, 50, 75, and 100%. Among all experts asked, six of them replied, and the average score of each image was calculated and reported.

Fibre diameter: Fibre bundle diameter was evaluated using an optical microscope (Wild Heerbrugg AG model, Gais, Switzerland). A total of 15 fibre bundles were randomly picked up from the output of each treatment. Each fibre bundle was glued on two aluminum cube blocks covered by a double-coated carbon conductive tape (Ted Pella, Inc.), placed under the microscope,

which was connected to a computer, and the diameter was measured. For each diameter, nine readings were taken along approximately a 25-mm of the fibre bundle length, and the average diameter was recorded. The average diameter value obtained from 15 specimens was reported for each treatment. Specimens were reused for the tensile test following this test.

Tensile properties: To measure tensile properties of the studied fibres, a 5 kN Instron (Ametek Instruments, LS model, USA) was used to perform the tests based on the ASTM D3822 standard [28]. The Instron was equipped via EXYGEN*Plus* software to set input alternatives and record the data. The main components of the Instron were a frame, a drive system, a controller, a load cell, and two grips to hold specimen. To prevent the risk of fibre bundle slippage from the grips, the fibre samples of 25 mm in length were maintained on a clipboard frame using permanent fabric adhesive. For each treatment, 15 specimens were selected. It was reported in the literature that natural fibres and their composites were dramatically affected by the wet environment, and their water absorption from the surrounding environment was sometimes beneficial to the fibres characteristics, while in other cases not [29–31]. Therefore, in this work 65 % relative humidity was considered to avoid being biased neither to very humid environment nor to arid one, as this may be the general case in most of Canada and Europe. To achieve an equilibrium condition, the specimens were kept in an environmental chamber for three days at 21˚C and 65 % relative humidity [32]. When a fibre specimen was fit between the grips, sides of the frame were cut, and the mobile grip was extended at a rate of 25 mm/min to apply tension load until the fibre broke. From each test, the fibre diameter was inserted into the software, and the software generated tensile strength, Young's modulus, and elongation at break of the fibre. The average values obtained from 15 specimens were reported for each treatment.

6.5. RESULTS AND DISCUSSION

6.5.1. Results from the experiment

The average measured values of the CR, FF, d, s, σ, EM, and δ for the 8 treatments are shown in Table 6.4. The highest CR was achieved when treatment 4 and 6 applied (60%), followed by treatment 2. In contrast, treatment 8 (9%) had the lowest percentage of the CR. Regarding the FF, treatment 4 had the highest effects in the decortication output (82%), followed by treatments 6 (77%). Similarly, the lowest FF was related to treatment 8 (34%). According to the ESEM images analysis, the highest quality fibre (i.e. the highest scores) was in treatments 8.

Results indicated that fibres obtained from treatment 6 had the smallest d (168.59 µm), followed by treatment 3, which resulted in fibres with d of 211.53 µm. The highest σ was related to treatment 4 (472.51 MPa) and the fibres obtained from treatment 1, had the lowest tensile strength (200.76 MPa). The EM of the extracted fibre obtained from treatment 3 was noticeably high, 92 GPa. The maximum δ was observed when treatments 2 and 4 were applied, 0.496 mm and 0.512 mm, respectively.

Table 6.4. The average measured values of C_R (core removal), F_F (Fibre fraction), s (ESEM score), d (Fibre diameter), σ (tensile strength), E_M (Young's modulus), and δ (elongation at break).

Treatment	CR (%)	FF (%)	s (%)	d (μm)	σ (MPa)	E_M (GPa)	δ (mm)
1	40	58	55	276.65	264.53	29.43	0.406
2	59	71	30	229.25	348.69	36.26	0.496
3	55	64	30	212.64	362.58	92.00	0.343
4	60	82	60	219.22	472.51	45.80	0.512
5	31	41	50	249.80	352.20	63.79	0.383
6	60	77	55	168.59	409.73	77.29	0.449
7	24	42	70	232.06	425.65	36.16	0.451
8	9	34	85	220.83	351.36	37.44	0.459

To calculate the estimated effect of each alternative on the measured factors (sub-criteria), which was the main objective of carrying out the experiments, the ASTM E-1169 standard [27] procedure was followed. First, the average of the results from high level (+1) and low level (-1) (Ave+ and Ave- respectively) were calculated (Table 6.5). For example, the average high level and low level of retting condition (A), M, was estimated by taking average from a, d, f, and g; the average low level of retting condition (A), N, was estimated by taking average from b, c, e, and h. The differences M-N was the main effect of alternative A. The estimated effect of the all alternatives which were the absolute value of the main effects were listed in Table 6.6.

Table 6.5. Ruggedness test calculation

Initial, balanced design								
Treatment	A*	B	C	D	E	F	G	Measured alternative†
1	+1	+1	+1	-1	+1	-1	-1	a
2	-1	+1	+1	+1	-1	+1	-1	b
3	-1	-1	+1	+1	+1	-1	+1	c
4	+1	-1	-1	+1	+1	+1	-1	d
5	-1	+1	-1	-1	+1	+1	+1	e
6	+1	-1	+1	-1	-1	+1	+1	f
7	+1	+1	-1	+1	-1	-1	+1	g
8	-1	-1	-1	-1	-1	-1	-1	h
Ave +	M¤	…	…	…	…	…	…	
Ave -	N¤	…	…	…	…	…	…	
Main effect	M-N	…	…	…	…	…	…	

*Alternatives effect: A: retting condition, B: Bundle feed size, C: Number of passes through the roller, D: Number of passes through the finisher, E: 3-comb shaker, F: 6-combs shaker, G: diameter variation.

†Measured alternatives in this investigation are the percentage of fibre product, the percentage of core within fibre product, fibre diameter, crimps, kinks, tensile strength, Young's modulus, and elongation at break.

¤M is the average value of the high level of measured alternative (a+d+f+g)/4, N is the average value of the low level of the measured alternative (b+c+e+h)/4, Correspondingly: M´= (j+k+m+p)/4, N´=(i+l+n+o)/4.

Table 6.6. The estimated effect of the alternatives on the CR (core removal), FF (Fibre fraction), s (ESEM score), d (Fibre diameter), σ (tensile strength), EM (Young's modulus), and δ (elongation at break).

Alternatives	CR	FF	s	d	σ	E_M	δ
A	7.5	12.25	11.25	4.00	39.40	10.20	0.03
B	7.5	11.25	6.25	41.62	51.28	21.72	0.010
C	22.5	17.75	23.75	8.69	54.05	12.95	0.03
D	14.5	12.25	13.75	5.68	57.90	0.57	0.03
E	8.50	5.25	11.25	26.90	20.90	10.97	0.05
F	20.50	18.25	11.25	18.83	44.75	7.03	0.05
G	0.5	5.25	6.25	20.72	28.27	30.08	0.06

6.5.2. Results of the criteria pairwise comparison

To find the relative importance of each alternative with respect to a criterion, the pairwise comparison was done by dividing the values of alternatives by each other, with respect to a given criterion. Then, to indicate relative importance of the alternative, the obtained ratios were converted to a suitable value using the 1–9 Saaty [26] scale. This strategy was applied to complete the pairwise comparison matrices, by considering the consistency ratio for the judgment acceptance.

Three sets of matrices, to illustrate pairwise comparison for all levels of the hierarchy, were developed based on taking the average of the eleven experts' response to the questionnaire (Table 6.7). The transitivity and reciprocity rules were followed to constitute other components of the matrix.

Table 6.7. Pairwise comparison matrices for all levels of the hierarchy

a. Pairwise compression matrix for the model's main criteria

Creation	Fibre quantity	Fibre quality
Fibre quantity	1	1.91
Fibre quality	1/1.91	1

b. Pairwise comparison matrix for the Fibre quantity

Sub-creation	Core removal	Fibre fraction
Core removal	1	2
Fibre fraction	1/2	1

c. Pairwise comparison matrix for the Fibre quality

Sub-creation	ESEM score	Fibre diameter	Tensile strength	Young's modulus	Elongation at break
ESEM score	1	1/1.85	1/3.35	1/3.09	1/2.09
Fibre diameter	1.85	1	1/2.82	1/2.41	1/1.5
Tensile strength	3.35	2.82	1	1.28	2.45
Young's modulus	3.09	2.41	1/1.28	1	2
Elongation at break	2.09	1.5	1/2.45	1/2	1

Figure 6.4a shows the contribution of each main criterion (e.g. fibre quantity and fibre quality) to the main goal, where the priority of fibre quantity (e.g. weight) is remarkably higher than quality. The reason that experts allocated high priority to the quantity compared to the quality is probably because the fibres' quality can be further modified in another process called surface modification. The inconsistency ratio for the main criteria with respect to the goal was 0.00 which was less than 10% and thus acceptable.

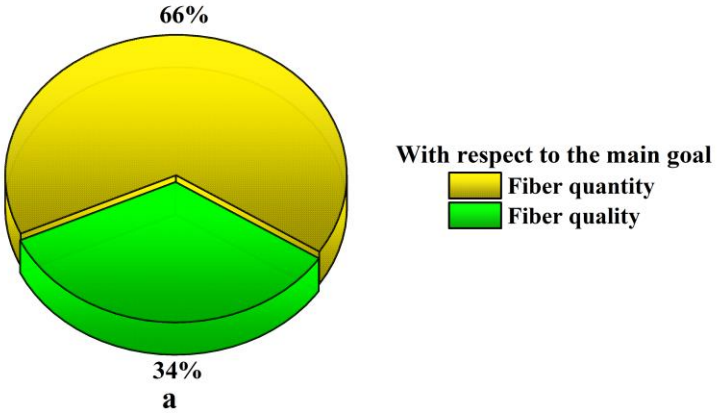

a

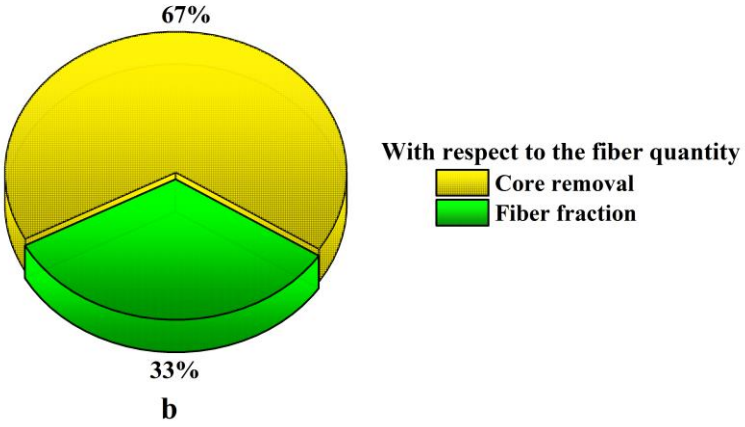

b

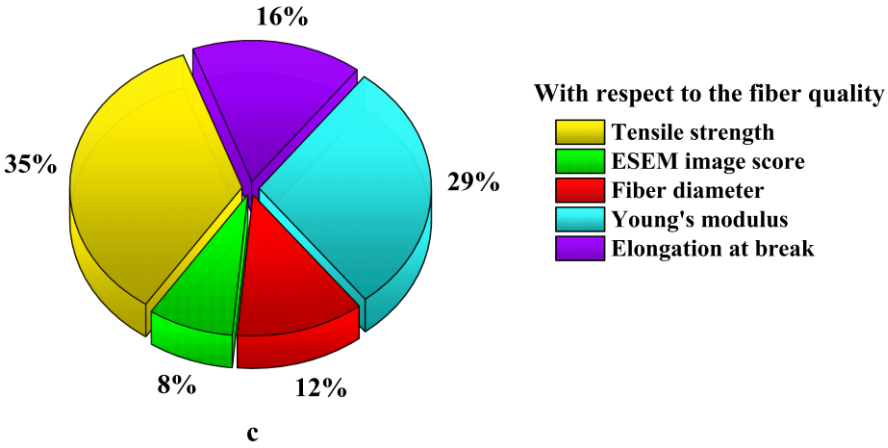

c

Figure 6.4. The contribution of the main criterions to the main goal (a), and the sub-criterions to the main criteria (b and c).

The contribution of the sub-criterion to their main ones is illustrated in Figs. 5.4b and 5.4c. The experts allocated high priority to the core removal (e.g. a weight of 67%) (Figure 6.4b) since high core removal shows high pure fibres were obtained during the decortication process. Considering the fibre quality as the main criterion, it was found that both tensile strength and Young's modulus were markedly the most important factors with a total aggregate weight of 64%. However, the ESEM image scores had the least important priority with a weigh of 8% (Figure 6.4c). The inconsistency ratio for sub-criterion to both fibre quantity and fibre quality was 0.0 and 0.01, respectively, which were acceptable.

6.5.3. Results of the alternative pairwise comparison

Considering the transitivity and reciprocity rules, the experimental results were used to constitute the relative pairwise comparison matrices of all alternatives with respect to each specific sub-criterion. For example, with respect to the core removal: the number of passes through the roller, retting condition, and the number of passes through the finisher, had the highest priorities, while the lowest priority was related to the stalk diameter variation (Figure 6.5a). Similarly, with respect to the fibre fraction, the highest priorities were the retting condition, number of passes through the rollers, and feed size, but the lowest priority were related to stalk diameter variations, and 3-comb shaker (Figure 6.5b). Because of conciseness, similar details for the other sub-criteria were not brought up.

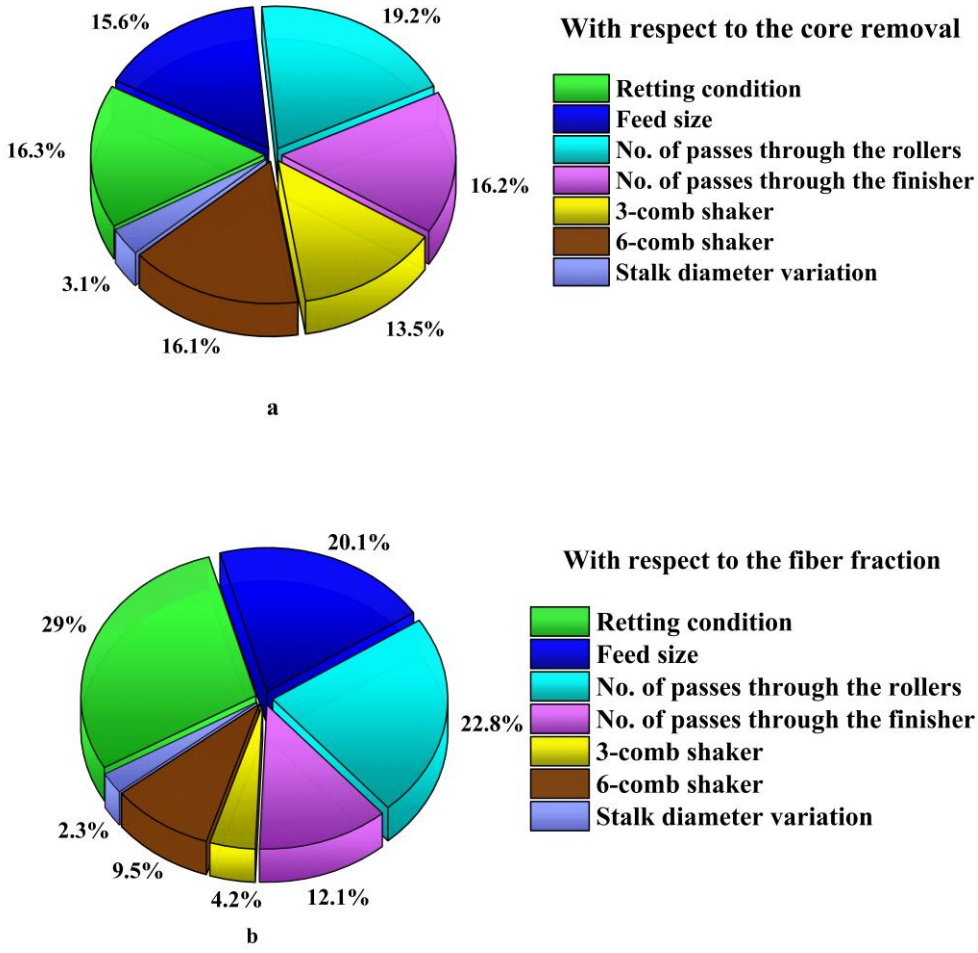

Figure 6.5. Priorities of the alternatives with respect to the (a) core removal and (b) fibre fraction.

Some calculations were done to develop the normalized relative pairwise comparisons (priorities) for all alternatives, with respect to the fibre quantity and fibre quality. The results are shown in Figure 6.6. Regarding the fibre quantity: stalk condition (A), feed size (B), number of passes through the rollers and finishers (C and D, respectively), and the 6-comb shaker, (F) had the highest priority in both core removal and fibre fraction, whereas the lowest priority was for stalk diameter variation (G) (Figure 6.6a). Although the 3-comb shaker noticeably affected core removal, it had a small effect on the fibre fraction. Regarding the fibre quality: retting condition

(A), feed size (B), and number of passes through the rollers (C), had the highest effect on both tensile strength and Young's modulus (Figure 6.6b). The influence of the 3-comb shaker (E), 6-comb shaker (F), and stalk diameter variation (G) on the Young's modulus was significantly higher than tensile strength. Retting condition (A) showed the highest priority to the elongation at break and ESEM images, while the lowest priorities were related to the stalk diameter variation (G).

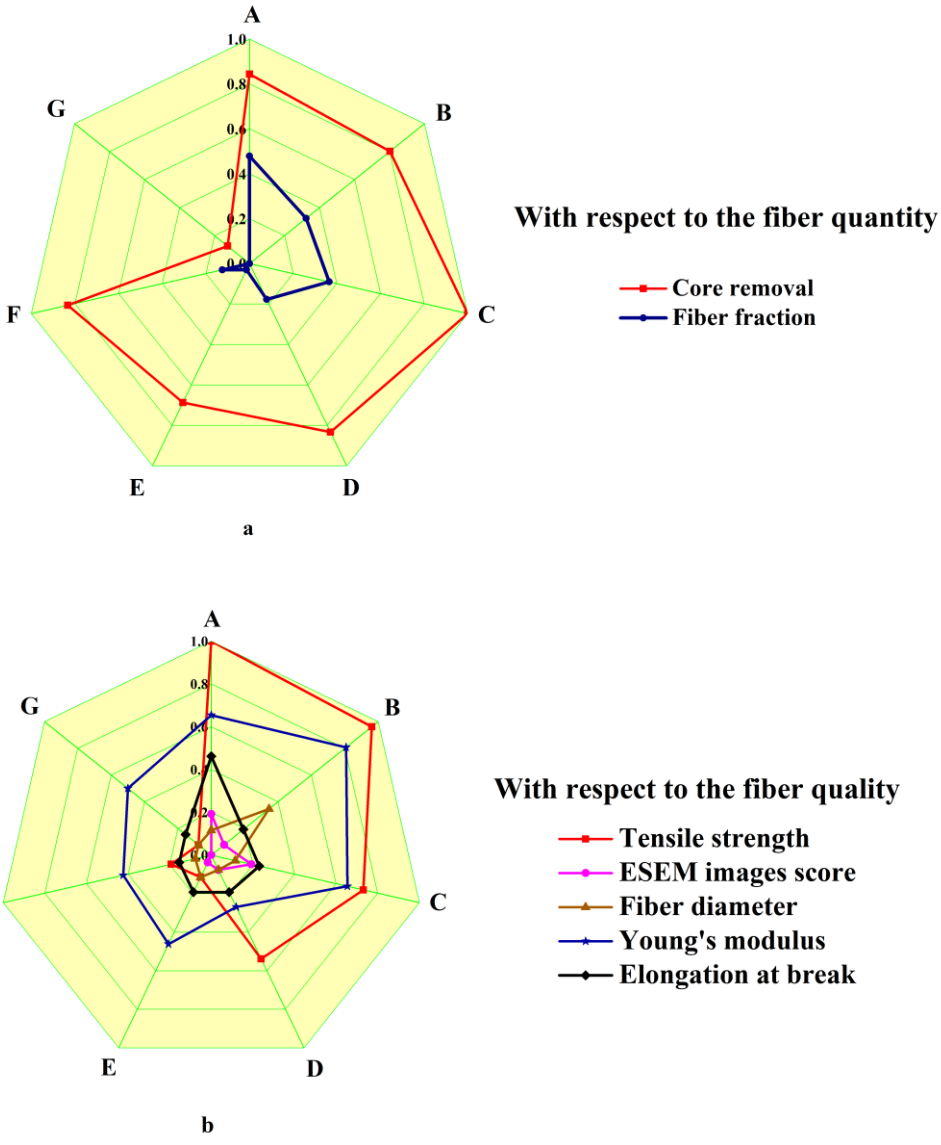

Figure 6.6. Priorities of the alternatives with respect to the (a) fibre quantity and (b) fibre quality. A: retting condition, B: Bundle feed size, C: Number of pass through the roller, D: Number of passes through the finisher, E: 3-comb shaker, F: 6-combs shaker, G: diameter variation.

The priority of the alternatives, with respect to the main goal (e.g. identifying the most influential parameters affecting mechanical extraction of bast fibres), was computed and presented in Figure 6.7. The most influential parameters (e.g. alternatives) affecting mechanical extraction of hemp fibres were the retting condition (20.4%), the number of passes through the rollers (19.4%), and the feed size (18.3%). The stalk diameter variation and the 3-comb shakers had respectively the least priorities; 4.4% and 10.7%.

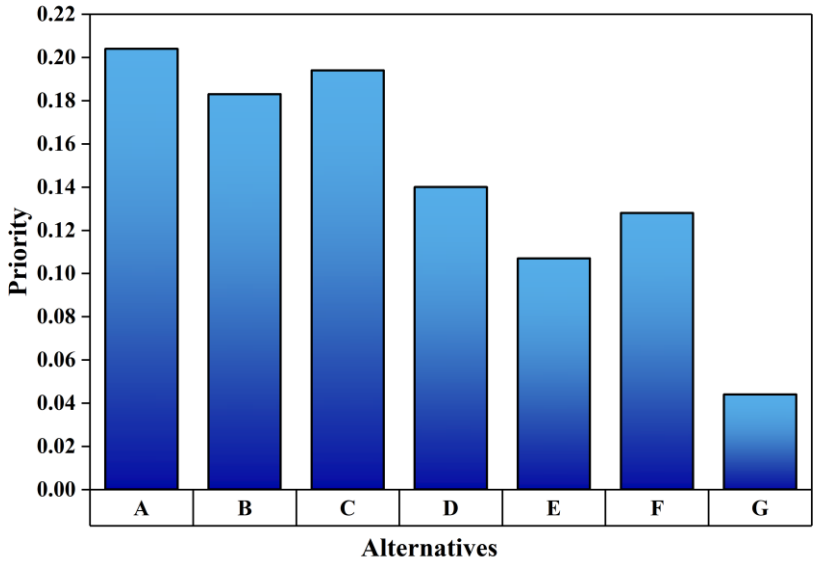

Figure 6.7. Priorities of the alternatives with respect to the main goal. A: retting condition, B: Bundle feed size, C: Number of passes through the roller, D: Number of passes through the finisher, E: 3-comb shaker, F: 6-combs shaker, G: diameter variation.

6.6. MODEL SENSITIVITY ANALYSIS

A sensitivity analysis was carried out to demonstrate the reliability of the drawn decisions under the influence of changing different alternatives of the model. To perform the analysis, the weight of the main criteria (e.g. fibre quantity and fibre quality) was altered to an unexpected exaggerated value to show an unreasonable change under normal conditions, to verify if a dominating alternative existed. According to AL-Oqla et al. (2015), increasing the weight of any criteria to more than 50% of the contribution in the model without making any dominant alternative

guarantees decisions drawn are confident and stable. In the current study, the weight of the fibre quality was increased from 34% to 74% (e.g. an unreasonable change under normal conditions), and the results were examined. Figure 6.8 demonstrates that the most influential parameters affecting mechanical extraction of hemp fibres were still the retting condition (A), with score of 22.9%; the feed size (F), with score of 22.5%%; and the number of passes through the rollers (C), with a score of 17.7%.

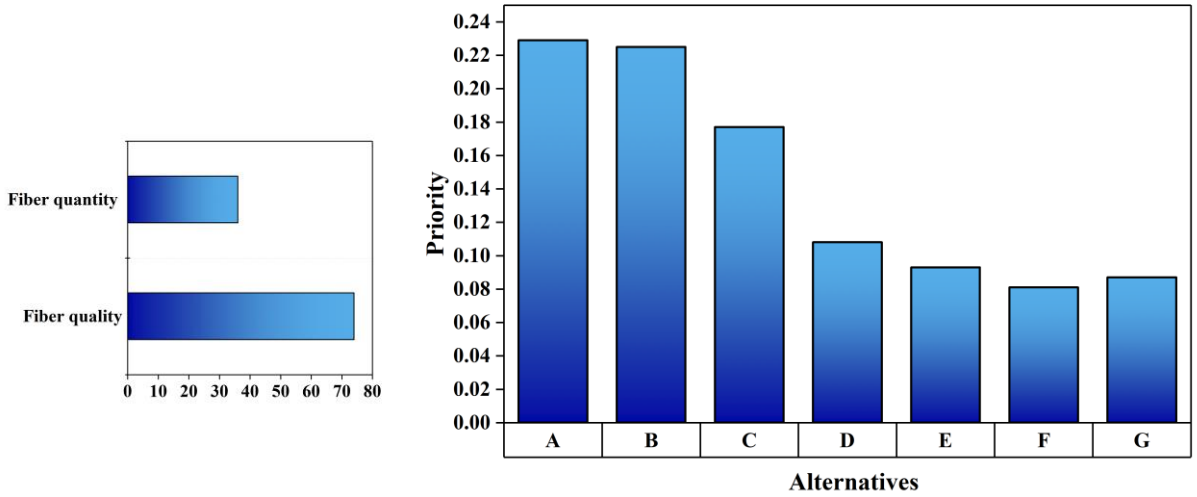

Figure 6.8. Dynamic sensitivity of the fibre quality criterion, the new assigned weights (left), and corresponding new scores of the alternatives (right). A: retting condition, B: Bundle feed size, C: Number of passes through the roller, D: Number of pass through the finisher, E: 3-comb shaker, F: 6-combs shaker, G: diameter variation.

Table 6.8 indicates the complete aggregate local and global weights of the developed AHP model items. The value of the local weights was obtained using pairwise comparison matrices. The global weights of the sub-criteria were calculated by multiplying the local weight of a sub-criteria with the local weight of the criteria to which it belongs. The most global contribution among all sub-criteria was related to the core removal and fibre fraction, while the least were coming from fibre diameter and ESEM images. The global score for core removal and fibre

fraction were 44% and 22%, and for ESEM images and fibre diameter were 3% and 4%, respectively.

Table 6.8. Local and global contributions of the AHP model items

Main criterion	Sub-criterion	Local priority	Global priority
Fibre quantity		0.66	0.66
	Core removal	0.67	0.44
	Fibre fraction	0.33	0.22
Fibre quality		0.34	0.34
	Tensile strength	0.35	0.12
	ESEM image score	0.08	0.03
	Fibre diameter	0.12	0.04
	Young's modulus	0.29	0.10
	Elongation at break	0.16	0.06

6.7. CONCLUSION

This work developed an AHP model to identify the most influential parameters that affected the quantity and quality of the extracted fibres. The results of the AHP model showed that the retting condition of the stalks (20.4%), the number of passes of stalks through the rollers (19.4%), and feed size (18.3%), were respectively the most influential parameters. The added values of the model include removing the bias of the expert's judgment, if any existed, and descending human error to select the most important alternatives. Industries will use the results of this work to enhance the design of the machine to improve fibre quality and quantity. It is highly recommended that in future work, different treatments of the number of passes through the rollers, in combination with different feed size, be studied to find the most desirable condition for the decorticator, in order to extract retted bast fibres.

6.8. ACKNOWLEDGMENT

This work was supported by the Composite Innovation Centre (CIC, MB, Canada) and Mitacs. The authors would like to thank Hamideh Sadrmanesh and Hanid Reza Fazeli for helping in developing the AHP model.

6.9. REFERENCES

[1] Sarasini F, Fiore V. A systematic literature review on less common natural fibres and their biocomposites. J Clean Prod 2018;195:240–67. https://doi.org/10.1016/j.jclepro.2018.05.197.

[2] Bourmaud A, Morvan C, Bouali A, Placet V, Perré P, Baley C. Relationships between micro-fibrillar angle, mechanical properties and biochemical composition of flax fibres. Ind Crops Prod 2013;44:343–51. https://doi.org/10.1016/j.indcrop.2012.11.031.

[3] Liu M, Fernando D, Meyer AS, Madsen B, Daniel G, Thygesen A. Characterization and biological depectinization of hemp fibres originating from different stem sections. Ind Crops Prod 2015;76:880–91. https://doi.org/10.1016/j.indcrop.2015.07.046.

[4] Le Duigou A, Baley C. Coupled micromechanical analysis and life cycle assessment as an integrated tool for natural fibre composites development. J Clean Prod 2014. https://doi.org/10.1016/j.jclepro.2014.07.027.

[5] Sadrmanesh V, Chen Y. Bast fibres: structure, processing, properties, and applications. Int Mater Rev 2018;0:1–26. https://doi.org/10.1080/09506608.2018.1501171.

[6] Pacaphol K, Aht-Ong D. Preparation of hemp nanofibres from agricultural waste by mechanical defibrillation in water. J Clean Prod 2017. https://doi.org/10.1016/j.jclepro.2016.09.008.

[7] Leduc PJ, Hill LG, Kelly DH, Stratton MA. Method for decorticating plant material. United States patent US 5720083 A. 1996 July 19., 1996.

[8] Gratton JL, Chen Y. Development of a field-going unit to separate fibre from hemp (cannabis sativa) stalk. Appl Eng Agric 2004;20:139–45.

https://doi.org/10.13031/2013.15882.

[9] Baker ML. Evaluation of a hammer mill and planetary ball mill for hemp fibre decortication [master's thesis]. Winnipeg (MB): University of Manitoba; 2009. 2009.

[10] Baker ML, Chen Y, Laguë C, Landry H, Peng Q, Zhong W, et al. Hemp fibre decortications using a planetary ball mill. Can Biosyst Eng 2010;52:7–15.

[11] Khan MMR, Y. Chen Y, C. Laguë C, H. Landry H, Q. Peng Q, W. Zhong W. Hemp (Cannabis sativa L.) decortication using the drop weight method. Appl Eng Agric 2013;29:79–87. https://doi.org/10.13031/2013.42521.

[12] Thakur S, Chen Y, Morrison J. Separation of Fibre and Shivesfrom Decorticated Flax. Appl Eng Agric 2017;33:113–20. https://doi.org/10.13031/aea.11335.

[13] Akin DE, Dodd RB, Foulk JA. Pilot plant for processing flax fibre. Ind Crops Prod 2005;21:369–78. https://doi.org/10.1016/j.indcrop.2004.06.001.

[14] Sadek M. Modelling biofibre (hemp) processing using the Discrete Element Method (DEM) [dissertation]. Winnipeg (MB): University of Manitoba; 2013. 2013.

[15] Parvin S. Separation of fibre and core from decorticated hemp [master's thesis]. Winnipeg (MB): University of Manitoba; 2011. 2011.

[16] Parvin S, Chen Y, Laguë C, Landry H, Peng Q, Zhong W. Post-decortication cleaning of hemp fibre using selected methods. AES Tech Rev Int Journal, Part C Int J Adv Trends Eng Mater Their Appl 2013;1:53–65.

[17] Al-Oqla FM, Sapuan SM. Natural fibre reinforced polymer composites in industrial applications: Feasibility of date palm fibres for sustainable automotive industry. J Clean

Prod 2014;66:347–54. https://doi.org/10.1016/j.jclepro.2013.10.050.

[18] Najafzadeh M, Rezaie-Balf M, Tafarojnoruz A. Prediction of riprap stone size under overtopping flow using data-driven models. Int J River Basin Manag 2018;16:505–12.

[19] Najafzadeh M, Zeinolabedini M. Derivation of optimal equations for prediction of sewage sludge quantity using wavelet conjunction models: an environmental assessment. Environ Sci Pollut Res 2018;25:22931–43.

[20] AL-Oqla FM, Salit MS. Materials selection for natural fibre composites. 2017.

[21] Kaur B, Bhatia R. Prioritizing parameters for software project selection using Analytical Hierarchical Process. vol. 118. 2015.

[22] AL-Oqla FM, Sapuan S, Ishak M. Predicting the potential of agro waste fibres for sustainable automotive industry using a decision making model. Comput Electron Agric 2015;113:116–27. https://doi.org/10.1016/j.compag.2015.01.011.

[23] Al-Oqla FM, Sapuan SM, Ishak MR, Nuraini AA. A Model for evaluating and determining the most appropriate polymer matrix type for natural fibre composites. Int J Polym Anal Charact 2015;20:191–205. https://doi.org/10.1080/1023666X.2015.990184.

[24] Sadrmanesh V, Chen Y. Simulation of tensile behavior of plant fibres using the Discrete Element Method (DEM). Compos Part A Appl Sci Manuf 2018;114:196–203. https://doi.org/10.1016/J.COMPOSITESA.2018.08.023.

[25] Saaty TL. The Analytic Hierarchy Process. New York: 1980.

[26] Saaty TL. Decision making with the analytic hierarchy process. Int J Serv Sci 2008;1:83–98.

[27] ASTM E-14. Standard Practice for Conducting Ruggedness Tests 2014:1–12.

[28] ASTM. Standard Test Method for Tensile Properties of Single Textile Fibres. ASTM Int USA 2015:1–10. https://doi.org/10.1520/D3822.

[29] AL-Oqla FM, Sapuan SM, Ishak MR, Nuraini AA. A novel evaluation tool for enhancing the selection of natural fibres for polymeric composites based on fibre moisture content criterion. BioResources 2014;10:299–312. https://doi.org/10.15376/biores.10.1.299-312.

[30] AL-Oqla FM, El-Shekeil YA. Investigating and predicting the performance deteriorations and trends of polyurethane bio-composites for more realistic sustainable design possibilities. J Clean Prod 2019;222:865–70. https://doi.org/10.1016/J.JCLEPRO.2019.03.042.

[31] Fares O, AL-Oqla FM, Hayajneh MT. Dielectric relaxation of mediterranean lignocellulosic fibres for sustainable functional biomaterials. Mater Chem Phys 2019;229:174–82. https://doi.org/10.1016/J.MATCHEMPHYS.2019.02.095.

[32] CGSB. Conditioning Textile Materials for Testing. Canadian General Standards Board and Standards Council of Canada.CAN/CGSB-4.2 no. 2-M88.; 2001.

Chapter 7: Multi-Objective Optimization of Canola Fibre Extraction Using a Hybrid Algorithm

7.1. ABSTRACT

Optimal retting conditions for high quantity and quality fibres are specific and have not been well documented for canola fibres. In this study, experiments were conducted to ret canola stalks in solutions under the following treatments: 12-72 hour for the retting time, 24-90 ºC for the temperature, and 0-10 % for the $NaHCO_3$ concentration (%w/w). The fibre yield, chemical compositions, crystallinity index, thermal stability, and maximum degradation temperature of the fibres were measured. The optimized retting parameters were predicted by developing a hybrid algorithm which was a combination of a genetic algorithm (GA) with consecutive sequential quadratic programming (SQP). Results showed the reaction time was the most important retting parameter, followed by reaction temperature and $NaHCO_3$ concentration. The optimum retting parameters for time, temperature, and $NaHCO_3$ concentration to achieve the highest quantity and quality fibres were 37.8 h, 57.7 ºC, and 5.62%, respectively.

7.2. INTRODUCTION

In Canada, one of the most potential fibre plants is Canola (Brassica Napus). Canola fibres can be potentially used as reinforcement for composite materials. The area of harvested canola in Canada increased from 7.12 MHA in 2010 to 9.27 MHA in 2017 [1]. After harvesting canola seeds, unfortunately, excessive amounts of canola stalks are left in the fields and considered as waste. Extracting fibres from canola stalks not only alleviates their side effects on the environment but also enhances the value-added of the planting canola. One potential way to extract canola fibre is

retting. In this process, cellulose of the fibre is kept, and other components such as hemicellulose, lignin, pectin, and waxy substances are removed [2]. If the process is performed correctly, high quality and quantity bast fibre can be separated from the plant stalks. As a result, the hydrophilic and polar properties of the fibres decrease, and their tendencies to blend with hydrophobic matrix increase. The reason for this improvement is the removal of hydroxyl groups. Hydroxyl groups are loosely linked with the fibre structure in the amorphous region of cellulose, hemicellulose, lignin, and pectin [3].

Alkali chemical retting decreases the amorphous hydroxyl groups and reduces the hydrophilic nature of the fibres. A cost effective chemical treatment is using commercial sodium bicarbonate (i.e. baking soda) ($NaHCO_3$) [4,5]. This solution is mildly alkaline because of constituting carbonic acid and hydroxide ion ($NaHCO_3 + H_2O \rightarrow Na^+ + HCO_3^-$, $HCO_3^- + H_2O \rightleftharpoons H_2CO_3 + OH^-$). Considering that OH groups existing in the fibres are related to the alcoholic hydroxyls, the interaction is like the traditional alkaline treatment with sodium hydroxide (Fibre-OH + NaOH → Fibre-$O^-Na^+ + H_2O$). The treatment also removes a specific amount of hemicellulose and lignin which leads to availability of large number of celluloses for matrix adhesion [6,7]. Sgriccia et al. (2008) reported that alkali treatment removed pectin and hemicellulose from the plant fibres. It was found that the alkali treatment increased crystallinity index and improved the mechanical properties of kenaf fibre composites [9]. The effectivity of the alkali treatment on the quantity and quality of the fibres depends on the reaction time and temperature. Uncontrolled retting deteriorates the quantity and quality of the fibres. For example, high alkali solution concentration excessively depolymerizes the cellulose and dignifies the fibre, which decreases the crystallinity index and as a result decrease the strength and stiffness of the fibres [9]. Therefore, optimizing

retting parameters such as time, temperature, and chemical concentration for optimal fibre quantity and quality is essential.

The parameters which were used to evaluate the quantity and quality of the fibres in this research were fibre yield, thermal stability, maximum degradation temperature, and crystallinity index. These parameters were considered as objectives where the maximum value of each of them is desirable. This multi-objective problem can be solved using either Pareto or scalarization methods. In the Pareto method, developing a continuously updated algorithm results in the dominated and non-dominated solutions. This method provides a compromise solution in the form of Pareto optimal front. In the scalarization method, all the objectives turn into a single objective using weighing. This method provides a scalar function which is incorporated in the fitness function [10]. When the maximum or minimum values of all the objectives is the intention, and there is no comparison solution, the scalarization method is a suitable option. Certain algorithms such as evolutionary algorithms or/and gradient-based can be used to determine the optimal value. The commonly used evolutionary algorithms and gradient based algorithm are Genetic Algorithm (GA) and Sequential Quadratic Programming (SQP), respectively. The GA maintains large sets (populations) of potential solutions and apply re-combination operators on them to reach an optimum solution. The SQP finds a search direction by solving an approximate problem based on linear approximations of the constraint functions and a quadratic approximation of the objective function. The GA is strong to global optima but slow and poor to identify the local optima. In contrast, the SQP is well-suited to find the local optima for constrained nonlinear optimization problems, but the solution may be not the global optimum of the problem. When the start point of the SQP is from a possible initial solution, a computational robustness is guaranteed.

The main objective of this study was to predict optimum value of time, temperature, and

$NaHCO_3$ concentration to extract high quantity and quality canola fibres. The experiments were designated based on the Response Surface Methodology (RSM). The quantity of the fibres was evaluated using drying and weighing the extracted fibres. The quality of the extracted fibres was estimated using FTIR, XRD, and TGA tests. The expert's knowledge was used to weight the measured parameters, then using a hybrid optimization algorithm, the optimized retting parameters were predicted.

7.3. MATERIALS AND METHODS

7.3.1. Design of retting experiments

Response surface methodology (RSM) was used to determine a functional relationship between the input variables (retting time, temperature, $NaHCO_3$ concentration) and the output parameters (yield, thermal properties, and crystallinity index of extracted fibre). Preliminary tests showed that the appropriate range for the retting time, temperature, and $NaHCO_3$ concentration were 12-72 hour, 24-90 ºC, and 0-10 %w/w. According to the three-factor central composite design in the RSM, the experiment conditions were as shown in Table 7.1.

Table 7.1. Experimental conditions based on central composite design in Response Surface Methodology.

Run number	Time (hr) (±0.2)	Temperature (ºC) (±0.4)	$NaHCO_3$ (%w/w)
1	24	77	8
2	12	57	5
3	60	37	8
4	72	57	5
5	42	57	5
6	42	57	10
7	42	57	5
8	42	57	5
9	42	57	0
10	60	77	8
11	42	90	5
12	42	57	5
13	42	24	5
14	24	77	2
15	24	37	2
16	42	57	5
17	24	37	8
18	60	37	2
19	42	57	5
20	60	77	2

7.3.2. Sample preparation

Canola seeds were planted in the middle of May and were harvested at the end of August. The canola stalks (vigor L241C variety) were then randomly collected from a research farm in Portage la Prairie, Manitoba, Canada. After that, they were stored indoor, and air-dried. Before performing the retting extraction trials, the stems were randomly selected, cleaned from the leaves, and cut into segments of 200 ± 10 mm in length.

7.3.3. Chemical retting procedures

A stable temperature digital utility water bath (Cole-Parmer, 5 L, Canada) was used for retting. The device had a 5-L water tank. A primary microprocessor-based temperature controller in the device provided ±0.1 °C precision and a secondary over-temperature safety sensor prevented the device from overheating. For a test, the tank was filled up with solution of a specific $NaHCO_3$ concentration. After adjusting the temperature and the reaction time, 20 ± 2 g of canola stems was immersed inside the device's tank. At the end of the retting time, the stems were taken out from the tank, and they were immediately put in water. Then, the fibres were manually peeled out. The extracted fibres were washed with warm water to remove the chemicals, dried at 55 °C for 72 h [11], weighed to compute the fibre yield, and stored in a zip-lock bag for further analyzes.

7.3.4. Measurements

7.3.4.1. Fibre yield

Fibre yield was measured to evaluate the effect of the chemical retting on the fibre quantity. The weight of the canola fibres obtained from each test was recorded as the output mass (m_o). With the initial mass (m_i) of the canola stems, the fibre yield (Y, %) was estimated based on the Eq. 7.1.

$$Y = \frac{m_o}{m_i} \times 100 \qquad (7.1)$$

7.3.4.2. Fourier Transform Infrared Spectroscopy (FTIR)

The chemical compositions of the extracted fibres were analyzed using Fourier Transform Infrared Spectrometry (FTIR) operating in attenuated total reflectance (ATR) (Nicolet iS10 FTIR spectrometer, ThermoFisher Scientific). The IR spectrum of the samples was recorded in the 4000-650 cm^{-1} region with 32 scans in each case at a resolution of 4 cm^{-1}. For each sample, five replications were carried out.

7.3.4.3. Thermogravimetric analysis (TGA)

To determine the thermal stability (TS) and maximum degradation temperature (MDT) of the extracted fibres, the samples were analyzed using a Perkin Elmer TGA 7 Thermogravimetric Analyzer apparatus whilst maintaining a static argon flow of 150 mL/min. The temperature was ranged from room temperature to 600 ºC at a rate of 2 ºC. For each sample, triplicate runs were done and averaged.

7.3.4.4. X-ray Diffraction (XRD)

The crystallinity index (CI) of the fibres was assessed using a Bruker D8 DaVinci diffractometer. A layer of each sample was attached to a circular disk, and the disk was maintained on the machine. The diffracted intensity of CuKα radiation was recorded over a range of 2Θ from 10° to 50° at a scanning speed of 0.03 mm/s, a current of 40 mA, and voltage of 40 mV.

7.3.5. Optimization of retting parameters

A method was proposed to effectively predict the optimized parameters for extracting canola fibres. Four main steps were followed. First, design of the experiments was performed based on the Response Surface Methodology to reduce the number of experiments to generate the data. Then, a surrogate model was developed for each measured parameter (e.g. each objective). After that, the multi-objective problem was turned into a single objective problem using the scalarization method. In the final stage, a hybrid algorithm was developed by combining a genetic algorithm (GA) with consecutive sequential quadratic programming (SQP) to predict the maximum solution. With these, the optimized retting parameters were identified. More details of the surrogate models, the scalarization method, and the hybrid GA-SQP algorithm are explained as follows. Figure 7.1 shows a schematic diagram of the optimization procedure.

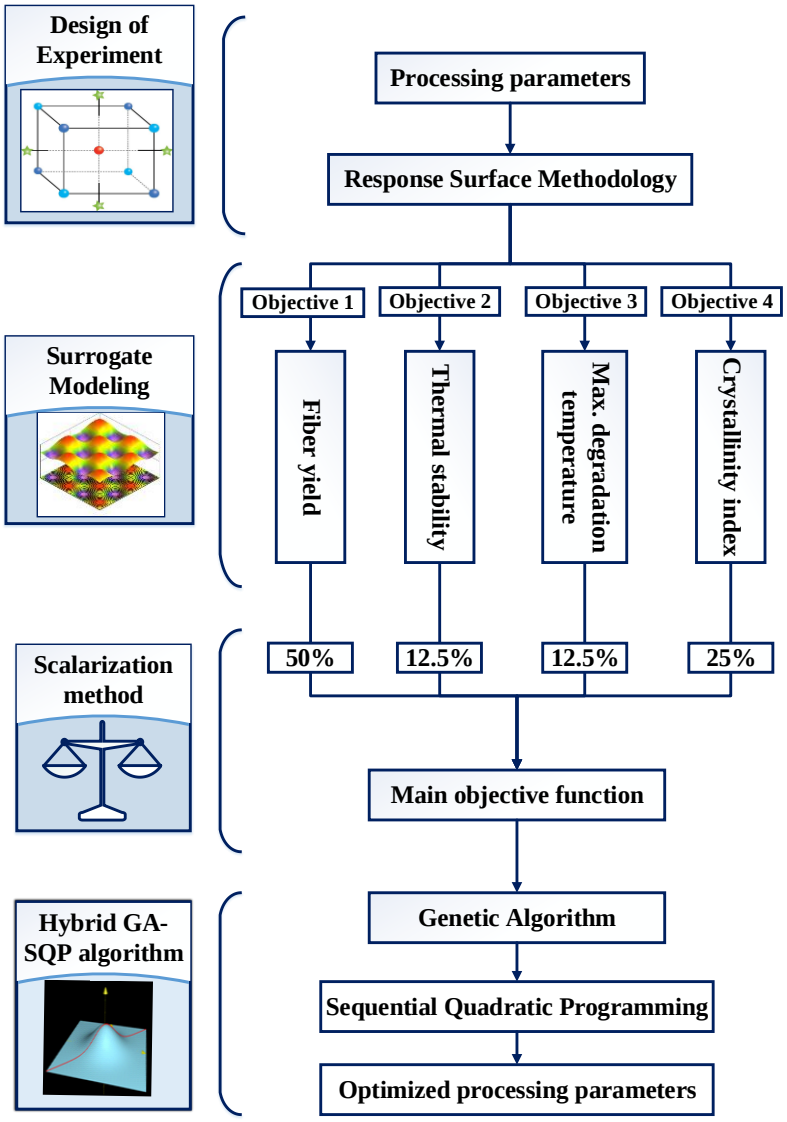

Figure 7.1. Procedure to predict the optimized retting parameters.

7.3.5.1. Surrogate model

Surrogate model is an efficient technique to decrease the costs of experiments using development of an approximate model for the true response surface. In this study, the data from the experiments were used to construct a surrogate model to predict a specific objective (e.g. fibre yield, thermal stability, maximum degradation temperature, and crystallinity index). For each specific objective, different types of surrogate models were tried, and it was found that kriging model was the most suitable one but the most time-consuming. This was probably because the kriging model was able

to be dynamically updated based on the responses during a given optimizing procedure. It makes the kriging model to be appropriated for a highly-nonlinear function with multi extremes.

Using the developed surrogate models, the sensitivity analysis was performed to identify the most influential variables affecting the output based on the main effect technique. In this technique, the differences between the average output values for all runs of an input variable at its upper and lower bond were calculated. The input variable with the largest main effect was selected as the most influential parameter.

7.3.5.2. Scalarization method

The scalarization method was more suitable than the Pareto method because the maximum values of all the objectives was the intention, and there was not any comprise solution. In the scalarization method, a single solution for the multi-objective functions is created. Specifically, the multi-objective problem turns into a single objective by allocating weight to each specific objective. In this study, the scalarization method was used to incorporate the multi-objective function into a scalar fitness function according to the following equation:

$$P(x) = w_1 FY(x) + w_2 TS(x) + w_3 MDT(x) + w_4 CI(x) \qquad (7.2)$$

where P(x) is performance indicator, w_n is the weight of each objective, *FY* is the fibre yield function, *TS* is the thermal stability function, *MDT* is the Maximum degradation temperature function, and *CI* is the crystallinity index function. Higher values of all the independent variables are desired. But each independent variable carried a weight in determining the retting performance. The fibre quantity (*FY*) was of the most importance, and thus it was given a higher weight factor ($w_1=0.5$). The weight factors associated with fibre quality were $w_2=0.125$, $w_3=0.125$, and $w_4=0.25$, determined based on the expert's knowledge.

7.3.5.3. Hybrid GA-SQP Algorithm

To take advantage of both the algorithms, a GA-SQP algorithm was developed to predict the optimum retting parameters. The GA was used to search the global optimum in the whole solution region to obtain the quasi-optimal solution. Then, the SQP was used to obtain the optimal solution in order to enhance the power of the GA regarding both solution quality and speed of convergence to the optimal. The hybrid GA-SQP algorithm had the ability to find an appropriate starting point, guarantee a faster convergence speed, and a higher convergence accuracy to predict the optimal solution [12]. This research does not intend to explain details about the GA and SQP methods. However, the GA and SQP parameters considered for this study are brought in Table 7.2.

Table 7.2. The Genetic Algorithm (GA) and Sequential Quadratic Programming (SQP) parameters

The GA parameters	Value	The SQP parameters	Value
Maximum Generations	1000	Maximum number of function evaluations	2000
Population size	50	Maximum number of iterations	75
Crossover	1	Number of optimizations runs	5
Mutation	0.1	Finite difference step size for calculating gradients	0.001
Maximum constraint violation	0.05	Tolerance on objective functions	0.001
Percent penalty	0.5	Tolerance on constrain feasibility	0.001
Stall generation limit	100	Tolerance on projected gradient	0.01

7.4. RESULTS AND DISCUSSION

7.4.1. Fibre yield

Based on the surrogate model developed according to the experimental results, the effect of $NaHCO_3$ concentration, time, and temperature on the fibre yield was plotted (Figure 7.2). The

sensitivity analysis showed that temperature had the highest effect on the fibre yield (e.g. 54%) followed by the chemical treatment (43%). At all levels of retting times, the lowest fibre yield was obtained when the temperature was more than 70 ºC, and the $NaHCO_3$ concentration was less than 5%. In contrast, the yield was maximum when the temperature and $NaHCO_3$ concentration ranges were between 50 to 60 ºC and 6 to 8%, respectively. The reason of increasing fibre yield at temperatures less than approximately 60 ºC and $NaHCO_3$ concentrations less than about 8% was probably because of pectin removal assisting to separate fibre from the stems. However, the high temperatures and chemical concentrations caused degradations of other chemical compositions, leading to a lower fibre yield. It was predicted that the optimum time, temperature, and $NaHCO_3$ concentration to reach the highest yield (11.24%) were respectively 54.86 hr, 57 ºC, and 6.43%.

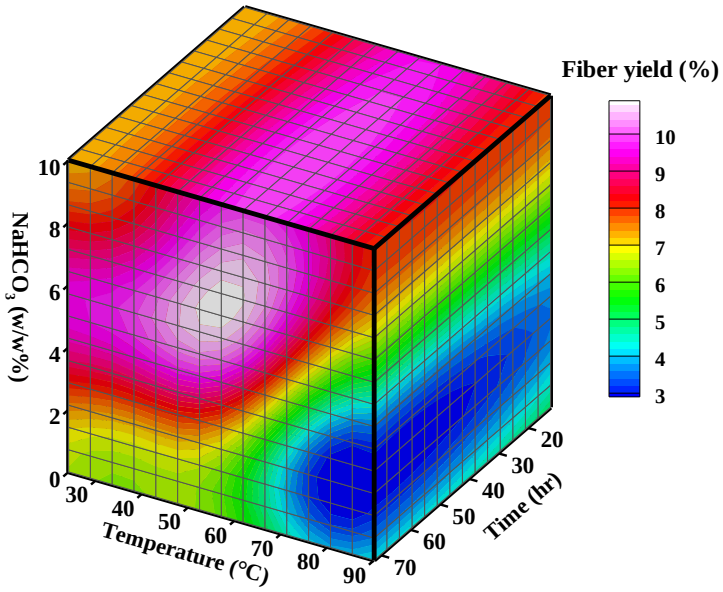

Figure 7.2. The effect of the retting parameters on the fibre yield.

7.4.2. Fourier Transform Infrared Spectroscopy

The spectra of the extracted fibres were seemingly similar because their major compositions of all the extracted fibres were cellulose and other polysaccharides such as hemicellulose and pectin

(Figure 7.3). However, there were some differences in the peaks for different tests, showing that the applied treatments changed the chemical compositions of the fibres. There were some peaks on all of the curves representing the chemical bonds related to the chemical compositions of the fibres. The peaks in the range of 3600 to 3100 cm^{-1} were attributed to O-H stretching via vibration in cellulose, hemicellulose, lignin, and pectin [13–15]. The absorption bands at around 2900 cm^{-1} were because of the C-H stretching vibration of the general organic material content of the fibre [16]. The peaks around 2920-2840 cm^{-1} were due to the C-H stretching vibration from CH and CH_2 in cellulose, hemicellulose, lignin, pectin, and waxes components (Konczewicz et al., 2017; Yang et al., 2007). The peaks centered around 1735 cm^{-1} represented the C=O stretching vibration of linkage of carboxylic acid in lignin or ester group in hemicellulose [4,16] while the peaks centered around 1600 cm^{-1} were due to the existence of O-H stretching group in the absorbed water [15,17]. The absorbance peak at around 1595 and 1505 cm^{-1} were explained by C=C stretching of aromatic ring of the lignin [15,18], and at around 1475 cm^{-1} were explained by CH_2 symmetric bending in cellulose, lignin, hemicellulose, and pectin [8,15]. The peaks at around 1365 and 1315 cm^{-1} were associated to the vibration of C-H and C-O groups of the aromatic ring in polysaccharides [4,19]. The absorbance at around 1235 cm^{-1} was the characteristic bands for the C-O stretching vibration of the acetyl group in lignin [4,20]. The C-C ring band at 1155 cm^{-1} and the C-O-C glyosidic ether band at 1105 cm^{-1} were as a consequence of the polysaccharide components which were largely cellulose [16]. The intense peaks at around 900 cm^{-1} were explained by b-glyosidic linkages between the monosaccharides of cellulose and hemicellulose [15,18].

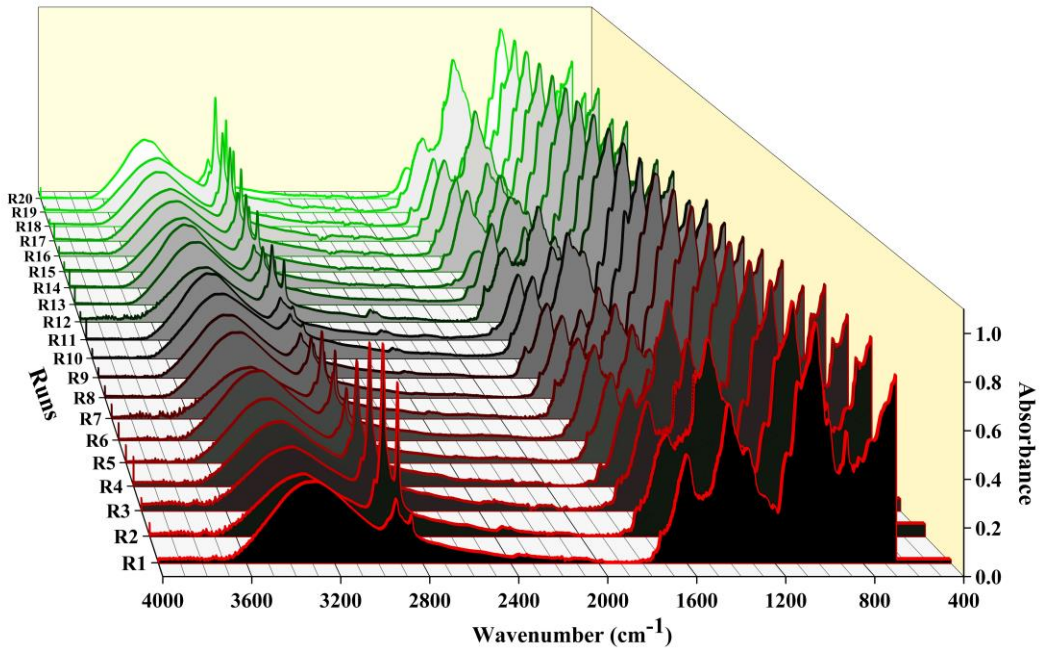

Figure 7.3. FTIR spectrum of canola fibre

7.4.3. Thermogravimetric analysis

The results of thermogravimetric analysis were used to plot TG and DTG graphs (Figure 7.4). TG graph was directly plotted from the obtained data and the DTG was plotted based on the first derivative values of the mass losses. Typically, several peaks were observed in the DTG graph which were related to (1) the vaporization of moisture, (2) decomposition of hemicellulose which was the first chemical composition to decompose due to its amorphous structure, (3) decomposition of cellulose which was more stable than hemicellulose because of several microfibrils positioned at the structure of the cellulose, and (4) oxidative degradation of the charred residue. No peaks were found for decomposition of lignin since lignin decompose from very low temperature to 600 ºC due to its complex composition structure of aromatic rings with various branches [2].

Thermal stability (TS), the temperature where hemicellulose starts decomposing, and maximum degradation temperature (MDT), where cellulose starts decomposing, are two important

temperatures to compare natural fibres from the thermal property standpoint. Figure 7.4 demonstrates the effects of the time, temperature, and $NaHCO_3$ concentration on the TS and MDT of the canola fibres. Based on the sensitivity analysis, it was found that among all retting parameters, the $NaHCO_3$ concentration treatment had the highest effect on the both TS and MDT.

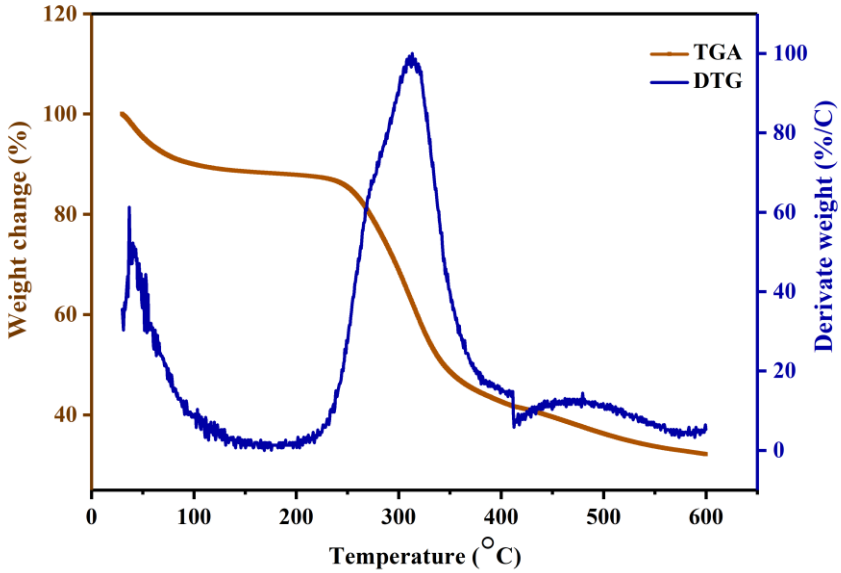

Figure 7.4. TG and DTG curves of a canola fibre

The developed surrogate model based on the experimental results was used to plot the effect of the retting parameters on the TS (Figure 7.5a). At $NaHCO_3$ concentrations less than 6%, the effect of time and temperature on the TS was negligible but a small change was found at high chemical concentrations. The desirable ranges of time, temperature, and $NaHCO_3$ concentration were 25 to 45 hr, 45 to 60 ºC, and 8 to 10%, respectively, where the value of the TS was in maximum. The reason was probably owing to removing hemicellulose from the chemical component of the fibres as hemicellulose was the first composition to degrade [4,6,21]. The other potential rationale was due to removing lignin but since no peak could be found on the DTG graph for lignin, no further consideration can be done [4]. The reason of decreasing the TS beyond the outlined desirable ranges was probably because of degradation of lignin bonded cellulose. It was projected that the

most desirable TS (284.69 ºC) would be achievable under the temperature of 52.29 ºC, the retting time of 37.71 hr, and the $NaHCO_3$ concentration of 8.57%.

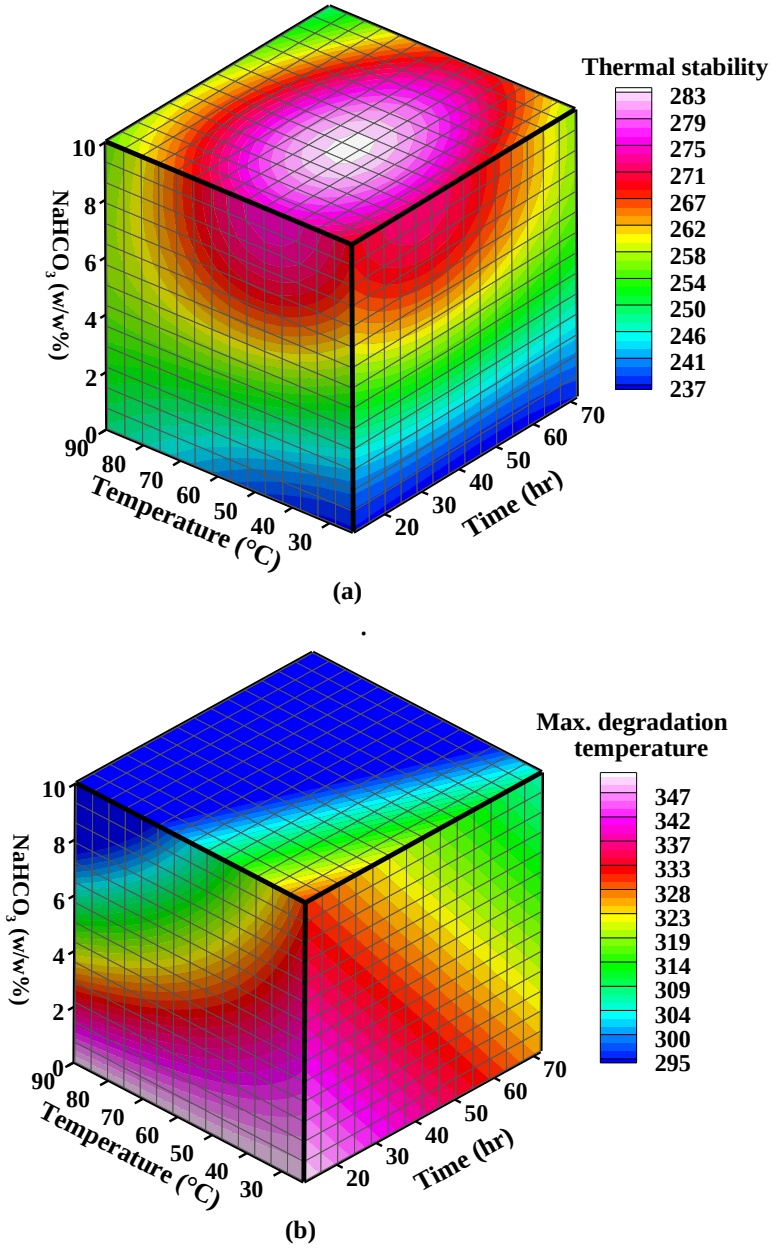

Figure 7.5. The effect of the retting parameters on the (a) thermal stability, and (b) maximum degradation temperature.

According to the experimental results, a surrogate model was developed and Figure 7.5b was plotted to show the effect of retting parameters on the MDT. The effect of time and temperature

on the MDT was more pronounced than on the TS. At $NaHCO_3$ concentrations less than 2%, only the retting time influenced the MDT, but at higher $NaHCO_3$ concentrations, increasing both time and temperature lead to the deterioration of MDT in which the value of MDT was at minimum at temperatures higher than approximately 70 ºC, and $NaHCO_3$ concentrations higher than 7%. The possible reason to decrease the MDT by increasing time, temperature, and $NaHCO_3$ concentration was exposing the cellulose network because of removing lignin [21]. The most desirable condition to obtain the maximum MDT was the lowest time (12 hr), temperature (24 ºC), and chemical concentration (0%).

7.4.4. Crystallinity index

Fibres with high crystallinity indices are stiffer. Crystallinity index was calculated using the following formula [22]:

$$CR = \frac{I_{002} - I_{amp}}{I_{002}} \times 100 \qquad (7.3)$$

where CR is crystallinity index, I_{002} is the peak intensity of the crystalline region which is located at $22^o<2\Theta<24^o$, and I_{amp} is in the amorphous region which is located at $18^o<2\Theta<20^o$. A surrogate model was fitted on the experimental data of CR, and the effect of time, temperature, and $NaHCO_3$ concentration was plotted (Figure 7.6). Sensitivity analysis demonstrated that the most effective treatments on the CR was temperature (66%) followed by $NaHCO_3$ concentration (30%). At high temperatures, the CR had high values when the $NaHCO_3$ concentration was between 4 to 6% and the retting time varied from 40 to 55 h. Under the applied treatment, amorphous materials (e.g. lignin, hemicellulose and wax) were eliminated from the fibre and the CR was enhanced. The reason for decreasing the CR above the outlined treatment was because of degradation of celluloses in addition to the amorphous materials. The CR would be maximum

(88.39%) when the extraction process was done for 46.29 h under 80.57 ºC, and 5% $NaHCO_3$ concentration.

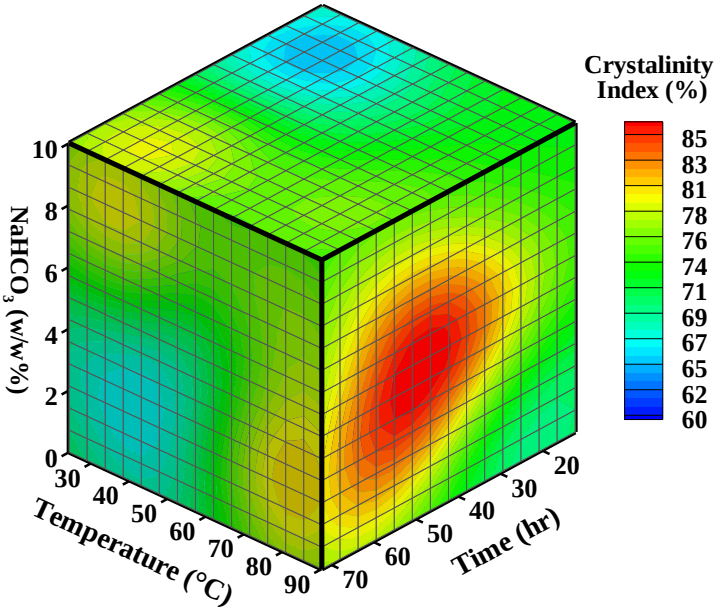

Figure 7.6. The effect of the retting parameters on the crystallinity index.

7.4.5. Predicting the optimum retting parameters

The effect of the retting parameters on the performance indicator (P(x)) was plotted according to the Eq. 3 (Figure 7.7). The sensitivity analysis showed that the importance of the retting parameters ranked as following: time, temperature, and chemical concentration. At short retting times, the ideal temperature and $NaHCO_3$ concentration ranges to reach the maximum value of the main objective were from 50 to 60 ºC and 4 to 6 %, respectively. When the retting parameters were set on the lowest levels, the value of the main objective was much better than the retting parameters being set at the highest levels.

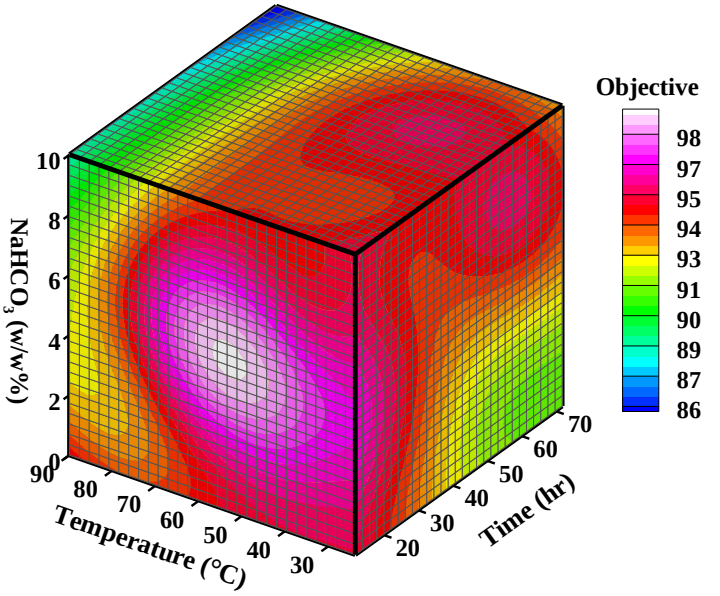

Figure 7.7. The effect of the retting parameters on the performance indicator

The optimization was done by maximizing the scalar fitness function, P(x) in equation 3 through changing retting parameters (*FY*, *TS*, *MDT*, and *CI*). The search space contained some local optima points which might lead to a local optimum solution. Therefore, an efficient algorithm was used to find global solution of the optimization problem. The GA was used to search the global optimum in the whole solution region to obtain the quasi-optimal solution. It gave an appropriate starting point for the SQP algorithm. After finding near global optimum point via NSGA–II, the obtained design point (e.g. starting point) was transferred to SQP as initial conditions to find the precise global solution and enhance the power of the optimization process regarding both solution accuracy and efficiency to the optimal retting parameters. Convergence history of the performance indicator (P(x)) in the SQP process is presented in Figure 7.8. The optimization problem was converged after 5 steps. It was found that the optimum retting parameters for retting time, temperature, and chemical concentration was 37.8 h, 57.7 ºC, and 5.62, respectively.

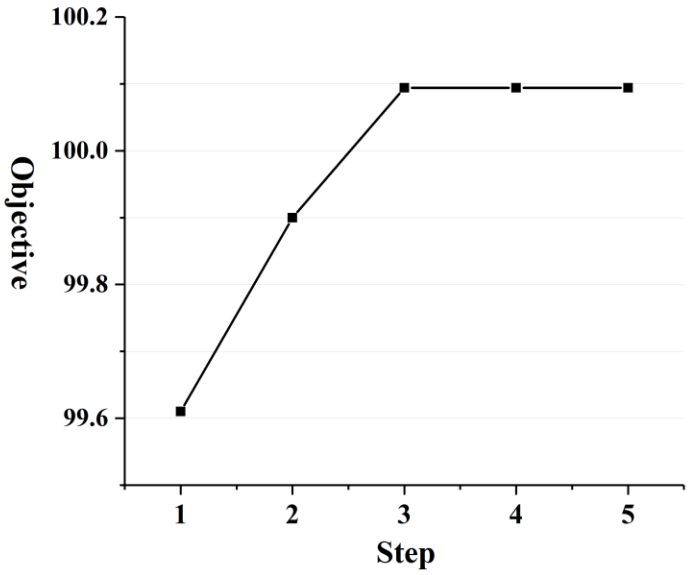

Figure 7.8. Convergence history of the objective function in the SQP process

7.5. CONCLUSION

Canola fibres were extracted under different levels of retting time, temperature, and $NaHCO_3$ solution treatments. The extracted fibres were analyzed using Fourier Transform Infrared Spectroscopy (FTIR), thermogravimetric analysis (TGA), and X-ray Diffraction (XRD). Then, a hybrid GA-SQP algorithm was developed to predict the optimum retting condition to obtain high quantity and quality fibres. The following conclusions were drawn:

- The fibre yield was maximum when the retting time was more than 50 h, the temperature level was in the range of 50 to 60 ºC, and $NaHCO_3$ concentration was in the range of 6 to 8%.
- The FTIR analysis of the extracted fibres showed that the applied retting condition changed the chemical compositions of the extracted fibres.
- Increased thermal stability of the extracted fibres was observed when the $NaHCO_3$ concentration was in the highest level, and the time and temperature levels were in the range of 30 to 45 h, and 45 to 65 ºC, respectively.

- The highest maximum degradation temperature was achieved when all of the fibres were extracted at the lowest levels of the retting parameters.
- At high temperatures, the crystallinity index was high when the fibres were extracted at retting time ranged from 40 to 55 h, and $NaHCO_3$ concentration from 4 to 6%.
- The results of the hybrid GA-SQP algorithm showed that the optimum retting parameters for time, temperature, and chemical concentration to achieve the highest quantity and quality fibres were 37.8 h, 57.7 ºC, and 5.62%, respectively.

7.6. ACKNOWLEDGMENTS

This work was supported by Natural Sciences and Engineering Research Council of Canada (NSERC). The authors would like to thank Med Habib Ben Khalifa for doing FTIR tests.

7.7. REFERENCE

[1] Statistics Canada. Table 001-0010 - Estimated areas, yield, production and average farm price of principal field crops, in metric units, annual, CANSIM. 2017.

[2] Sadrmanesh V, Chen Y. Bast fibres: structure, processing, properties, and applications. Int Mater Rev 2018;64:381–406. https://doi.org/10.1080/09506608.2018.1501171.

[3] Sarasini F, Fiore V. A systematic literature review on less common natural fibres and their biocomposites. J Clean Prod 2018;195:240–67. https://doi.org/10.1016/j.jclepro.2018.05.197.

[4] Fiore V, Scalici T, Nicoletti F, Vitale G, Prestipino M, Valenza A. A new eco-friendly chemical treatment of natural fibres: Effect of sodium bicarbonate on properties of sisal fibre and its epoxy composites. Compos Part B Eng 2016;85:150–60. https://doi.org/10.1016/j.compositesb.2015.09.028.

[5] Fiore V, Scalici T, Valenza A. Effect of sodium bicarbonate treatment on mechanical properties of flax-reinforced epoxy composite materials. J Compos Mater 2018;52:1061–72. https://doi.org/10.1177/0021998317720009.

[6] Kabir MM, Wang H, Lau KT, Cardona F. Effects of chemical treatments on hemp fibre structure. Appl Surf Sci 2013;276:13–23. https://doi.org/10.1016/j.apsusc.2013.02.086.

[7] Al-Oqla FM, Sapuan SM. Natural fibre reinforced polymer composites in industrial applications: Feasibility of date palm fibres for sustainable automotive industry. J Clean Prod 2014;66:347–54. https://doi.org/10.1016/j.jclepro.2013.10.050.

[8] Sgriccia N, Hawley MC, Misra M. Characterization of natural fibre surfaces and natural

fibre composites. Compos Part A Appl Sci Manuf 2008;39:1632–7. https://doi.org/10.1016/j.compositesa.2008.07.007.

[9] Razak NIA, Ibrahim NA, Zainuddin N, Rayung M, Saad WZ. The influence of chemical surface modification of kenaf fibre using hydrogen peroxide on the mechanical properties of biodegradable kenaf fibre/poly(Lactic Acid) composites. Molecules 2014;19:2957–68. https://doi.org/10.3390/molecules19032957.

[10] Gunantara N. A review of multi-objective optimization: Methods and its applications 2018. https://doi.org/10.1080/23311916.2018.1502242.

[11] ASABE. Moisture Measurement. Moisture Meas 2005:3–5.

[12] Yengui F, Labrak L, Frantz F, Daviot R, Abouchi N, O'connor I. A Hybrid GA-SQP Algorithm for analog circuits sizing. Circuits Syst 2012;3:146–52. https://doi.org/10.4236/cs.2012.32019.

[13] Seki Y, Sarikanat M, Sever K, Durmuşkahya C. Extraction and properties of Ferula communis (chakshir) fibres as novel reinforcement for composites materials. Compos Part B Eng 2013;44:517–23. https://doi.org/10.1016/J.COMPOSITESB.2012.03.013.

[14] Yang H, Yan R, Chen H, Lee DH, Zheng C. Characteristics of hemicellulose, cellulose and lignin pyrolysis. Fuel 2007;86:1781–8. https://doi.org/10.1016/j.fuel.2006.12.013.

[15] Konczewicz W, Zimniewska M, Valera MA. The selection of a retting method for the extraction of bast fibres as response to challenges in composite reinforcement. Text Res J 2018;88:2104–19. https://doi.org/10.1177/0040517517716902.

[16] Garside P, Wyeth P. Identification of Cellulosic Fibres by FTIR Spectroscopy - Thread and

Single Fibre Analysis by Attenuated Total Reflectance. Stud Conserv 2003;48:269–75. https://doi.org/10.1179/sic.2003.48.4.269.

[17] Olsson A-M, Salmén L. The association of water to cellulose and hemicellulose in paper examined by FTIR spectroscopy. Carbohydr Res 2004;339:813–8. https://doi.org/10.1016/J.CARRES.2004.01.005.

[18] De Rosa IM, Kenny JM, Puglia D, Santulli C, Sarasini F. Morphological, thermal and mechanical characterization of okra (Abelmoschus esculentus) fibres as potential reinforcement in polymer composites. Compos Sci Technol 2010;70:116–22. https://doi.org/10.1016/J.COMPSCITECH.2009.09.013.

[19] Le Troedec M, Sedan D, Peyratout C, Bonnet JP, Smith A, Guinebretiere R, et al. Influence of various chemical treatments on the composition and structure of hemp fibres. Compos Part A Appl Sci Manuf 2008;39:514–22. https://doi.org/10.1016/J.COMPOSITESA.2007.12.001.

[20] Li Y, Pickering KL. Hemp fibre reinforced composites using chelator and enzyme treatments. Compos Sci Technol 2008;68:3293–8. https://doi.org/10.1016/j.compscitech.2008.08.022.

[21] George M, Mussone PG, Bressler DC. Surface and thermal characterization of natural fibres treated with enzymes. Ind Crops Prod 2014;53:365–73. https://doi.org/10.1016/j.indcrop.2013.12.037.

[22] Segal L, Creely JJ, Martin AE, Conrad CM. An empirical method for estimating the degree of crystalline of native cellulose using the X-Ray Diffractometer. Text Res J 1959;29:786–94. https://doi.org/10.1177/004051755902901003.

Chapter 8: General Conclusions and Future Recommendations

8.1. GENERAL CONCLUSIONS

Canola and sweet clover fibres were introduced as two alternative plant fibres. Their main chemical elements, chemical bonds, and crystallinity index were in the same ranges with the traditional plant fibres (hemp and flax). Canola and sweet clover fibres had high desirable thermal stability and wettability; however, they were associated with low Young's modulus and low tensile strength.

The tensile behaviour of plant fibres were investigated using the discrete element modelling (DEM). The model fibre contained sufficient numbers of particles and bonds to represent the solid nature of a plant fibre. The most critical micro-parameters of the model were identified to be the micro-Young's modulus of particles and micro-strength (tensile) of bonds. Their relationships with the model outputs (macro-Young's modulus and macro-strength) were linear.

A series of mechanical extraction tests were carried out on hemp fibre. The AHP model showed that the retting condition of the stalks, the number of passes of stalks through the rollers of the machine, and feed stalk size were the most influential parameters. The tests to extract canola fibres using mechanical extraction were unsuccessful.

Chemical retting tests were performed to extract canola fibres. The hybrid GA-SQP algorithm predicted that the optimum retting condition occurred at 37.8 h for reaction time, 57.7 ºC for temperature, and 5.62% for $NaHCO_3$ solution concentration. Under this condition, the highest quantity and quality fibres were obtained.

8.2. LIMITATIONS AND RECOMMENDATIONS

For improving the performance of mechanical extraction, it is recommended that in future work, different types of decorticators, in combination with different fibrous plants, be studied to find the most desirable conditions of feed stalk and machine parameters.

One of the challenges for chemical retting was that the process generates large amount of wastewater. This issue should be addressed before the retting process is scaled to commercial production.

In this study, a multi-objective optimization was done to predict the optimized condition to extract canola fibres. It is recommended to apply the same approach to optimize surface modifications to improve the properties of the fibres for better fibre products.

One of the main limitations of canola was its low percentage of fibre yield. Most breeding efforts in canola are directed to increase oil production and decrease fibre content. It is highly recommended to maintain, or enhance fibre content for a viable, multi-purpose canola crop.

The environmental benefit of utilizing bast fibre needs to be further investigated, as compared to fossil fuel based products. A systematic approach is to do Life Cycling Assessment analysis to understand the energy aspects of plant fibre.